University of Stavanger

FACULTY OF SCIENCE AND TECHNOLOGY

MASTER'S THESIS

Study program/specialization: Petroleum Engineering/Drilling Technology	Spring semester, 2019 Open
Author: Hassan Hmayed	_____ (Signature of author)
Supervisor: Mesfin Belayneh	
Title of Master's thesis: **Ormen Lange 6305/7 drilling data based ROP modelling and its application**	
Credits (ECTS): 30	
Keywords: ROP Modelling Ormen Lange field MSE Mutliple linear regression D-exponent Warren model Drilling optimization	Number of pages: 118 Supplemental material/other: 8 Stavanger, 15-06-/2019

ABSTRACT

During design and planning phase, determination of the accurate rate of penetration (ROP) is essential for efficient drilling operations. Optimized ROP predictions improve the drilling efficiency in terms of decreasing operation time per drilling depth and hence lowering the drilling cost. Thus, the application of the best ROP modelling procedure is crucial.

This thesis work presents a total of four different ROP modelling techniques, which are applied and tested on three wells in the Ormen Lange field. The modelling methods are the multiple linear regression, mechanical specific energy (MSE) model, d-exponent model and Warren model. The modelling approaches used were based on the whole well data and similar geologically grouped based data. The applicability of the models was tested only on the near-by wells, but not on far-away ones from the considered block.

ROP modelling of old well's drilling data and testing the model on the near-by wells showed that the stratigraphic groups-based modelling approach provides the best fit results with the field data and predicts the near-by well's ROP data quite good. Moreover, this thesis work developed and illustrated a step-by-step process for ROP optimization in terms of modelling of drilled well's data and its application for the near-by well to be drilled.

ACKNOWLEDGMENTS

I would like to thank and show my full appreciation for my supervisor Dr. Mesfin Belayneh, who has been there to support from the start and give guidance and advice when needed. I would also like to thank Andreas Habel and the Norwegian Petroleum for the well data that was required for this thesis. Lastly, I would like to thank my family and friends that supported me while writing this thesis.

TABLE OF CONTENTS

ABSTRACT ..... **ii**

ACKNOWLEDGMENTS ..... **iii**

TABLE OF CONTENTS ..... **iv**

LIST OF FIGURES ..... **vii**

LIST OF TABLES ..... **x**

NOMENCLATURE ..... **xi**

LIST OF ABBREVIATIONS ..... **xii**

1 INTRODUCTION **1**

1.1 Background 1

1.2 Problem Formulation 2

1.3 Objective 2

2 LITERATURE STUDY **3**

2.1 Drill Bit 3

2.1.1 Roller Cone Bits 4

2.1.2 Fixed Cutter Bits 5

2.1.3 Hybrid–Ktymira Bits 7

2.2 Factors affecting ROP 8

2.2.1 Formation Characteristics 8

2.2.2 Drilling Mud Weight and Overbalance 9

2.2.3 Plastic Viscosity and Solid Content 11

2.3 Operational Factors 13

2.4 Drilling Bit Optimization 14

3 THEORY **16**

3.1 Bourgoyne and Young ROP model 16

3.2 Warren ROP model 17
3.2.1 Perfect-Cleaning Model 17
3.2.2 Imperfect-Cleaning Model 18
3.3 Modified Warren ROP model 19
3.4 Mechanical Specific Energy vs ROP 21
3.5 D-Exponent vs ROP 23
3.6 Drag Bit Model 24
3.8 Maurer Model 24
3.7 Bingham Model 25
4 ORMEN LANGE FIELD DATA MODELLING AND WORKFLOW 26
4.1 Ormen Lange field description 26
4.2 Drilling data filtration 28
4.2.1 Moving Average Filter 28
4.2.2 Exponential Smoothing 30
4.3 ROP modelling techniques 31
4.3.1 Multiple Linear Regression 31
4.3.2 D-exponent 33
4.3.3 MSE – Mechanical Specific Energy 34
4.3.4 Warren Model 35
5 RESULTS 38
5.1 Multiple Regression 39
5.1.1 Total Well Data Modelling 39
5.1.2 Geological Well data modelling 46
5.2 MSE 56
5.3 D-exponent 61
5.4 Warren Model 66
5.4.1 Modelling with data from the whole well 67

5.4.2 Modelling with data from geological groups 74

6 SUMMARY AND DISCUSSION 81

6.1 Plot comparisons 81

6.2 Mean absolute percentage error (MAPE) 87

6.3 Time analysis 90

6.4 Parametric sensitivity study 93

6.5 Analysis summary 99

6.6 Optimization methods for the field application 101

7 CONCLUSIONS 102

8 REFERENCES 103

APPENDIX I: More Reviewed ROP Models 107

Bourgoyne and Young model 107

Drag Bit Model 109

Maurer Model 109

Bingham Model 110

APPENDIX II: Modelling Application 111

Moving Average 111

Multiple Linear Regression 112

Warren Model 113

LIST OF FIGURES

Figure 1. Rotatory drilling using both indentation and cutting [11]. 4
Figure 2. Roller Cone bit and its components [13]. 5
Figure 3. PDC bit and its components [15]. Figure 4. PDC cutter component [16]. 6
Figure 5. Baker Hughes Kymera bit [17]. 7
Figure 6. Unconfined compression test [22]. 9
Figure 7. Rate of Penetration (ROP) vs. drilling mud density (oil-based) [26]. 10
Figure 8. Relation between the normalized rate of penetration and overbalance [27]..... 11
Figure 9. Rate of penetration vs Plastic viscosity, non-normalized to the left and normalized to the right [24]. 12
Figure 10. Rate of penetration (ROP) vs solid content- non-normalized to the left and normalized to the right [24]. 12
Figure 11. Rate of penetration (R) vs. weight on bit (W) (Bourgoyne et al. 1991). 13
Figure 12. Rate of penetration (R) vs. the rotation speed (N) (Bourgoyne et al. 1991). 14
Figure 13. Mechanical efficiency vs. the depth of cut. Bits are between 30-40% efficient..... 22
Figure 14. Location of the Ormen Lange field on the NCS {NPD, #29}. 27
Figure 15. Location of the three wells used in the modelling in block 6305/7. 28
Figure 16. Example of moving average. 30
Figure 17. Example of exponential smoothing for alfa = 0.9 and 0.75. 31
Figure 18. Multiple linear regression workflow [21]. 33
Figure 19. D-exponent Workflow. 34
Figure 20. MSE Workflow 35
Figure 21. Warren Model Workflow 37
Figure 22. Multiple regression using whole field data from 6305/7-D-1 H on itself. 40
Figure 23. Multiple regression using whole field data from 6305/7-D-2 H on itself. 41
Figure 24. Multiple regression using whole field data from 6305/7-D-3 H on itself. 41
Figure 25. Multiple regression using whole field data from 6305/7-D-1 H on 6305/7-D-2 H.42
Figure 26. Multiple regression using whole field data from 6305/7-D-1 H on 6305/7-D-3 H.42
Figure 27. Multiple regression using whole field data from 6305/7-D-2 H on 6305/7-D-1 H.43
Figure 28. Multiple regression using whole field data from 6305/7-D-2 H on 6305/7-D-3 H.44
Figure 29. Multiple regression using whole field data from 6305/7-D-3 H on 6305/7-D-1 H.45
Figure 30. Multiple regression using whole field data from 6305/7-D-3 H on 6305/7-D-2 H.45
Figure 31. Multiple Regression (using geological sections) of well 6305/7-D-1 H on itself. . 51
Figure 32. Multiple Regression (using geological sections) of well 6305/7-D-2 H on itself. . 51
Figure 33. Multiple Regression (using geological sections) of well 6305/7-D-3 H on itself. . 52
Figure 34. Multiple regression using geological group data from 6305/7-D-1 H on 6305/7-D-2 H. 53
Figure 35. Multiple regression using geological group data from 6305/7-D-1 H on 6305/7-D-3 H. 53
Figure 36. Multiple regression using geological group data from 6305/7-D-2 H on 6305/7-D-1 H. 54
Figure 37. Multiple regression using geological group data from 6305/7-D-2 H on 6305/7-D-3 H. 54
Figure 38. Multiple regression using geological group data from 6305/7-D-3 H on 6305/7-D-1 H. 55
Figure 39. Multiple regression using geological group data from 6305/7-D-3 H on 6305/7-D-2 H. 55

Figure 40. Calculated MSE for wells 6305/7-D-1 H, 6305/7-D-2 H and 6305/7-D-3 H vs. total depth. 57
Figure 41. Modelled ROP (using MSE values from 6305/7-D-1 H). 58
Figure 42. Modelled ROP (using MSE values from 6305/7-D-1 H). 58
Figure 43. Modelled ROP (using MSE values from 6305/7-D-1 H). 59
Figure 44. Modelled ROP (using MSE values from 6305/7-D-2 H). 60
Figure 45. Modelled ROP (using MSE values from 6305/7-D-3 H). 61
Figure 46. Modelled ROP (using MSE values from 6305/7-D-3 H). 61
Figure 47. Calculated d-exponent for 6305/7-D-1 H, 6305/7-D-2 H and 6305/7-D-3 H. 62
Figure 48. Modelled ROP (using d-exponent from 6305/7-D-1 H). 63
Figure 49. Modelled ROP (using d-exponent from 6305/7-D-1 H). 63
Figure 50. Modelled ROP (using d-exponent from 6305/7-D-2 H). 64
Figure 51. Modelled ROP (using d-exponent from 6305/7-D-2 H) 65
Figure 52. Modelled ROP (using d-exponent from 6305/7-D-3 H). 65
Figure 53. Modelled ROP (using d-exponent from 6305/7-D-3 H). 66
Figure 54. Warren ROP for 6305/7-D-1 H (using coefficients for the same well). 68
Figure 55. Warren ROP for 6305/7-D-2 H (using coefficients for the same well). 68
Figure 56. Warren ROP for 6305/7-D-3 H (using coefficients for the same well). 69
Figure 57. Warren ROP for 6305/7-D-2 H (using coefficients from 6305/7-D-1 H). 70
Figure 58. Warren ROP for 6305/7-D-3 H (using coefficients from 6305/7-D-1 H). 70
Figure 59. Warren ROP for 6305/7-D-1 H (using coefficients from 6305/7-D-2 H). 71
Figure 60. Warren ROP for 6305/7-D-3 H (using coefficients from 6305/7-D-2 H). 72
Figure 61. Warren ROP for 6305/7-D-1 H (using coefficients from 6305/7-D-3 H). 73
Figure 62. Warren ROP for 6305/7-D-3 H (using coefficients from 6305/7-D-2 H). 73
Figure 63. Warren ROP for 6305/7-D-1 H (using coefficients from the geological groups for the same well). 76
Figure 64. Warren ROP for 6305/7-D-2 H (using coefficients from the geological groups for the same well). 77
Figure 65. Warren ROP for 6305/7-D-3 H (using coefficients from the geological groups for the same well). 77
Figure 66. Warren ROP for 6305/7-D-2 H (using coefficients from the geological groups from 6305/7-D-1 H). 78
Figure 67. Warren ROP for 6305/7-D-3 H (using coefficients from the geological groups from 6305/7-D-1 H). 78
Figure 68. Warren ROP for 6305/7-D-1 H (using coefficients from the geological groups from 6305/7-D-2 H). 79
Figure 69. Warren ROP for 6305/7-D-3 H (using coefficients from the geological groups from 6305/7-D-2 H). 80
Figure 70. ROP deviations plot vs total depth. 82
Figure 71. Application of the “IF” model. 83
Figure 72. Calculation of the percentage deviation of the modelled ROP. 83
Figure 73. calculating the MAPE for each datapoint 88
Figure 74. Calculating the MAPE for the modelling technique 88
Figure 75. calculating drilling time for interval. 91
Figure 76. The effect of increasing or decreasing WOB by 10% on the modelled ROP. 94
Figure 77. The effect of increasing or decreasing torque by 10% on the modelled ROP. 95
Figure 78. The effect of increasing or decreasing RPM by 10% on the modelled ROP. 95
Figure 79. The effect of increasing or decreasing flow rate by 10% on the modelled ROP. 96
Figure 80. Average of the modelled ROP (using 10% deviations from the filtered operational parameters). 97

Figure 81. Sensitivity analysis – modelled ROP for 305/7-D-2 H after increasing RPM by 10 % and decreasing torque by 10 % vs. modelled ROP (using coefficients from 6305/7-D-1 H). 98
Figure 82. Sensitivity analysis – modelled ROP for 305/7-D-3 H after increasing RPM by 10 % and decreasing torque by 10 % vs. modelled ROP (using coefficients from 6305/7-D-1 H). 98
Figure 83. percentage decrease in drilling time for wells 6305/7-D-2 H and 6305/7-D-3 H when using +10% RPM and -10% torque. 99
Figure 84. Moving Average filter using the data analysis package 111
Figure 85. Moving average equation applied in Excel by the package 111
Figure 86. Multiple rinear regression application 112
Figure 87. Calculating the first Warren Term in Excel 113
Figure 88. Calculating the second Warren Term in Excel 113
Figure 89. Calculating the third Warren Term in Excel 113
Figure 90. Calculation of Warren coefficients in Matlab 114
Figure 91. Warren ROP calculating in Excel 114

LIST OF TABLES

Table 1. Drilling performance comparison between PDC and hybrid bits [18]..... 7
Table 2. Regression coefficients from well 6305/7-D-1 H. 39
Table 3. Regression coefficients from well 6305/7-D-2 H. 39
Table 4. Regression coefficients from well 6305/7-D-3 H. 40
Table 5. Geological groups and their depths for well 6305/7-D-1 H..... 46
Table 6. Geological groups and their depths for well 6305/7-D-2 H..... 47
Table 7. Geological groups and their depths for well 6305/7-D-3 H..... 47
Table 8. Regression Coefficients for the Nordland group from well 6305/7-D-1 H. 47
Table 9. Regression Coefficients for the Hordaland group from well 6305/7-D-1 H..... 48
Table 10. Regression Coefficients for the Rogaland group from well 6305/7-D-1 H. 48
Table 11. Regression Coefficients for the Nordland group from well 6305/7-D-2 H. 49
Table 12. Regression Coefficients for the Hordaland group from well 6305/7-D-2 H. 49
Table 13. Regression Coefficients for the Rogaland group from well 6305/7-D-2 H. 49
Table 14. Regression Coefficients for the Nordland group from well 6305/7-D-3 H. 50
Table 15. Regression Coefficients for the Hordaland group from well 6305/7-D-3 H. 50
Table 16. Regression Coefficients for the Rogaland group from well 6305/7-D-3 H. 50
Table 17. Warren coefficients for 6305/7-D-1 H (using data from the whole well)..... 67
Table 18. Warren coefficients for 6305/7-D-2 H (using data from the whole well)..... 67
Table 19. Warren coefficients for 6305/7-D-3 H (using data from the whole well)..... 67
Table 20. Warren coefficients for 6305/7-D-1 H (Nordland group)..... 74
Table 21. Warren coefficients for 6305/7-D-1 H (Hordaland group)..... 74
Table 22. Warren coefficients for 6305/7-D-1 H (Rogaland group)..... 74
Table 23. Warren coefficients for 6305/7-D-2 H (Nordland group)..... 75
Table 24. Warren coefficients for 6305/7-D-2 H (Hordaland group)..... 75
Table 25. Warren coefficients for 6305/7-D-2 H (Rogaland group)..... 75
Table 26. Warren coefficients for 6305/7-D-3 H (Nordland group)..... 75
Table 27. Warren coefficients for 6305/7-D-3 H (Hordaland group)..... 76
Table 28. Warren coefficients for 6305/7-D-3 H (Rogaland group)..... 76
Table 29. percentage of data within a 5 % margin using all the modelling methods..... 83
Table 30. percentage of data within a 10% margin using all the modelling methods..... 85
Table 31. MAPE values for the multiple modelling methods..... 88
Table 32. Drilling time deviation for the different models. 91
Table 33. Analysis of the modelling techniques. 100

NOMENCLATURE

A – Area
A_B – Bit area
C_b – Cost of bit
d – Bit diameter / D-exponent
D – Depth
d_B – Bit diameter
d_c – Corrected d-exponent
d_n – Bit nozzle diameter
e – Specific energy
F – Thrust
f_c – Chip hold down function
F_j – Jet impact force
F_{jm} – Modified jet impact force
g_p – Pore pressure gradient of formation
hr – Hour
m – Meter
N – Rotational speed (RPM)
P_e – Effective differential pressure
P_w – Penetration loss due to wear of cutter
q – Flow rate
R – ROP
S – Rock strength
T – Torque
t_b – Rotating time
t_c – Non-rotating time
t_t – Trip time
V_D – Volume each cutter is worn down per rotation
v_f – Return fluid velocity
v_n – Nozzle velocity
w – Bit weight
ρ – Fluid density
ρ_c – ECD at the hole-bottom
γ_f – Fluid specific gravity
μ - Bit specific coefficient of sliding friction

LIST OF ABBREVIATIONS

coeff. – Coefficient(s)
CCS – confined compression strength
D-Exp – D-exponent
DSP – Digital signal processing
ECD – Equivalent circulating density
Eq. – Equation
FLOW – Flowrate
FP – Formation pressure
GPM – Mud flow rate
IADC – International Association of Drilling Contractors
KA – Apparent nozzle area of bit
log – Logarithm
MAPE – Mean absolute percentage error
Mult. Reg. – Multiple regression
MW – Mud weight
MSL – Mean sea level
MSE – Mechanical specific energy
NCS – Norwegian continental shelf
NPP – Normal pore pressure
NPD – Norwegian Petroleum Directorate
PDC – Polycrystalline diamond compact
ROP – Rate of penetration
ROP_{mod} – Rate of penetration
RPM – Revolutions per minute
TRQ – Torque
TVD – True vertical depth
UCS – Unconfined compressive strength
WOB – Weight on bit
WOB_{mech} – Mechanical weight on bit

1 INTRODUCTION

This thesis work presents the ROP modelling and application on the Ormen Lange field in block 6305/7 in Norwegian Sea. A total of six modelling approaches were employed and their performance are evaluated. The thesis presents an ROP optimization procedure to be applied when drilling a new well

1.1 Background

Rotary drilling operations comprise of rotating, hoisting and circulation systems. Among these, drill bits are part of the rotary system. It is connected to the very end of the drill string. Upon the application of rotational and axial load, the drill bit crushes the formation into pieces and hence allows drilling deeper into the formation.

There are different types of drill bits available on the market. Among others, roller cone, PDC and hybrid (kymira) are the commonly used ones. Their performance and efficiency on drilling vary, based on the geology of the well and the handling of the vibrations control in the well. During design phases, the choice of the bit with respect to higher ROP and minimum bit wear is the key for reducing cost by reducing the undesired number of tripping and drilling in shortest period possible.

Determination of the rock strength or ‘’drillability’’ associated with different geological formation is important [1]. There are several methods to quantify or estimate the rock strength for instance through mechanical testing of cored rock samples [2], rock cuttings [3], Sonic logs derived empirical models [4], and ROP modeling analyses [5]. During design phase, the ROP optimization is conducted using software. For instance, drilling optimization Simulator (DROPS) software is developed to simulate ROP optimization. The basic principle with the design is that first it calculates the apparent rock strength logs using drilling parameters obtained from the old well [6-9]. Using the MSE theory, it calculates the uniaxial compressive strength (ASRS), which is to estimate the strength of the formation for the nearby well. By selecting different drilling parameters and running several simulations, the software provides an optimized ROP and bit wear expected for drilling the new well. Moreover, for optimizing drilling operation in the newly planned well, it is important to learn the challenges encountered in the previously drilled wells in

the same field, investigate the effects of the drilling parameters on the ROP and determine which parameters are most sensitive to ROP optimization for when planning to drill the new well. It can be investigated through modelling and sensitivity study by computing the ROP and total drilling time for a given drilling depth. In this thesis, this approach will be implemented by modelling an old well and applying the model on a nearby well in the Ormen Lange field in Norwegian Sea. Several modeling techniques will be implemented and compared.

1.2 Problem Formulation

Among many others, drilling rate optimization is a key factor for reducing drilling cost. This is done during planning phases. As mentioned, there are several analytical simulation software available in the industry. In this thesis, using drilled wells data, different types of modelling techniques will be employed to model ROP for planning to drill new well. The issues to be addressed are:

- how reliable are the newly modelling techniques?
- how reliable are the models when applied for nearby wells?
- what is the effect of the geological properties on the modelling?
- how can the literature established models be modified to generate new correlation parameters

1.3 Objective

The primary objective of this thesis is to answer the issues addressed in section 1.2. The main activities include:

- To review the ROP models
- To model wells located in the Ormen Lange field in block 6305/7 using different modelling approaches and the well data for each well
- To evaluate the performance of the models on the nearby wells in the same field
- Evaluate the effect of dissecting the well into multiple geological groups
- To perform and propose an ROP optimization technique.
- To indicate the best ROP modeling approach

2 LITERATURE STUDY

This chapter will discuss and present the literature around the factors that influence the rate of penetration (ROP) as well as multiple ROP models that have been published and tested, however not all the models presented in the literature will be tested.

2.1 Drill Bit

The drill bit is a drilling tool used for drilling a wellbore and is located at the tip of the drilling string below the drilling collar. The main role of the bit is cutting and penetrating the rocks at the bottom of the well. It usually consists of cutters or "teeth" and nozzles. The cutters on the bit head are designed so they are harder than the rock formation they are being pushed on and break the rock. The material that is used for these teeth depends upon the hardness of the rock and can vary from:

- Steel
- Tungsten carbon
- Diamond

The nozzles of the bit are the passage through which the drilling fluid is circulated down to the well. The drilling fluid that is pumped down help cooling down the bit during drilling operation. It also circulates out the broken-down formation rocks that where drilled to the surface through the annulus in the wellbore. The drilling fluid that is pumped down the nozzles applies a jet force on the formation. This Jet force improves the penetration of the formation. As well as that, the drilling fluid applies a hydrostatic overbalance in the well that protects the well from any influx of reservoir fluids.
As R TEALE described, bits work on the formation by a combination of two actions, as shown in Figure 1 [10]:

- Indentation, where the drill bit is pushed into the rock formation through weight on bit (WOB) and this gives the drilling bit a grip on the rock
- Cutting, where lateral movement is applied to the drilling bit to chip the formation rock and break it out.

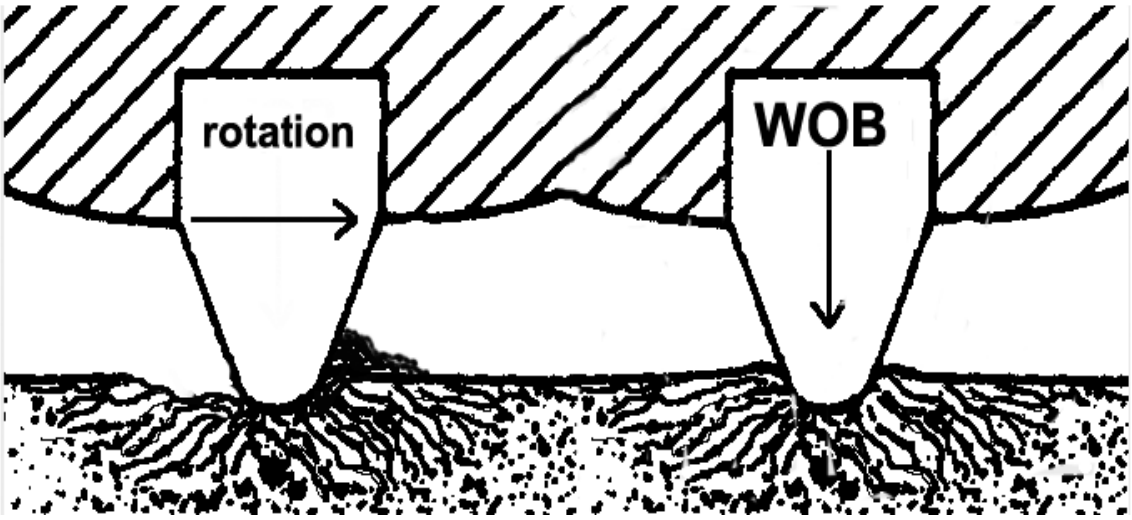

Figure 1. Rotatory drilling using both indentation and cutting [11].

Drilling bits come in many different forms and shapes depending on the hardness of the rock formation and the size of the wellbore. They can be divided into two groups: Roller cone bits and fixed cutter bits, where there also exist bits that combine properties from both.

2.1.1 Roller Cone Bits

Roller cone bits are the traditional and most used bits in the E&P industry since 1909 when it was patented by Howard Hughes. They usually consist of three equally sized metal cones that can rotate independently with cutters on them used to crush the rock formation located. As well as that, nozzles are located on the bit that direct the mud flow through them. The number of nuzzles, their direction and angle all are design based and impact the performance of the roller cone bit, where the best drilling performance is seen when the nozzles are positioned so they direct the mud flow onto the cones to help with the removal of the cuttings. Figure 2 represents a typical roller cone bit.

Roller cone bits can be classified into two sub-categories depending on the structure of the cuttings located on the cones [12]:

- Steel milled-tooth bits: These are created of steel and are made as parts of the cone; they are then coated to protect them from wear.
- Insert bits or Tungsten Carbide Inserts (TCI): These are fabricated from tungsten carbide and are pressed on the cones through small holes that are made.

The length of the cutters used vary depending on the compressive strength of the formation rock, where longer cutters are used on soft rock formations with weak compressive strength and shorter cutters are used on hard rock formations with high compressive strength.

The design of the roller bit cone, from the materials used, the nozzles and type of cutters is to avoid the wear of the bit while maintaining high ROP. This avoids unnecessary trips to replace a damaged bit and minimizes non-productive time (NPT).

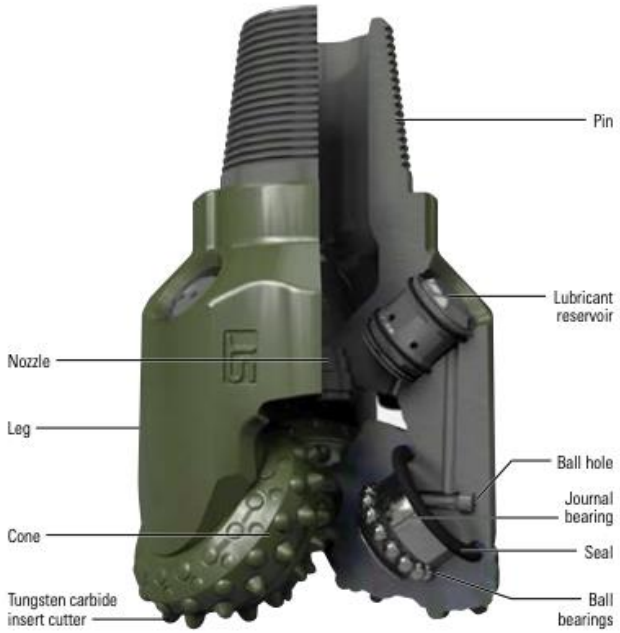

Figure 2. Roller Cone bit and its components [13].

2.1.2 Fixed Cutter Bits

Fixed cutter bits are one of the biggest advances for the drilling tools industry ever since their introduction in 1976 and have become as popular as the traditional roller cone bits. The whole bit rotates as a single unit and has no components that move independently of the bit such as bearings or cones. Instead of crushing and gauging the rock formation as

a traditional roller cone bit, the fixed cutter bit will use a shearing motion for formation rock excavation. The most prominent type of fixed cutter bit that is used worldwide is the polycrystalline diamond bit. [13] The body of the fixed cutter bit is manufactured in two different styles: steel-body bit or a matrix-body bit. The two materials have both their advantages and disadvantages and the use of one or the other is dependent on the needs of application. The matrix is made of a hard, yet brittle, composite material of tungsten carbide and an alloy that has higher resistance to abrasion and corrosion and can withstand higher compression loads than steel, where steel is softer than the matrix. However, the steel-body bit has the advantage over the matrix-body bit when it comes to resisting high impact loads. The cutters that are used in a fixed cutter are permanently located on blades on the bit and the first component of the bit that makes contact with the formation rock. PDC cutters use polycrystalline diamond that is created by diamond grit and then used in the diamond table and is the first thing that makes contact with the formation rock. This diamond table is sintered to a tungsten carbide substrate that provides structural support to the diamond and a method to withstand brazing [12, 14]. An example of a PDC bit and its cutter can be seen in Figures 3 and 4, respectively.

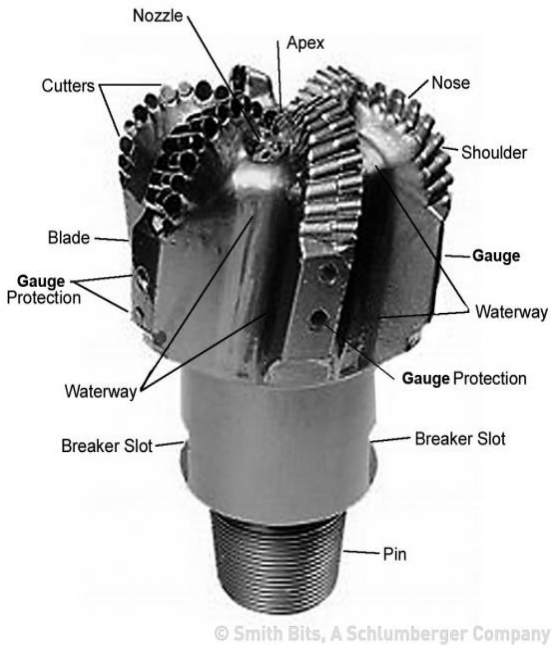

Figure 3. PDC bit and its components [15].

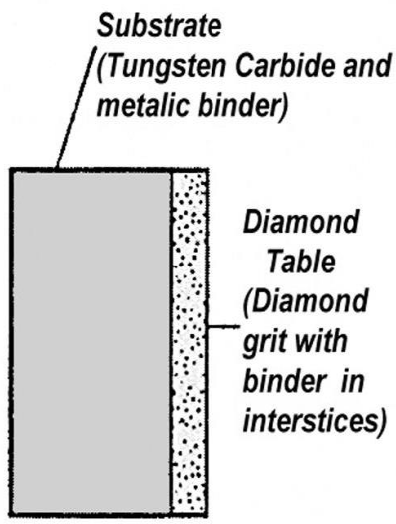

Figure 4. PDC cutter component [16].

2.1.3 Hybrid–Ktymira Bits

The drilling bit has improved since its introduction to meet higher demands and challenges in the oil industry and is still being improved upon to access deep reservoirs that have high compressive strength and are under extremely high pressures and temperature. This has led to the introduction of new types of drilling bits such as the hybrid drilling bits which are a mix of the PDC bits and the roller cone bits. Hybrid bits have improved drilling efficiency in terms of drilling at higher speeds and controlling stick slip vibrations. An example of such bit is illustrated in Figure 5

Figure 5. Baker Hughes Kymera bit [17].

As shown in Table 1, the hybrid bit drilled with an ROP of 13 ft/hr, achieving 108% higher ROP with less cost per foot compared to the previous runs which drilled the same formation in the same well.

Type	Depth In [ft]	Depth Out [ft]	Int. Ft.	Tot.Hr.	On Btm Hr	ROP [ft/hr]
Bit A – PDC	10870	11101	231	50.5	44.8	5.16
Bit B – PDC	11101	11440	339	50	48.6	6.98
Hybrid	11440	12049	609	51.5	48.6	12.5
Bit C - PDC	12049	12236	187	35.5	30.2	6.19

Table 1. Drilling performance comparison between PDC and hybrid bits [18].

2.2 Factors affecting ROP

2.2.1 Formation Characteristics

Formation properties such as elasticity, formation strength, porosity and formation pressure play a major role in both drilling and completion and can be the deciding factors for bit choice, casing design and completion design. During drilling operations, these properties will affect the rate of penetration (ROP) during drilling operations and determining these properties and using them will impact the drilling efficiency [19].

Out of the properties mentioned above, the formation elasticity and the formation strength, traditionally represented by the Unconfined compressive strength (UCS), are the biggest factors that determine the rate of penetration and can be seen as the resistance the formation rock puts up against the bit that is pushed on them. The unconfined compressive strength is the maximum compressive stress that a cylindrical-shaped core can withstand before breaking under atmospheric pressure.

Calculation and estimation of the uniaxial compressive strength of rocks has been established and standardized by both, The International Society for Rock Mechanics (ISRM) and the American Society for Testing and Materials (ASTM). This involves laboratory tests using a machine that applies axial to a circular cylindrical specimen that represents the formation until it breaks. This test in its nature is destructive and requires multiple core samples that are nearly identical to replicate the results and compare them. An example of such test can be observed in Figure 6. Other methods have been devised to estimate the UCS that avoids destroying the specimen, one of these methods would be using P-waves, Schmidt hammer, rebound slake durability index, and shore hardness [20, 21].

However, there remains an issue with using the unconfined compression strength of the rock. The laboratory environment that the core sample are tested upon are not representative of downhole conditions. During operations, clear fluid like the one used for the laboratory is substituted by drilling mud that creates a mud filter cake which acts as an impermeable membrane, and the formation rock is affected by confined pressure that gives an increase in the apparent compressive strength of the formation rock.

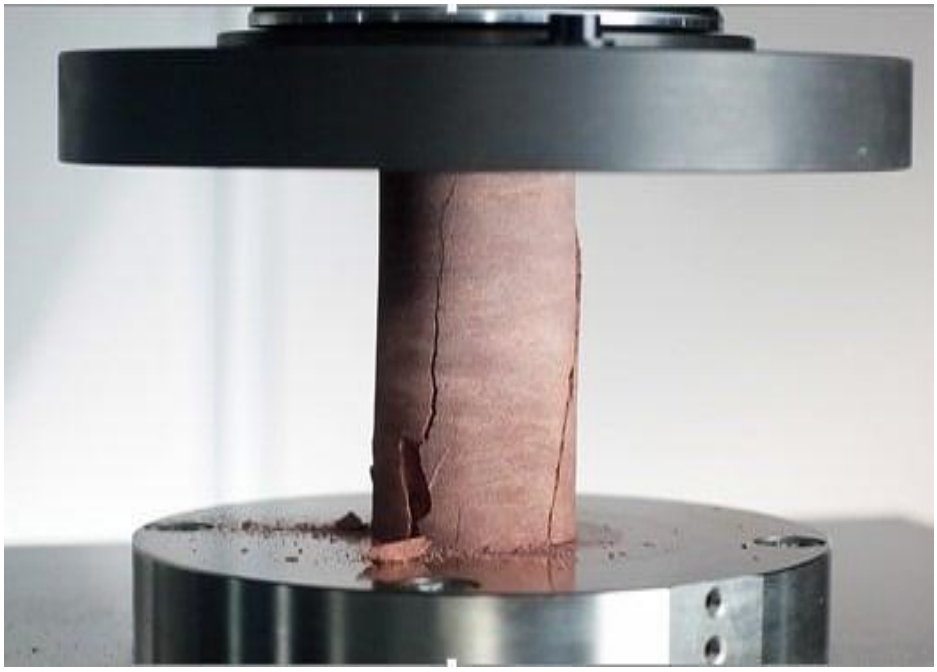

Figure 6. Unconfined compression test [22].

This was solved by using the confined compression strength (CCS), which takes into account the issues mentioned above, and can be derived from the unconfined compression strength, the confining stress, the pore pressure of the formation and the rock internal angle of friction, which is between 30° and 40° for most rocks. The equation can be shown as followed [23]:

$$CCS = UCS + DP + \frac{2*DPsin(FA)}{(1-\sin(FA)} \tag{2.1}$$

Where CCS is the confined compressive strength, UCS is the unconfined compressive strength, DP is differential pressure, or the confined stress and FA is the rock internal angle of friction.

2.2.2 Drilling Mud Weight and Overbalance

The drilling mud used in drilling operations has been documented to influence the rate of penetration (ROP). The mud used under drilling operations is responsible for cleaning the wellbore of any rock debris after drilling and transport them to the surface so the bit can make contact with the formation below, and to cool down the rotating bit. The drilling

mud's efficiency in drilling the well depends on the many properties that compose it, such as [24, 25]:

- Rheology
- Mud weight
- Overbalance
- Type of mud used (Water-based or oil based)
- Solid content
- Plastic viscosity

Mud Weight and Overbalance

A study in 1985 by Cheatham and Nahm [26] shows that the weight of the drilling mud has an inversely relation with the rate of penetration (ROP). This is seen in Figure 7. where the higher the density of the drilling mud, the lower the rate of penetration (ROP). This is when all the other known factors are kept constant and is regardless of the type of drilling fluid used, whether it be water-based mud or oil-based mud.

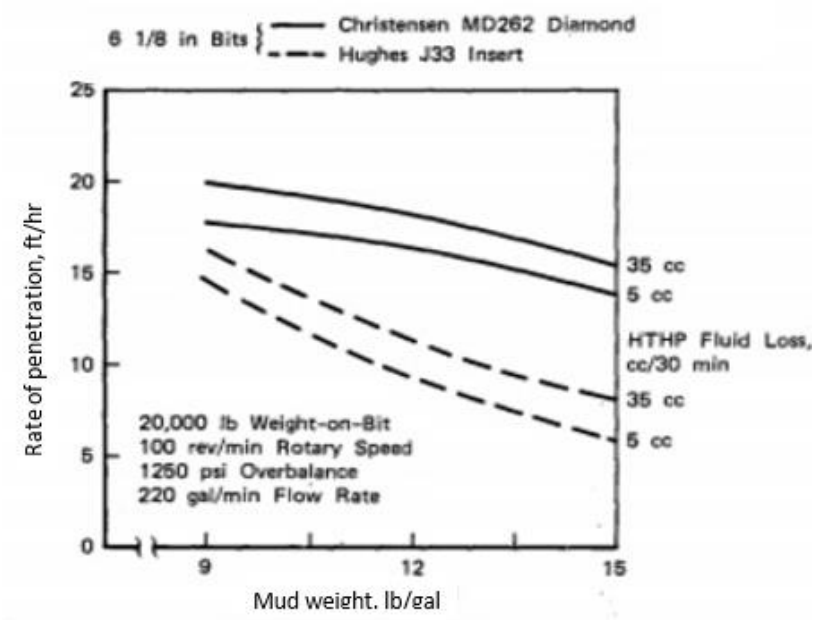

Figure 7. Rate of Penetration (ROP) vs. drilling mud density (oil-based) [26].

As well as that, an increase in drilling mud weight would increase the pressure differential between the bottomhole pressure and the pore pressure, known as the overbalance. In

1974, Bourgoyne and Young observed that this increase in overbalance was met by a decrease in the rate of penetration. This can be seen in Figure 8, and the relationship between the logarithm of the normalized rate of penetration (ROP), which is the ratio of the rate of penetration under overbalance and the rate of penetration with zero overbalance, and the overbalance gives a straight line and is thus linear. Thus, the following relation can be made between the two:

$$\log \frac{R}{R_0} = -m(P_{Bh} - P_f) \tag{2.2}$$

Where R is the is the rate of penetration, R_0 is the rate of penetration under zero overbalance, m is the slope of the line, P_{Bh} is the bottomhole pressure and P_f is the formation-fluid pressure or pore pressure [27].

Bourgoyne and Young decided to express the overbalance term in the equation with a term that includes the ρ_f, the equivalent circulating density (ECD), i.e. the density of the mud at bottomhole conditions and the pore pressure gradient g_p. Eq. 2.2 can then be written as follows:

$$\log \frac{R}{R_0} = 0.052mD(g_p - \rho_f) \tag{2.3}$$

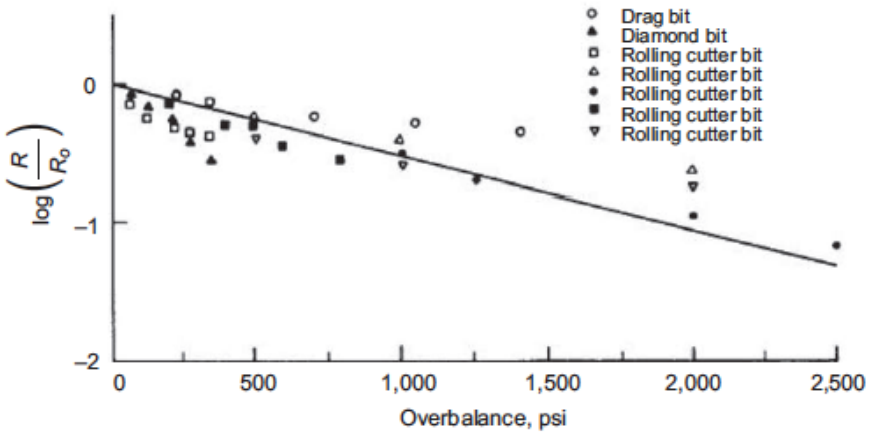

Figure 8. Relation between the normalized rate of penetration and overbalance [27].

2.2.3 Plastic Viscosity and Solid Content

In a study by Abouzar Mirzaei-Paiaman and Mohsen Masihi in 2009 [24] on the effects of drilling fluid properties on rate of penetration (ROP), they found that a change in plastic viscosity and the solid content of the fluid used for operation impacts the rate of penetration.

When keeping all other factors constant and only increasing the plastic viscosity (PV), they observed that both the rate of penetration (ROP) and the normalized rate of penetration (NROP) decreased. This can be seen in Figure 9.

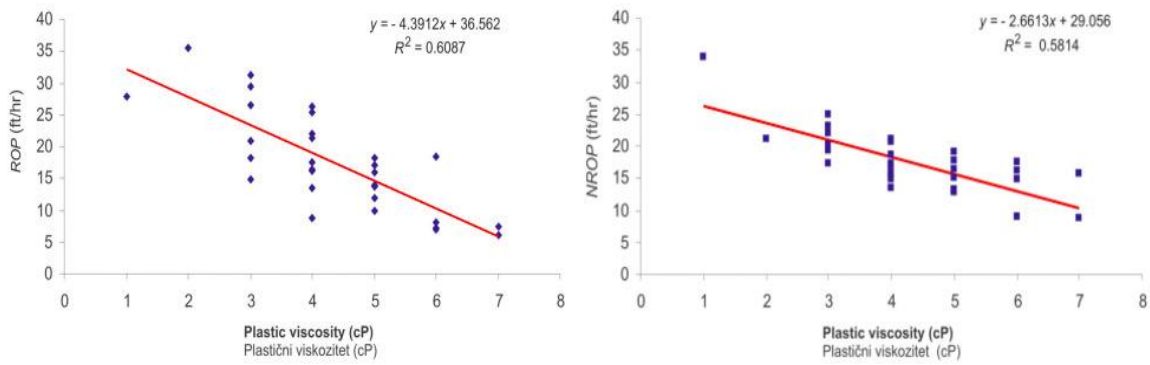

Figure 9. Rate of penetration vs Plastic viscosity, non-normalized to the left and normalized to the right [24].

An increase in the solid content of the drilling mud, while keeping the plastic viscosity constant, proved to give a behavior similar to that of the plastic viscosity. Where an increase in the solid content resulted in a lower normalized and non-normalized rate of penetration (ROP). This is observed in Figure 10.

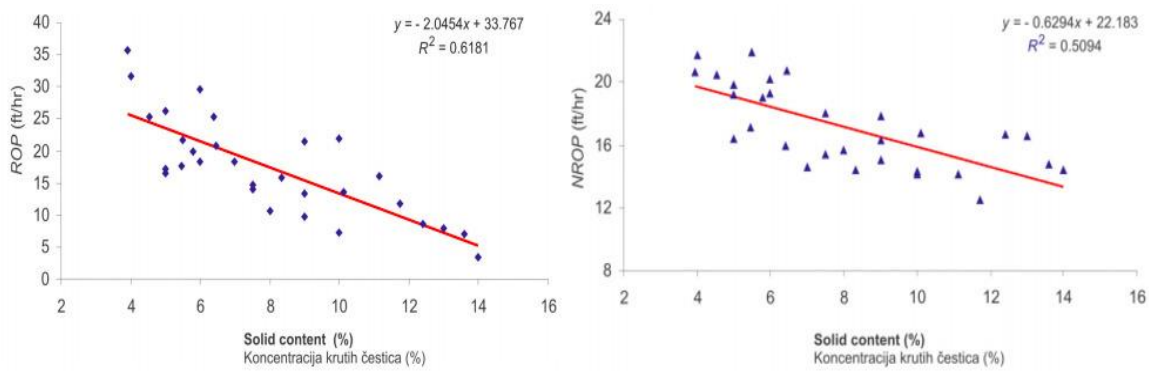

Figure 10. Rate of penetration (ROP) vs solid content- non-normalized to the left and normalized to the right [24].

2.3 Operational Factors

During drilling operation, the driller has control over two factors that majorly affect the rate of penetration (ROP), these are the rotation speed (RPM) and the weight on bit (WOB). Many studies have been performed by authors to show the relation between the change in one of the two factors mentioned and the rate of penetration (ROP)[28].

An increase in the weight on bit (WOB) has been documented to respond with an increase to the rate of penetration (ROP) until a limit has been reached, this can be seen in Figure 11. To initiate drilling and get any penetration, a threshold of weight on bit (WOB), point "a" on the Figure, needs to be applied. Penetration starts after that and increases gradually, yet linearly, from "a" to "b". This increase becomes more rapidly from "b" to "c", and this is due to the change of the failure-rock mode from scarping to shearing. After that slight increases in rate of penetration (WOB) are observed for increasing the weight on bit (WOB), "c" to "d". Increasing the weight on bit (WOB) beyond that has shown in some cases to reduce the rate of penetration (ROP), "d" to "e", this can be referred to as bit foundering. The negative results of increasing the weight on bit (WOB) too high are usually due to low hole cleaning efficiency. This could be due to the hydraulics for the operation not being changed and the rate of cuttings being created has increased or that the cutters on the bit are penetrating the formation rock with no clearance to allow proper cleaning [29].

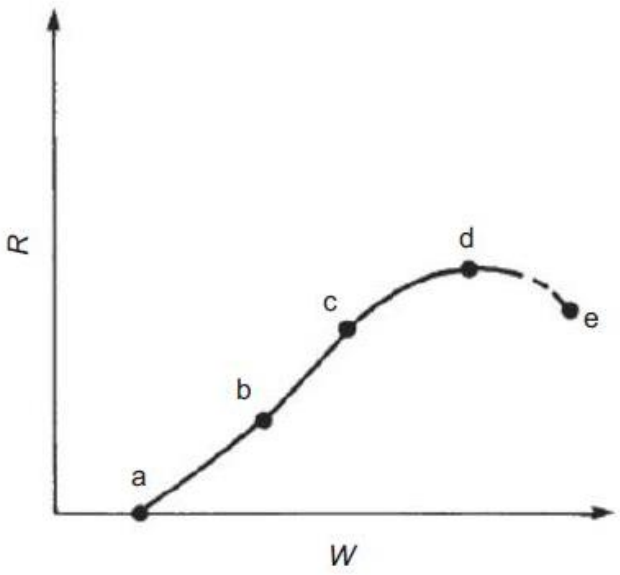

Figure 11. Rate of penetration (R) vs. weight on bit (W) (Bourgoyne et al. 1991).

The generalized relationship between the rotational speed (RPM) during drilling operations and the rate of penetration (RPM) can be seen in Figure 12. Penetration rates increase linearly as rotation speed increases, until a value of rotation speed is reached at which any further increase will result in diminishing increases in the rate of penetration (ROP) [27, 30].

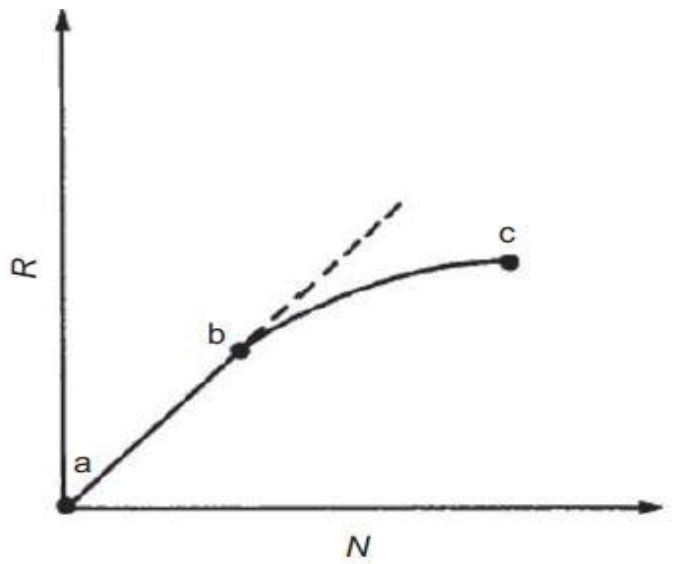

Figure 12. Rate of penetration (R) vs. the rotation speed (N) (Bourgoyne et al. 1991).

2.4 Drilling Bit Optimization

Drilling bits that are used for a specific well are one of the main factors that decide the rate of drilling and the cost of drilling that well. This can be seen in Eq. 2.4, which shows the calculation of the drilling cost [31].

$$C_d = \frac{(t_c+t_d+t_t)C_r+C_m t_d+C_b}{\Delta D} \tag{2.4}$$

Where t_c, t_d, and t_t are the connection time, the drilling time and the trip time in [hrs] respectively. ΔD is the drilling length in [ft] and C_d, C_r, C_m and C_b are the drilling cost, the drilling rig cost, the drilling motor cost and the bit cost in [USD/ft] respectively.

The design and type of drilling bit used have a big impact on the drilling cost, where optimization of the drilling bit will lead to decreased drilling time due to increased rate of penetration, less trip time to change the bit since bit wear is reduced under optimization. The decision of what type bit to use along with its performance depend the type of formation that is going to be drilled, the models used to determine the optimal bit and the experience and prior performance of previous bits. Many design factors of the drilling bit will decide the bit's performance such as size, weight, type of the bit, either roller cone bit or fixed cutter bit, number of nozzles and their positioning, the material used for the cutters and the body of the bit and wear resistance. All of these will have an impact on how the bit will perform.

As well as the bit factors mentioned above, many drilling operational factors impact the performance of the bit. These can be the compressive strength of the rock formation, weight on the bit, RPM, hydraulics and the mud properties used [32].

3 THEORY

Modelling the ROP has been done and documented on several occasions by multiple authors. This is because of the impact of the rate of penetration on the drilling expenses and the need to optimize it. The exacts factors that affect the ROP are extremely complex and have partially been understood, with more research needed. Nevertheless, multiple researchers and academics have tried to model the ROP using factors such as the WOB, RPM and the strength of the formation rock. This is done through multiple experiments and using drill data from multiple wells. The usage of such models has been noted by many to reduce the drilling operation expenses. These models that were derived by multiple academics, what they can do to optimize the ROP and how they do it will be presented and discussed in the next chapters. [27, 30]

3.1 Bourgoyne and Young ROP model

Bourgoyne and young developed a simplified model in 1974 that can predict the ROP for roller cone bits using previously gathered drilling data. Since the model they used was linear, multiple regression method is used to determine the coefficients needed from the gathered data. This model has been the dominant method to estimate the ROP in the oil and gas industry [33]. The Bourgoyne and Young model estimates that the ROP is a function of 8 individual parameters that are multiplied with each other and that include a coefficient that is locally dependent [33]. The Bourgoyne and Young is a function of eight parameters and given as:

$$ROP = f_1 x f_2 x f_3 x f_4 x f_5 x f_6 x f_7 x f_8 \tag{3.1}$$

The parameters are: formation drill ability, formation strength and bit type, compaction on drilling penetration, overbalance on drilling rate, undercompaction found in abnormally pressured formations, weight on bit, rotary speed, tooth wear and the bit hydraulics. The model parameters are defined in the Appendix I. Due to the limitations of data to be used in the eight parameters, in this thesis work the model was not used for modelling of the field data.

3.2 Warren ROP model

In 1981, Warren devised a model to predict the rate of penetration (ROP) for soft-formation roller cone bits that would reflect their characteristics and would take into account the adequate cleaning of the borehole and the cuttings removal. The models presented at the time for soft-formation bits failed under certain circumstances, such as the one proposed by Galle and Woods which could not be applied without breaking its assumptions. The same goes for the "perfect cleaning" model published by Maurer, where it is not applicable for most soft-formation drilling scenarios. Another model presented by Cunningham failed to match experimental data [34].

Warren's model attempts to reflect on the shortcomings of the previous ones and to take into account what they did not. Due to the complexity and the number of factors that affect the penetration of the bit and its rate, the model that warren proposed is one that uses tests and data from research drilling rigs and takes into account the weight on bit (WOB), the rotary speed, hydraulic capacity and torque.

According to Warren, the model does not explain the drilling process but rather quantifies the parameters that affect it and can be changed during drilling operations [35].

3.2.1 Perfect-Cleaning Model

The perfect cleaning model developed by Warren in 1981 was a starting point for developing a model for imperfect cleaning. This model assumes steady-state drilling operations where the rate of the removal of the cuttings is equal to the rate at which new cuttings is being made. Thus, the rate of penetration (ROP) is determined by the cuttings generation process, the cuttings removal process or a combination of both and the cuttings removal does not affect the rate of penetration (ROP) [34]. The model is similar, but not identical, to a dimensionless model developed by Wardlaw which was modified to fit better with experimental data from laboratory tests. The resulting model was [35]:

$$ROP = \left(\frac{aS^2 d_b^3}{N^b WOB^2} + \frac{c}{N d_b}\right)^{-1} \tag{3.2}$$

Where a, b and c are dimensionless bit constants, S is the rock strength, d_b is the bit diameter, N is the bit rotary speed and WOB is the weight on bit.

The first term in the model, $aS^2 d^3_b/N^b WOB^2$, describes the maximum rate at which the formation rock is broken down into cuttings assuming that the WOB is assisted by a constant number of teeth on the bit, independent of the penetration depth of the tooth. The second term in the model, c/Nd_b, changes the modelled ROP to account for the distribution of the applied WOB to more teeth on the bit as the WOB is increased and the teeth penetrate deeper into the formation rock. It also serves as an upper limit for the modelled ROP for a constant rotary speed. At low values for the WOB, the ROP increases at an increasing rate when the WOB is increased. This continues until the ROP hits an inflection point and after that increases at a decreasing rate. This happens because the first term of the Eq. 3.2, $aS^2 d^3_b/N^b WOB^2$, is predominant for low ROP values, whereas the second term, c/Nd_b , is predominant for higher ROP values [35].

3.2.2 Imperfect-Cleaning Model

The perfect-cleaning model published by Warren was devised to predict the ROP without the presence of the complication cutting-removal effects. This was to be a start point to devise a more complex model that included these effects to reflect real world drilling conditions. Thereby, Warren published in 1987 his imperfect-cleaning model after modifying the previous perfect-cleaning model.

Unlike the perfect-cleaning model, this model does not assume steady-state drilling operations and the rate at which cuttings is being produced does not have to equal the rate at which they are removed. Warren used dimensional analysis to isolate a group of variables consisting of the modified impact force (F_{jm}) and the mud properties used during drilling. Warren incorporated these variables into the perfect-cleaning model to account for the cutting-removal until an equation that satisfied the experimental data was found. The results of this was the imperfect-cleaning model:

$$ROP = \left(\frac{aS^2 d_b^3}{NWOB^2} + \frac{b}{Nd_b} + \frac{cd_b \gamma_f \mu}{F_{jm}}\right)^{-1} \tag{3.3}$$

Where “a”,”b” and “c” are bit coefficients that are constant for the model, γ_f is the fluid specific gravity, μ is the plastic viscosity. The modified impact force is presented as:

$$F_{jm} = (1 - A_v^{-0.122})F_j \tag{3.4}$$

Where the theoretical measured impact force (F_j) and the ratio of jet velocity to return velocity (A_v) are presented as:

$$F_j = 0.000516\rho q v_n \tag{3.5}$$

$$A_v = \frac{v_n}{v_f} = \frac{0.15d_b^2}{3d_n^2} \tag{3.6}$$

Where q is the flow rate, ρ for the fluid density, v_n for the nozzle, v_f is the return fluid velocity and d_n is the nozzle diameter.

3.3 Modified Warren ROP model

The modelling of a complete ROP model that takes into account all the factors that affect the ROP is a demanding task, since we still do not have a complete understanding of these parameters. In the Warren model presented above, Warren did not include two important factors that affect the ROP. These are the "chip hold down effect" and the "bit wear effect". Thus, Hareland and Hoberock modified Warren's model in 1993 to include both effects [8, 36].

Chip hold down effect

The chip hold down effect has a significance impact on the ROP and Hareland and Hoberock addresses it and implanted it in the modified warren through data from laboratory full scale drilling experiments. During these tests, the bottomhole pressure was set as a variable while everything else was constant. The resultant equation that described chip hold down effect was:

$$f_c(P_e) = c_c + a_c(P_e - 120)^{b_c} \tag{3.7}$$

Where P_e is the differential pressure, (a_c, b_c and c_c) are the lithology dependent constants and $f_c(P_e)$ is the "chip hold down function". The coefficients where made so that the chip hold down function would be dimensionless [8]. Eq. 3.3 can thus be modified to include the chip hold down function as follows:

$$ROP = \left[f_c(P_e)\left(\frac{aS^2d_b^3}{NWOB^2} + \frac{b}{Nd_b}\right) + \frac{cd_b\gamma_f\mu}{F_{jm}}\right]^{-1} \tag{3.8}$$

Bit wear effect

Bit wear has a significant effect on the performance of the drilling bit during operations. The higher the bit wear the lower the ROP. This effect was not addressed in the original Warren Model and thus Hareland and Hoberock included it in the modifield Warren model. They did this by introducing a bit wear function W_f into the model. The model thus becomes:

$$ROP = W_f\left[f_c(P_e)\left(\frac{aS^2d_b^3}{NWOB^2} + \frac{b}{Nd_b}\right) + \frac{cd_b\gamma_f\mu}{F_{jm}}\right]^{-1} \tag{3.9}$$

$$W_f = 1 - \frac{\Delta BG}{8} \tag{3.10}$$

Where ΔBG is the change in the bit tooth wear which is a function of WOB, ROP, Confined rock strength and relative rock abrasiveness. ΔBG is given as:

$$\Delta BG = \sum_{i=1}^{n} WOB_i . RPM_i . Ar_{abr_i} . S_i \tag{3.11}$$

$$S_i = S_0(1 + a_s P_e^{b_s}) \tag{3.12}$$

Where S_i and S_0 are unconfined and confined rock strength respectively and (a_s and b_s) are coefficients that depend on the formation permeability

3.4 Mechanical Specific Energy vs ROP

As mentioned before, R. Teale described the drilling process as one that mechanically crushes and breaks the formation rock using a bit rather than one that cuts the formation rock. Therefore, the relationship between the "specific energy" used to crush the rock and the volume it excavates is of importance. Teale described the amount of energy needed to excavate one volume of formation rock as the MSE [37]. This can also be described as a relationship between the input energy and the ROP

$$MSE \approx \frac{Input\ Energy}{Output\ ROP} \tag{3.13}$$

In rotatory drilling, the energy the system uses is represented by a number of factors. According to Teale's MSE, these are the thrust, the torque, the rotational speed, the area of the hole being drilled, and the penetration rate (F, T, N, A and u respectively). The work done in one minute can be described by the term ($Fu + 2\pi NT$) and the volume of formation rock crushed in one minute is (Au). Using these two terms, the specific energy can be translated in equation 3.13:

$$e = \left(\frac{F}{A}\right) + \left(\frac{2\pi}{A}\right)\left(\frac{NT}{u}\right) \tag{3.14}$$

$$e_t = \left(\frac{F}{A}\right) \tag{3.15}$$

$$e_r = \left(\frac{2\pi}{A}\right)\left(\frac{NT}{u}\right) \tag{3.16}$$

The e_t term describes the thrust component of the specific energy and is equivalent to the mean pressure done by the thrust on the cross-sectional area of the bottomhole. The e_r term describes the rotary component of the specific energy. Thus, Eq. 3.14 can be translated into:

$$MSE = \frac{480 * T * N}{{d_b}^2 * ROP} + \frac{4 * WOB}{{d_b}^2 * \pi} \tag{3.17}$$

Theoretical perfect efficiency would indicate that the MSE is equal to the rock compressive strength. However, drilling bits are around 30-40% efficient at best performance, as seen in Figure 13. Due to this, the MSE value needs to be around three times the compressive strength of the rock and a new term representing the mechanical efficiency (EFF_M) is introduced [38], adjusting equation 2.15 to

$$MSE_{adj} = EFF_M * MSE \tag{3.18}$$

$$MSE_{adj} = EFF_M * \left(\frac{480 * T * N}{{d_b}^2 * ROP} + \frac{4 * WOB}{{d_b}^2 * \pi}\right) \tag{3.19}$$

Figure 13. Mechanical efficiency vs. the depth of cut. Bits are between 30-40% efficient.

Eq. 3.19 includes torque (T) as a variable for the MSE. However, during drilling operations, the majority of field data that is produced are in the form of WOB, N and ROP. Thereby, R.C. Pessier and M.J. Fear introduced in 1992 the bit coefficient of sliding friction (μ) as a means to represent torque as a function of WOB and the bit diameter [39]. This relationship, the new MSE term and the ROP that can be extracted are represented below:

$$T = \mu * \frac{d_b * WOB}{36} \tag{3.20}$$

$$MSE_{adj} = EFF_M * WOB * \left(\frac{13.33 * \mu * N}{d_b * ROP} + \frac{4}{{d_b}^2 * \pi}\right) \tag{3.21}$$

$$ROP = \frac{13.33 * \mu * N}{d_b * \left(\frac{MSE_{adj}}{EFF_M * WOB} - \frac{4}{{d_b}^2 * \pi}\right)} \tag{3.22}$$

3.5 D-Exponent vs ROP

Formation pressure is of major importance during drilling operations and locating overpressured formations is knowledge drillers need to consider in order to optimize the ROP and prevent any incidents from occurring. Laboratory experiments have shown that the differential pressure, i.e. the difference in pressure between the mud column and the formation pressure, have a relationship with the ROP, where the higher the mud column the lower the ROP. However, the research also showed that no relationship was found between the overburden pressure and the ROP [40]. The detection of the differential pressure through drilling data is a goal that helps in quick detection of overpressured formations and allows for quick reactions to such cases. However, the complexity of the drilling bottomhole environment and the multiple factors that affect the ROP has presented to a difficulty in achieving such a goal. Normalizing the ROP proved to be a method to negate this hurdle. This was referred to as the d-exponent. [40, 41]

The D-exponent was devised by Bingham in 1964 as a means to detect overpressued formations from drilling and data and the model that was developed is as follows [42]:

$$ROP = A_M N^E \left(\frac{WOB}{d_b}\right)^{d_{exp}} \tag{3.23}$$

Where "E" is the rotary speed exponent, "A_M" is the rock matrix strength constant. This model holds true for variations in the factors that it includes if all other factors remain constant and some ideal constants are held. In 1966, Jorden and Shirley simplified the

model presented by Bingham using the assumptions that ($A_M = 1$) and that ($E = 1$). Using these and rearranging the model, gives the d-exponent as:

$$d_{exp} = \frac{log\left(\frac{ROP}{60N}\right)}{log\left(\frac{120WOB}{10^6 d_b}\right)} \tag{3.24}$$

For the calculation of the d-exponent, it is desirable to keep the mud density functions constant, so the resulting d-exponent only reflects the formation pressure and the differential pressure. This was done by Rehm And McClendon in 1971 by using an empirical basis. This gives the following expression [43]:

$$d_c = d_{exp}\left(\frac{NMW}{ECD}\right) \tag{3.25}$$

Where "d_c" is the corrected d-exponent, "NMW" is the normal mud weight of the area and "ECD" is the equivalent circulating density.

3.6 Drag Bit Model

The models presented before, have mostly been to the application of roller cone bits and with the ever-increasing usage of drag bits in drilling operations, a new model was required. In 1994, Hareland and Rampersad developed an ROP model for drag bits such as Natural diamond bits, PDC bits or any Geoset bit. The model assumes conservation of mass where the ROP is equivalent to the rate of cuttings removal. The model takes into consideration the bit geometry, cutter geometry, bit wear and UCS. Further elaboration on the model is included in Appendix I [44].

3.8 Maurer Model

In 1962, Maurer developed his "perfect-cleaning theory" of rotary drilling for predicting the ROP when using roller con bits. This model assumes perfect cleaning during drilling, i.e., condition where all the drilling cuttings are removed between tooth impacts. The model developed my Maurer is based on two observations [45]:

- The crater volume (V_c) is proportional to the square of the depth of penetration (X) for craters made by wedge-shaped chisels: $V_c \propto X^2$
- The depth of penetration (X) is inversely proportional to the drillability strength of the rock (S) if constant force is applied on the tooth: $X \propto 1/S$

The model will be further elaborated in Appendix I.

3.7 Bingham Model

In 1965, Bingham developed a simplistic model to estimate the value of ROP. This model is a simplistic modified version of the model developed by Maurer. This model is applicable for low values of WOB and N. It neglects the drilling depth and thus has low real-world reliability [46]. Further explanation of the model will be found in Appendix I

4 ORMEN LANGE FIELD DATA MODELLING AND WORKFLOW

The modelling in this thesis is done through multiple databases in order to find a relationship between the ROP and the various factors that affect it while drilling. In order to do so, access to large databases of recorded values of the ROP and the factors that affect it is required.

The Norwegian Petroleum Directorate (NPD) has drilling reports for the vast majority of the wells drilled on the Norwegian continental shelf (NCS) and records all the ROP data in them. Having access to such data from a well and a model for ROP, helps predicting the ROP for a new well.

This thesis revolves around modelling ROP and testing the models on nearby wells to validate and improve the model. The modelled ROP will be compared to the filtered one for these wells and the model will be evaluated. The ROP modelling will be done with regression of the datasets and will be tested against well-established methods such as the MSE, warren and the d-exponent. Worth mentioning is that Morten Adamsen Husvæg and Malik Alsenwar previously used similar modelling methods.

4.1 Ormen Lange field description

Drilling data represented in drilling logs and mud reports that where enquired from the NPD were exported to a spreadsheet in Excel where it was filtered before being modelled.

The field of application in this thesis is the Ormen Lange field, located in block 6305 and around 120 Km northwest off Kristiansund. The field is a natural gas field with water depths ranging from around 800 m to 1100 m. The field was discovered in 1997 and started producing natural gas in 2007 and is still producing until today with a declining productivity from the well due to reduction in reservoir pressure [47]. The location of the field and the wells can be observed in Figures 14 and 15, respectively. The ROP model

coefficients are derived from data from wells 6305/7-D-1 H, 6305/7-D-2 H and 6305/7-D-3 H. Each of the three models is tested by modelling the ROP of the other two wells.

The more the model is tested, the more valid and robust it becomes. The modelling method using linear regression, the warren model, MSE model and the d-exponent will be further discussed in this chapter.

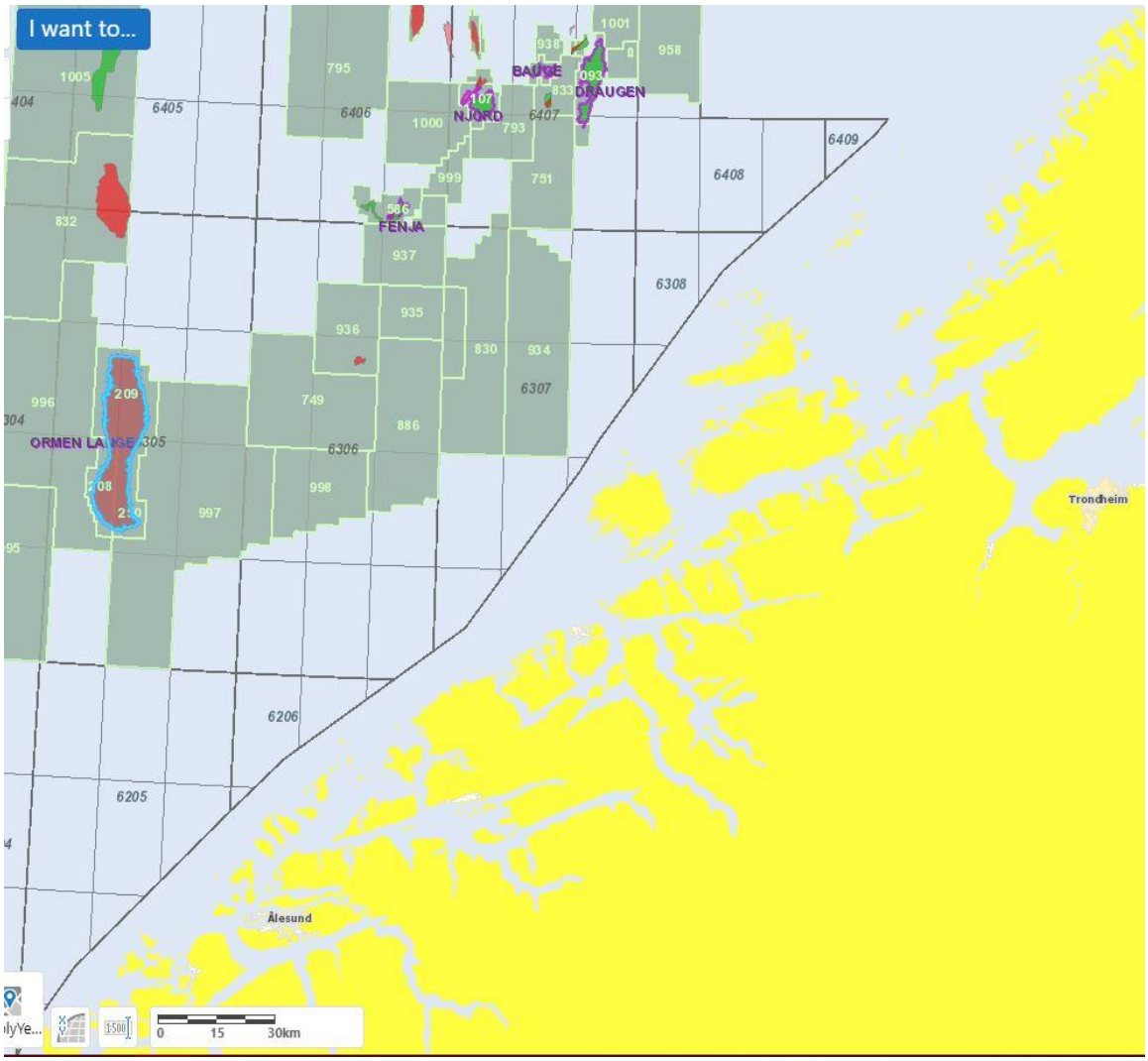

Figure 14. Location of the Ormen Lange field on the NCS [48].

Figure 15. Location of the three wells used in the modelling in block 6305/7 [48].

4.2 Drilling data filtration

Filtering was done to refine the ROP and its parameters and to remove any outliers and counter any noise present in the data creating a more solid representative model. More details about the filtering method will be discussed later in the chapter.

4.2.1 Moving Average Filter

The moving average filter is one of the simplest yet most effective low pass filters in Digital signal processing (DSP). Despite being one of the simplest filters, the moving average filter is optimal for reducing any noise present in a signal while retaining any sharp step response. The moving average filter takes the average of a number of points from the input signal to calculate one point of the output signal, this is seen in equation 4.1 [49]:

$$y\,[i] = \frac{1}{M}\sum_{i=0}^{M-1} x\,[i+j] \tag{4.1}$$

Where "$y\,[i]$" is the outcome signal of the filter, "M" is the number of points in the moving average filter. The smoothening of the signal or data is dependent on the value of "M" where the larger the number of points we average, the smoother the signal or data gets. However, a too high value of "M" will cause the signal to lose the sharpness at the edges. All of this can be seen in Figure 16 below [50].

In this thesis, moving average filter was used on both the drilling parameters and the actual ROP prior to regression. This was done to smooth down, reduce the noise and eliminate any offsets in the data provided because linear regression provides better models when the noise and offsets are removed. Thus, for ROP, Eq. 4.1 becomes:

$$ROP_{filt}\,[i] = \frac{1}{M}\sum_{i=0}^{M-1} ROP\,[i+j] \tag{4.2}$$

Where ROP_{filt} is the filtered value of the ROP. The same is done for all the parameters that are being used for the modelling. This is done in Microsoft Excel. Figure 16 shows an example of moving average calculated for window =5. Application of this filtering method is shown in Appendix II.

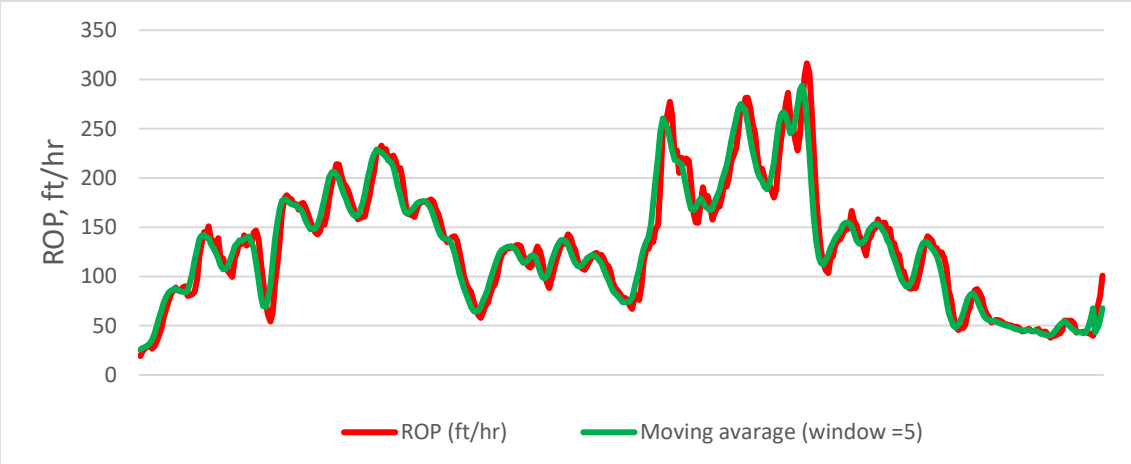

Figure 16. Example of moving average.

4.2.2 Exponential Smoothing

An exponential smoothing technique was also employed to filter drilling data. The principle of forecasting is based on using weighted averages where the weights exponentially decrease. It can also be written as [51]:

$$S_t = \alpha * y_{t-1} + (1-\alpha)S_{t-1} \tag{4.3}$$

α is the smoothing parameter and is between 0 and 1.

Here the two weighted moving average with two weights: α and 1−α. The previous expected $\hat{y}_{t-1}$ value is multiplied by 1−α and makes the expression recursive.

The forecast at time t+1 is equal to a weighted average between the most recent observation y_t and the most recent forecast $\hat{y}_{t|t-1}$.

Figure 17 shows an example of exponential smoothing applied on the field measured ROP data. The examples displayed are for smoothing parameters (alpha = 0.9 and alpha = 0.75). As shown, the smoothing parameter alfa =0.9 reduced the spikes as compared with the alfa =0.75.

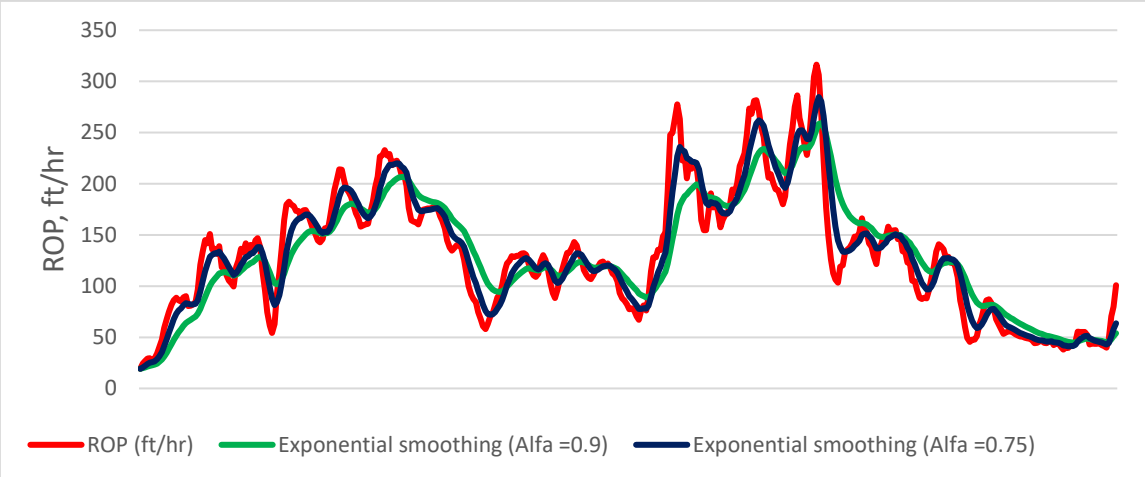

Figure 17. Example of exponential smoothing for alfa = 0.9 and 0.75.

4.3 ROP modelling techniques

4.3.1 Multiple Linear Regression

The modelling of the ROP consists of more than one independent variable, due to this, multiple linear regression is used with the assumptions that the factors share a linear relationship with the ROP. Regression is a method to find a quantitative relationship between an outcome and multiple independent variables or regressors, while taking into account any independent or simultaneous change in the variables. This modelling does not care nor know of the underlying physics and mechanics behind the values introduced and attempts to best fit the regressors using coefficients to result in the outcome. Thus, the model from the regression will be more of a quantitative analysis of the variables that uses logical reasoning than a logical model. The equation that represents such modelling is given by: [52]

$$y = \beta_0 + \beta_1 X_1 + \beta_2 X_2 + \beta_3 X_3 + \cdots + \beta_n X_n \tag{4.4}$$

Where “y” is the dependent outcome, "β_{0-n}" are the regression coefficients, “β_0” is the intercept and “X_{1-n}” are the regressors.

Prior to the modelling workflow, filtering of the data was applied, and the model uses the filtered RPM, torque, WOB, formation pressure, mud weight, the flowrate and the UCS

as the regressors with the observed and filtered ROP as the outcome of the model. The UCS for the various depths is not presented in the drilling reports and is calculated from the MSE. This is more explained in chapter 3.4.

After the modelling is completed and coefficients are determined, the model will be tested on other wells using the filtered data of that well. Throughout the thesis, the filtering must be consistent and done in a manner that all the data are filtered using the same number of points in the moving average filter as illustrated in section 4.2.1.

Thus, the ROP is the "y" in Eq. 4.4 and all the other parameters are represented in the different "X" values. Thus, Eq. 4.4 can be written as:

$$ROP = \beta_0 + \beta_1 WOB + \beta_2 Torque + \beta_3 RPM + \beta_4 Flow\,rate + \beta_5 FP + \beta_6 MW + \beta_7 UCS \quad (4.5)$$

Well deviation is not considered as part of the variables in this modelling. This can be a major parameter that affects the ROP due to the changing formation strength when changing from vertical to deviated. The wells used from the field are correlated for the same geological sections and are modelled accordantly. The coefficients from the regression are applied on the same geological sections of the wells. The data from wells 6305/7-D-1 H, 6305/7-D-2 H and 6305/7-D-3 H are filtered in Excel and after that, modelled using the data analysis package. A workflow representation can be seen in Figure 18. More details on the Excel workflow will be presented in Appendix II.

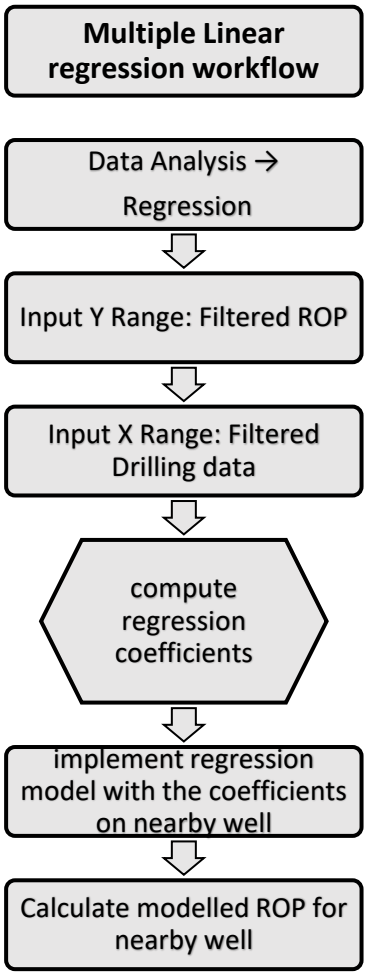

Figure 18. Multiple linear regression workflow [21].

4.3.2 D-exponent

The drillability exponent, d-exponent, is a normalized value that represents the drillability of a formation using drill data such as the WOB, ROP, RPM and the bit diameter; as shown in Eq. 3.24. This equation was further corrected by Rehm et. Al to include the effect of the ECD while drilling. This is established in Eq. 3.25. In the thesis, the d-exponents from the reference well are used for modelling the ROP for the close-by wells. Due to lacking data on the ECD, the corrected d-exponent cannot be used for modelling and thus Eq. 3.25 is not used. The values of the d-exponent for one well are computed using Eq. 3.24. These values are then implemented in Eq. 4.6, which is a modified version of Eq. 3.24 that gives ROP as an output. The workflow for this application is represented in Figure 19.

$$\text{Eq. 3.24} \rightarrow log\left(\frac{ROP}{60N}\right) = d * \log\left(\frac{12WOB}{10^6 d_b}\right)$$

$$\rightarrow \log ROP = d * log\left(\frac{12WOB}{1000 d_B}\right) + \log(60N) \tag{4.6}$$

$$\rightarrow \quad ROP = 10^{d*\log\left(\frac{12WOB}{10^6 d_b}\right)+\log(60N)}$$

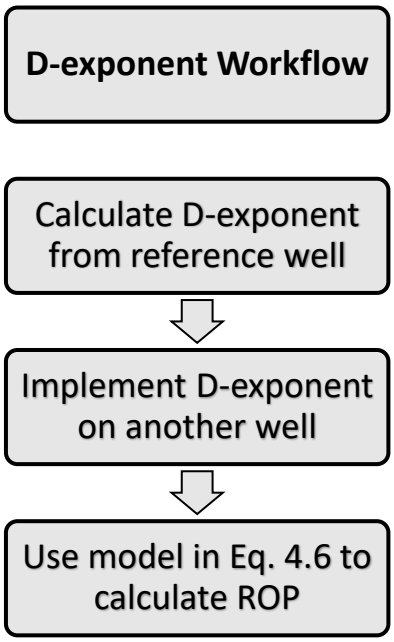

Figure 19. D-exponent Workflow.

4.3.3 MSE – Mechanical Specific Energy

The MSE describes the energy needed to excavate one volume of the formation rock. This model was developed by Teale and has been used as a method to estimate the formation strength in the oil and gas industry. MSE is used in this thesis work to model the ROP. This is done by calculating the MSE values using data from the reference well and Eq. 3.17. These values are then implemented into Eq. 4.7 to compute the ROP values for a different well. This assumes that the MSE value for same depth is correlative between the different wells. The Workflow of such a procedure is shown in Figure 20.

$$\text{Eq. 3.17} \rightarrow MSE * 1000\, {d_b}^2 = \frac{4\, WOB}{\pi} + \frac{480\, RPM\, T}{ROP}$$

$$\rightarrow \quad \frac{480\, RPM\, T}{ROP} = MSE\, 1000\, {d_b}^2 - \frac{4\, WOB}{\pi}$$

$$\rightarrow \quad \frac{1}{ROP} = \frac{MSE\, 1000\, {d_b}^2 - \frac{4\, WOB}{\pi}}{480\, RPM\, T} \tag{4.7}$$

$$\rightarrow \quad ROP = \left[\frac{MSE\, 1000\, {d_b}^2 - \frac{4\, WOB}{\pi}}{480\, RPM\, T}\right]^{-1}$$

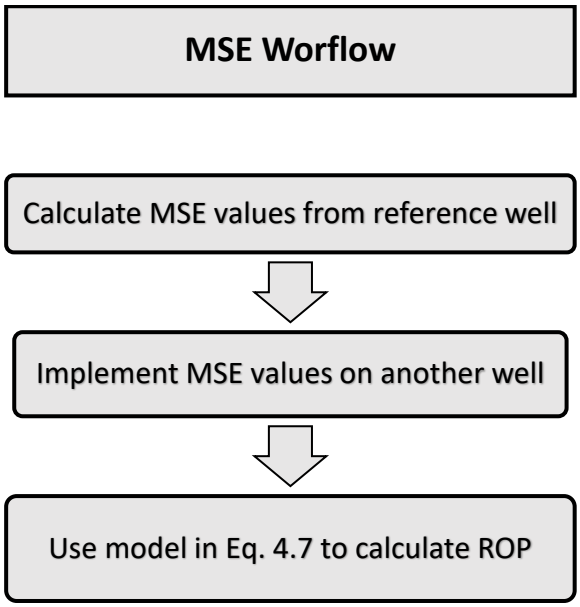

Figure 20. MSE Workflow

4.3.4 Warren Model

The Warren model presented in 1981 for roller cone soft formation bits aims at relating the ROP to multiple drilling parameters such as the WOB, d_b, the modified impact force (F_{jm}), formation strength, N, fluid specific gravity (γ_f) and the plastic viscosity (μ). This model was established through laboratory testing using real life drilling data. The Warren model was established first as the "perfect-cleaning" model that assumes perfect cleaning under the drilling bit and equal return of the drilling fluid and the "imperfect-cleaning" model which is a modified version of the prior one that does not consider perfect cleaning.

In order to calculate the ROP using this model, data for these parameters needs to be available. Unfortunately, rock strength is not provided in the drilling reports. In order to tackle that, Teale's definition of the MSE is used to estimate the rock strength. Teale assumes that the MSE is equal to the UCS of the rock. Thus, the value of the rock strength can be replaced by the MSE.

The "imperfect-cleaning" model will be used to model ROP for the selected fields. This will be done by expressing Eq. 3.3 as follows:

$$ROP = \left(\frac{aS^2d_b^3}{NWOB^2} + \frac{b}{Nd_b} + \frac{cd_b\gamma_f\mu}{F_{jm}}\right)^{-1}$$

$$\rightarrow \frac{1}{ROP} = \frac{aS^2d_b^3}{NWOB^2} + \frac{b}{Nd_b} + \frac{cd_b\gamma_f\mu}{F_{jm}} \tag{4.8}$$

$$\rightarrow a\left(\frac{S^2d_b^3ROP}{NWOB^2}\right) + b\left(\frac{ROP}{Nd_b}\right) + c\left(\frac{d_b\gamma_f\mu ROP}{F_{jm}}\right) = 1$$

The terms $\left(\frac{S^2d_b^3ROP}{NWOB^2}\right)$, $\left(\frac{ROP}{Nd_b}\right)$ and $\left(\frac{d_b\gamma_f\mu ROP}{F_{jm}}\right)$ are calculated for all the datapoints in the Microsoft Excel sheet for the reference well . Eq. 4.8 can be expressed as a matrix in the form of:

$$\begin{bmatrix} x_1 & y_1 & z_1 \\ \vdots & \vdots & \vdots \\ x_n & y_n & z_n \end{bmatrix} \begin{bmatrix} a \\ b \\ c \end{bmatrix} = \begin{bmatrix} 1 \\ \vdots \\ 1 \end{bmatrix} \tag{4.9}$$

Where x, y and z are the three terms in Eq. 4.8 respectively. The matrix is then solved in Matlab to calculate the values of "a"," b" and "c". These values are then applied to Eq. 3.3. A representation of the workflow is shown in Figure 21 and the detailed work will be further discussed in Appendix II.

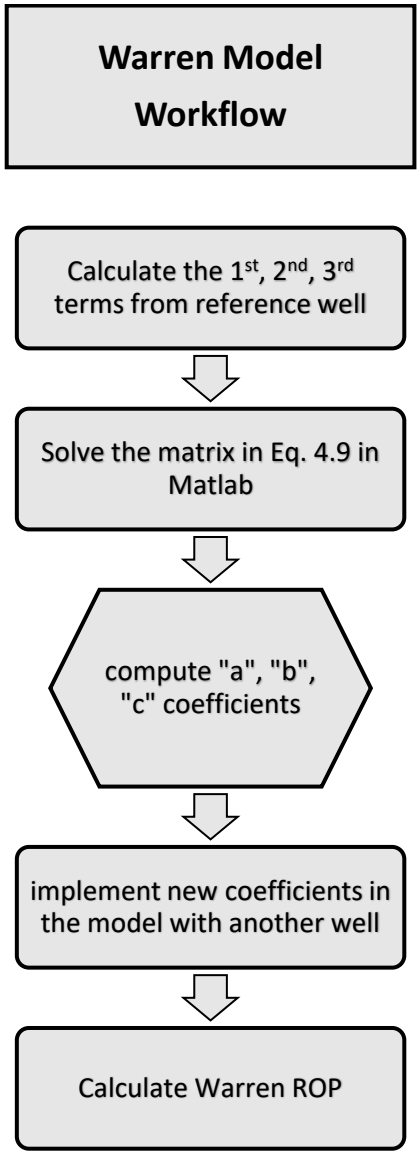

Figure 21. Warren Model Workflow

5 RESULTS

This chapter will present the results of the ROP modelling techniques shown in chapter 4. Previous work by Malik and Morten has shown that ROP modelling for far away fields yields poor results. Thus, the main focus in this thesis work is to improve the reliability and accuracy of the ROP modelling in nearby wells in the same field. This will result in better predictions of the ROP when drilling a well close to an already drilled one and having the drilling results of the old one.

The results of the modelling are presented in graphs that show both the actual filtered ROP and the modelled ROP in ft/hr. In the graphs, the blue line always represents the actual filtered ROP for the well, while the orange line indicates the modelled ROP using the technique being discussed. The x-axis for the graphs will represent the true depth of the fields in ft.

The field that is chosen for this thesis is the Ormen Lange field, using wells 6305/7-D-1 H, 6305/7-D-2 H and 6305/7-D-3 H. All the techniques previously mentioned will be applied to all 3 wells and the results for each well be tested on the other two. By using multiple wells in the same field and multiple techniques, the validity of the modelling techniques will be verified and assured.

The modelling in the thesis, will be done using two techniques:

- Modelling using data from the whole well
- Modelling using data from the different geological groups in the well

This is done to test the old method of modelling the whole well and applying it on nearby wells and compare it to a new approach.

5.1 Multiple Regression

This modelling technique was presented in chapter 4.3.1 and the workflow used for the achieving the results was presented in Figure 18. Both modelling techniques will be used to calculate the ROP

5.1.1 Total Well Data Modelling

This subchapter will present the modelling of the wells using data from the whole well. The modelling will be done first on the wells using the coefficients extracted from them, then on the other two near-by wells. The resultant coefficients of the modelling from the three wells is presented in tables 2, 3 and 4.

Table 2. Regression coefficients from well 6305/7-D-1 H.

6305/7-D-1 H	*Coefficients*
Intercept	-256,095
X Variable 1	-0,00102
X Variable 2	0,013662
X Variable 3	-0,20776
X Variable 4	0,095136
X Variable 5	25,2423
X Variable 6	3,951088
X Variable 7	-2,41145

Table 3. Regression coefficients from well 6305/7-D-2 H.

6305/7-D-2 H	*Coefficients*
Intercept	233,6515
X Variable 1	-7,1E-05
X Variable 2	0,004147
X Variable 3	0,848821
X Variable 4	0,019269
X Variable 5	-16,8295
X Variable 6	-68,5821
X Variable 7	-0,75308

Table 4. Regression coefficients from well 6305/7-D-3 H.

6305/7-D-3 H	*Coefficients*
Intercept	354,93
X Variable 1	0,001585
X Variable 2	-0,00073
X Variable 3	1,232096
X Variable 4	-0,35803
X Variable 5	-14,1769
X Variable 6	186,4217
X Variable 7	-2,22376

Testing the models on the fields they were derived from

The multiple regression model using the coefficients in the tables 2, 3 and 4 is tested on wells 6305/7-D-1 H, 6305/7-D-2 H and 6305/7-D-3 H. The resultant ROP is presented in Figures 22, 23 and 24 respectively.

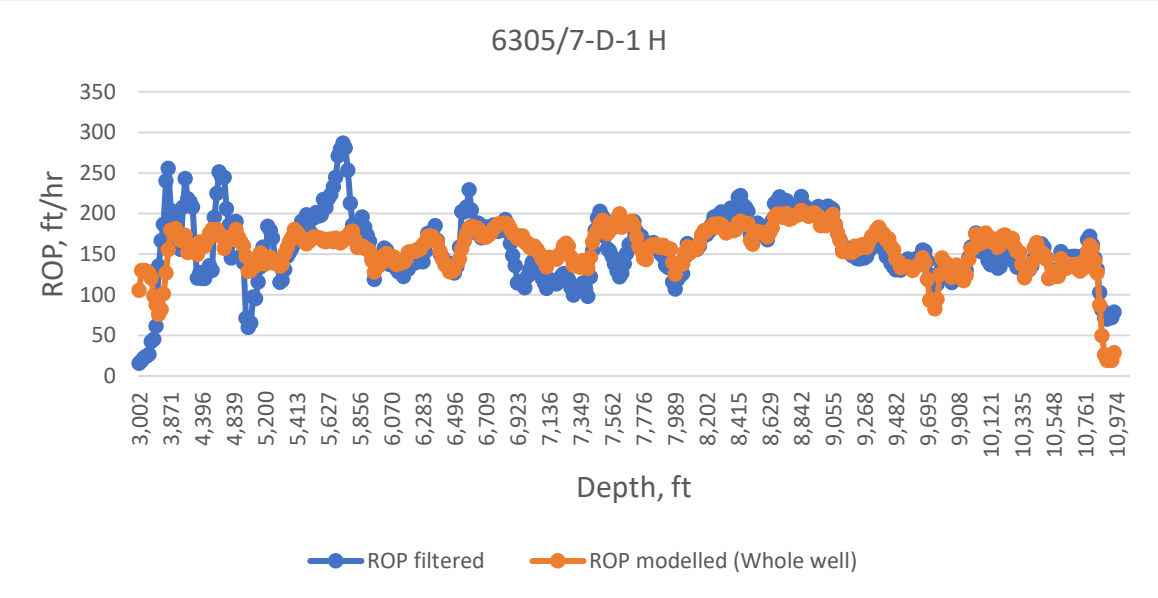

Figure 22. Multiple regression using whole field data from 6305/7-D-1 H on itself.

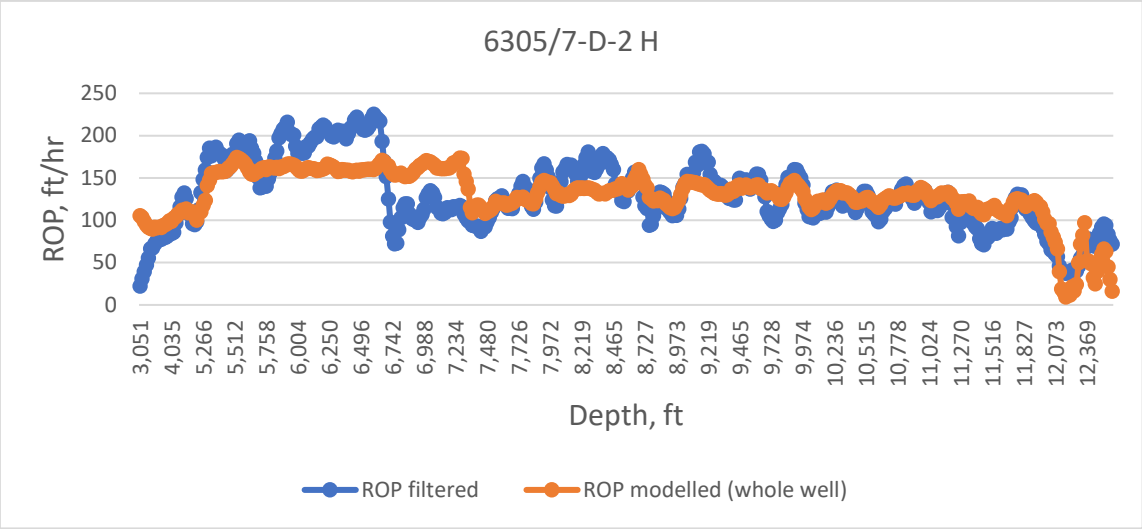

Figure 23. Multiple regression using whole field data from 6305/7-D-2 H on itself.

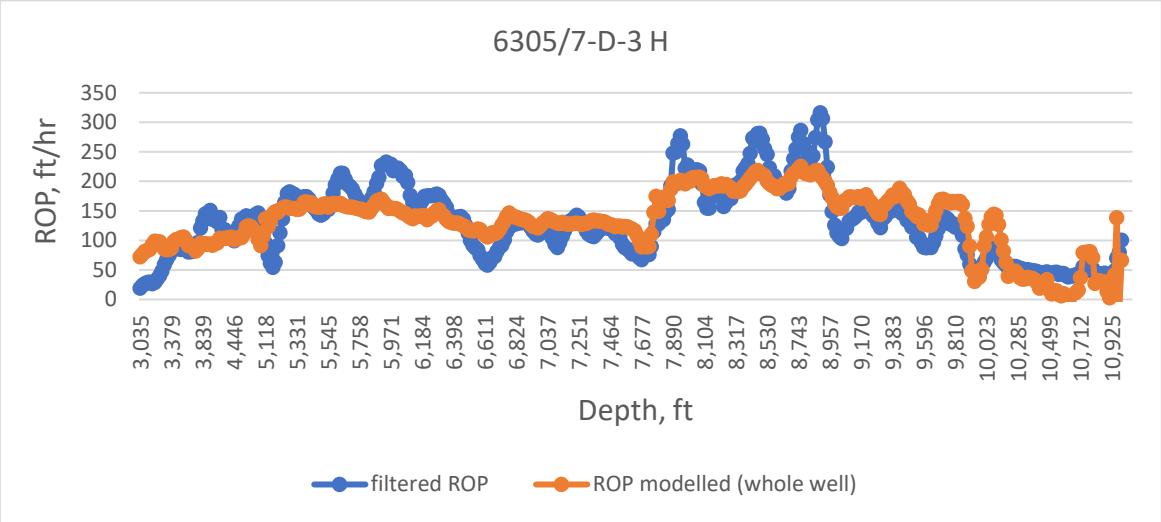

Figure 24. Multiple regression using whole field data from 6305/7-D-3 H on itself.

There is good correlation overall when testing the model on the wells, this was done to indicate that the model was good and to go further into the modelling section later. The model showed good results in the lower sections of the wells towards the Rogaland group, as well as the middle sections, where the Hordaland group is present. Wells 6305/7-D-1 H and 6305/7-D-2 H showed some deviation at depths 5331 ft to 5881 ft and 5600 ft to 6200 ft. This is most likely due to geological properties at those depths.

Testing the model with coefficients from well 6305/7-D-1 H

The coefficients derived from well 6305/7-D-1 H presented in table 2 are used in the multiple regression model to predict the ROP for wells 6305/7-D-2 H and 6305/7-D-3 H. The results are shown in Figures 25 and 26 respectively.

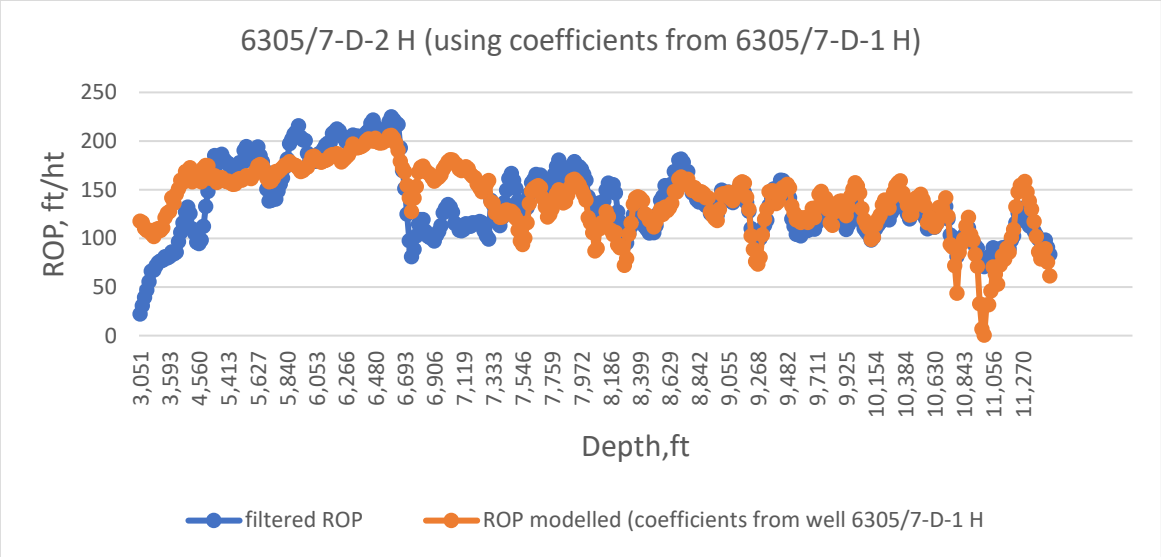

Figure 25. Multiple regression using whole field data from 6305/7-D-1 H on 6305/7-D-2 H.

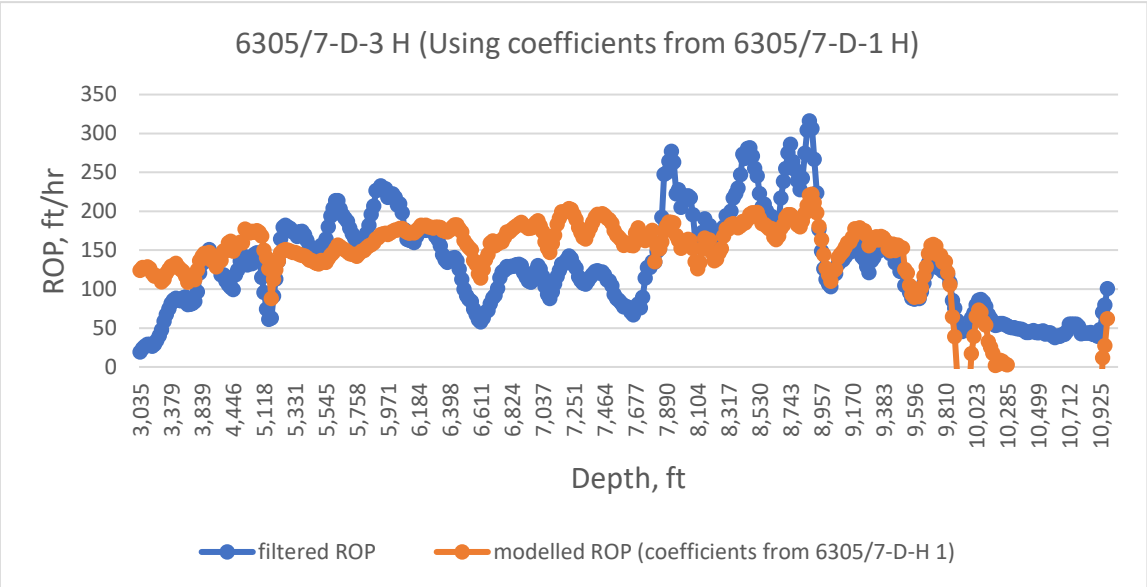

Figure 26. Multiple regression using whole field data from 6305/7-D-1 H on 6305/7-D-3 H.

The modelled ROP values from well 6305/7-D-2 H in Figure 25 show good correlation with the filtered ROP values from well 6305/7-D-1 H. This is an indication of similarities in the geological environment of the two wells. Using well coefficients from well 6305/7-D-3 H to model the ROP gave worse correlation that that of well 6305/7-D-2 H, where it showed correlation with the filtered ROP for most of the well except that the amplitudes where lower towards the start and higher during the middle of the well. However, towards the end of the field, after 9800 ft, the correlation fell off.

Testing the model with coefficients from 6305/7-D-H 2

The coefficients from well 6305/7-D-H 2 presented in table 3 are applied in the model to model the ROP for wells 6305/7-D-H 1 and 6305/7-D-H 3. The results of this is presented in Figures 27 and 28.

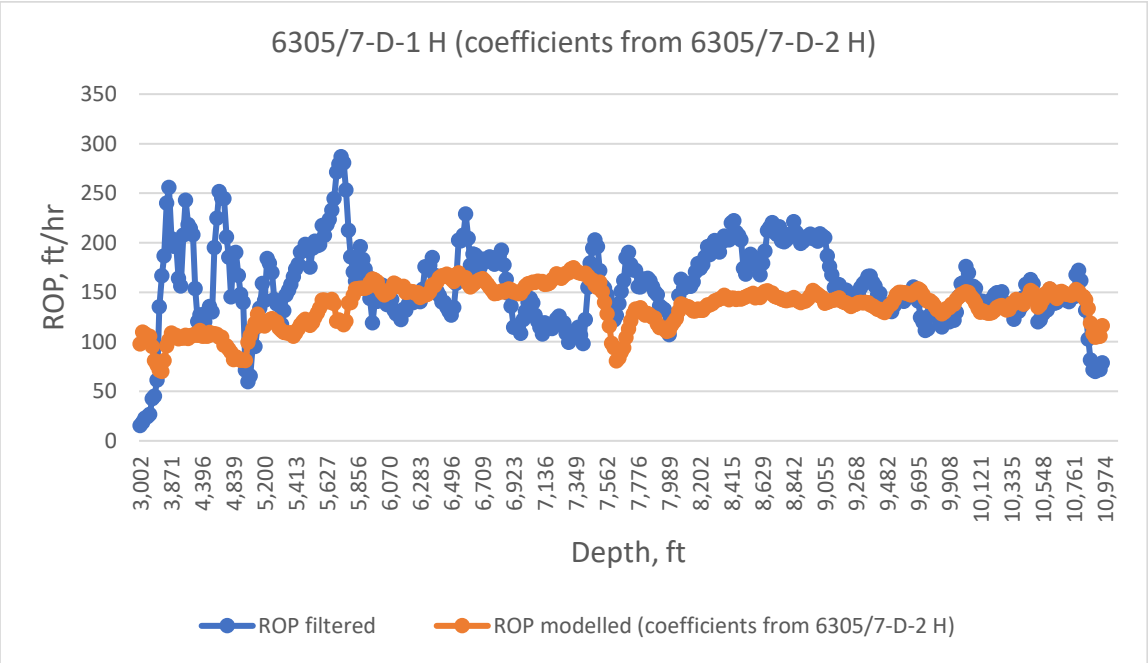

Figure 27. Multiple regression using whole field data from 6305/7-D-2 H on 6305/7-D-1 H.

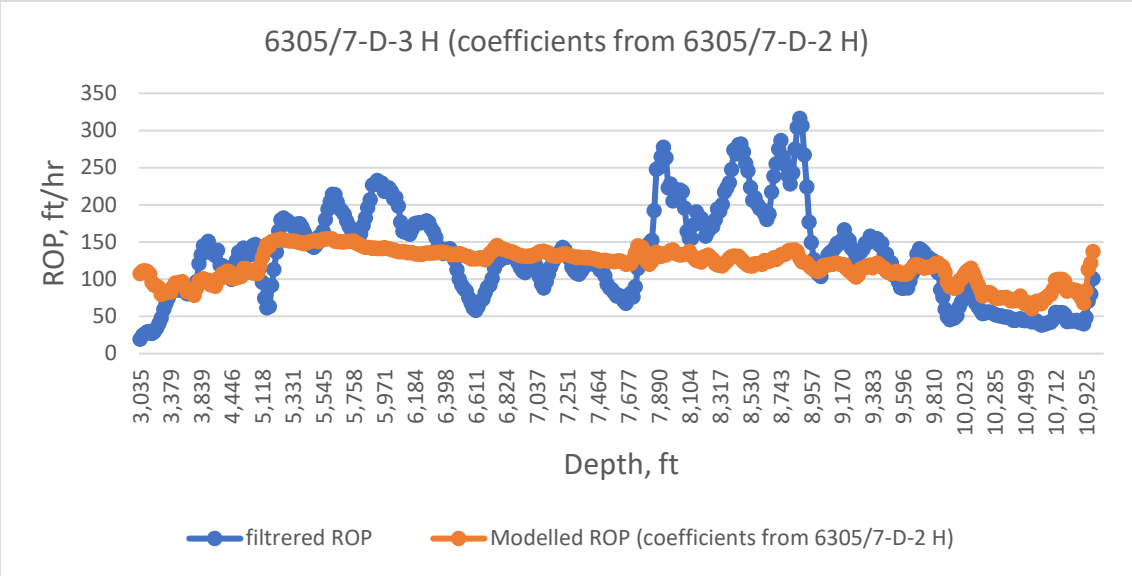

Figure 28. Multiple regression using whole field data from 6305/7-D-2 H on 6305/7-D-3 H.

Using well 6305/7-D-1 H to model the ROP of 6305/7-D-1 H gave fairly good results, especially towards the end. The filtered ROP is seen to have a lot of bouncing up and down of the values which can be most likely attributed to bit bouncing. The results became excellent towards the Rogaland formation at the end of the field. The model applied on well 6305/7-D-3 H gave good correlation towards the start of the field in the Nordland group and towards the end in the Rogaland group. However, the model overestimated the ROP in the interval (6430 ft to 7700 ft) and underestimated the ROP in the intervals (5200 ft to 6300 ft) and (7800 ft to 8960 ft). This is most likely due to geological differences between the wells at those depths and the inclination of the well at those depths.

Testing the model with coefficients from 6305/7-D-3 H

The model is lastly tested on wells 6305/7-D-1 H and 6305/7-D-2 H using the coefficients from well 6305/7-D-3 H located in table 3. The results of this modelling are presented in Figures 29 and 30.

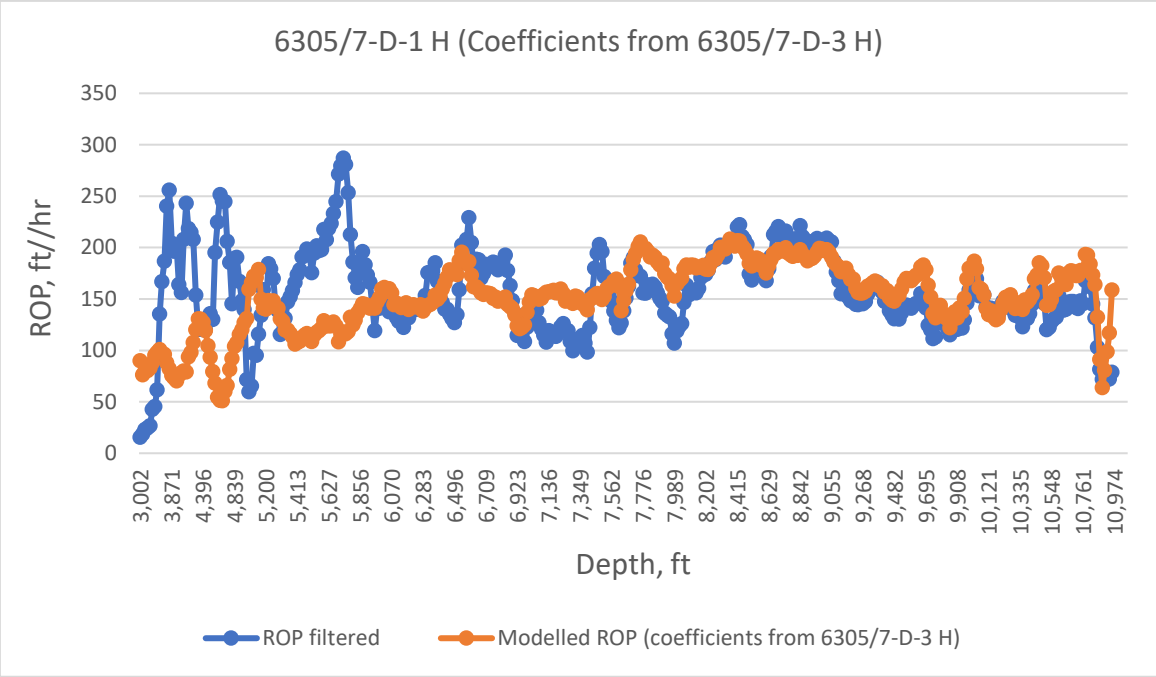

Figure 29. Multiple regression using whole field data from 6305/7-D-3 H on 6305/7-D-1 H.

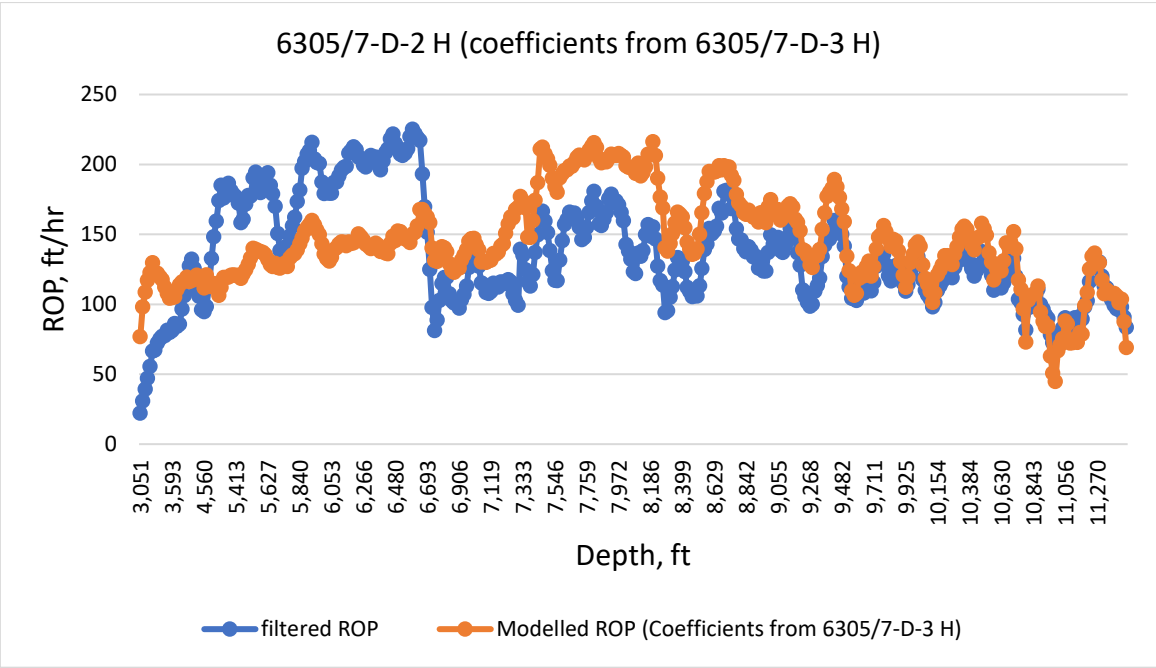

Figure 30. Multiple regression using whole field data from 6305/7-D-3 H on 6305/7-D-2 H.

The ROP model using the coefficients from well 6305/7-D-3 H proved to give good correlation with the filtered ROP of the other two wells. Well 6305/7-D-1 H showed poor

correlation with the modelled ROP values at the start, being shifted to the left until 5250 ft and started giving good correlation after 8000 ft towards the Rogaland formation. This can be due to a difference in the depth of the geological formations between the two wells at the measured depth. Well 6305/7-D-2 H gave underestimated values of the ROP from the start until 6700 ft and overestimated values from then until 9400 ft. This was then followed by excellent correlation with the filtered ROP values. It is worth mentioning that, though the values where higher or lower than the filtered ROP, the shape of the lines was very similar between the modelled ROP and the filtered one.

5.1.2 Geological Well data modelling

Using the drilling reports for the wells being modelled. The depth interval of the multiple geological groups was established and each of the groups was modelled using the drilling data for those depths. The main focus of this thesis will be the Nordland, Hordaland and Rogaland groups that three wells share. The coefficients for the model of a group was then taken to another well, to be modelled on the depth interval of the same geological group and not the same depth interval. The results of the multiple models at the different depths are then set together and compared to the filtered ROP of the well. This was done to minimize any effect of the geological environment on the modelling. The following subchapter will present and discuss the results of this technique; first presenting the result of the modelling on the wells the coefficients were extracted from, followed by the results of using the model on the other two nearby wells.

For the three wells, the depths at which the different geological formations where located are presented in the tables 5,6 and 7.

Table 5. Geological groups and their depths for well 6305/7-D-1 H.

Total Depth (ft)	Geological group
5265 to 5735	Nordland
5736 to 8448	Hordaland
8448 to 10990	Rogaland

Table 6. Geological groups and their depths for well 6305/7-D-2 H.

Total Depth (ft)	Geological group
4960 to 5557.7	Nordland
5558 to 8448	Hordaland
8448 to 12660	Rogaland

Table 7. Geological groups and their depths for well 6305/7-D-3 H.

True Depth (ft)	Geological group
5164 to 5603	Nordland
5604 to 8667.9	Hordaland
8668 to 11522	Rogaland

The regression coefficients that were derived from the wells for the three different geological groups are presented in the following tables.

Well 6305/7-D-1 H:

Table 8. Regression Coefficients for the Nordland group from well 6305/7-D-1 H.

Nordland Group	*Coefficients*
Intercept	-1282,4178
X Variable 1	0,00100507
X Variable 2	0,04323143
X Variable 3	0,55129937
X Variable 4	1,2699148
X Variable 5	-6,7957517
X Variable 6	-307,71777
X Variable 7	-11,67909

Table 9. Regression Coefficients for the Hordaland group from well 6305/7-D-1 H.

Hordaland Group	*Coefficients*
Intercept	-840,4591402
X Variable 1	0,00134773
X Variable 2	-0,006655235
X Variable 3	0,756484313
X Variable 4	-0,121865015
X Variable 5	41,23263227
X Variable 6	602,3079495
X Variable 7	-4,921434062

Table 10. Regression Coefficients for the Rogaland group from well 6305/7-D-1 H.

Rogaland group	*Coefficients*
Intercept	335,5733314
X Variable 1	0,000624926
X Variable 2	-0,005130162
X Variable 3	0,935142244
X Variable 4	-0,203348922
X Variable 5	5,407532883
X Variable 6	22,24859395
X Variable 7	-2,30457278

Well 6305/7-D-2 H:

Table 11. Regression Coefficients for the Nordland group from well 6305/7-D-2 H.

Nordland Group	*Coefficients*
Intercept	-2528,3687
X Variable 1	-0,0049897
X Variable 2	0,02735047
X Variable 3	0,37624936
X Variable 4	0,62766009
X Variable 5	-33,038602
X Variable 6	1742,10626
X Variable 7	-18,428776

Table 12. Regression Coefficients for the Hordaland group from well 6305/7-D-2 H.

Hordaland group	*Coefficients*
Intercept	213,9518225
X Variable 1	0,000656666
X Variable 2	-0,001875314
X Variable 3	0,303233038
X Variable 4	-0,316254321
X Variable 5	11,53332675
X Variable 6	259,2394217
X Variable 7	-6,230105632

Table 13. Regression Coefficients for the Rogaland group from well 6305/7-D-2 H.

Rogaland Group	*Coefficients*
Intercept	39,4557011
X Variable 1	0,00068047
X Variable 2	-0,0023738
X Variable 3	1,83471135
X Variable 4	-0,485557
X Variable 5	0,77095859
X Variable 6	275,183786
X Variable 7	-0,7506833

Well 6305/7-D-3 H:

Table 14. Regression Coefficients for the Nordland group from well 6305/7-D-3 H.

Nordland group	*Coefficients*
Intercept	1149,25302
X Variable 1	0,00849489
X Variable 2	-0,0042855
X Variable 3	0
X Variable 4	0,15770134
X Variable 5	-8,4993114
X Variable 6	-972,90026
X Variable 7	-2,9643069

Table 15. Regression Coefficients for the Hordaland group from well 6305/7-D-3 H.

Hordaland group	*Coefficients*
Intercept	762,8720289
X Variable 1	0,001768878
X Variable 2	-0,003741035
X Variable 3	0
X Variable 4	-0,538295434
X Variable 5	1,791043548
X Variable 6	133,461745
X Variable 7	-6,58277937

Table 16. Regression Coefficients for the Rogaland group from well 6305/7-D-3 H.

Rogaland group	*Coefficients*
Intercept	-12049,238
X Variable 1	0,00092087
X Variable 2	0,03030958
X Variable 3	0
X Variable 4	-3,5615349
X Variable 5	13,0681548
X Variable 6	11202,0481
X Variable 7	-1,106502

Using the coefficients in the tables above, the ROP was calculated for each well using its own data. This is represented in the Figures 31, 32 and 33.

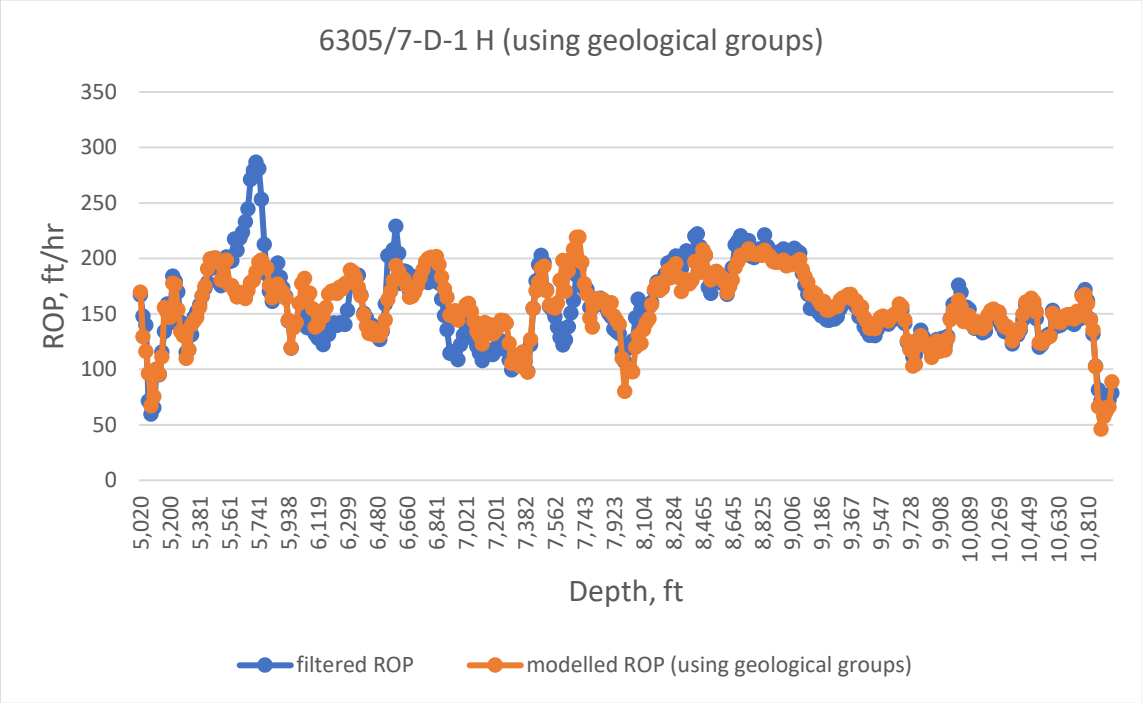

Figure 31. Multiple Regression (using geological sections) of well 6305/7-D-1 H on itself.

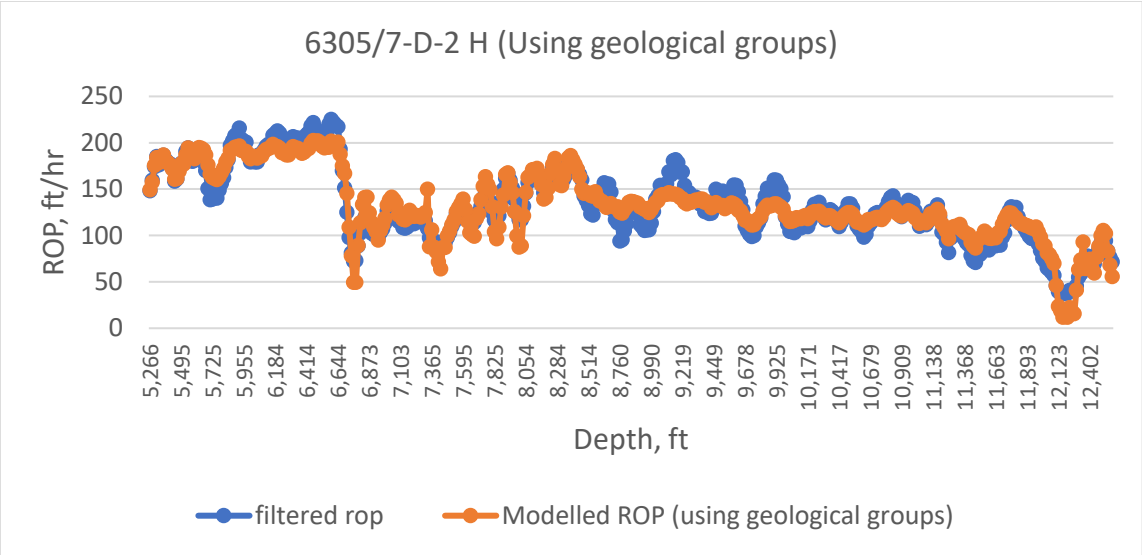

Figure 32. Multiple Regression (using geological sections) of well 6305/7-D-2 H on itself.

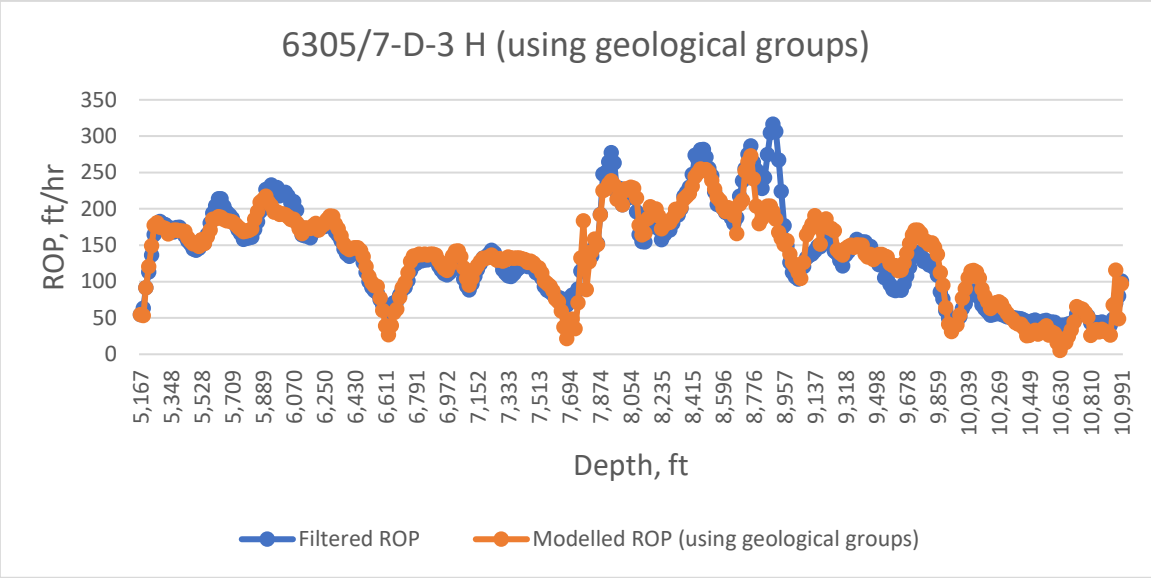

Figure 33. Multiple Regression (using geological sections) of well 6305/7-D-3 H on itself.

When modelling by geological groups, the results showed excellent correlation with the filtered ROP, with small to no deviations from the filtered ROP. The results are an improvement over using the whole well as shown in Figures 22, 23 and 24. This indicates that the model used for the multiple linear regression is good.

Testing the model with coefficients from 6305/7-D-1 H

The coefficients from well 6305/7-D-1 H presented in tables 8, 9 and 10 for the Nordland, Hordaland and Rogaland groups respectively are used to model the ROP for wells 6305/7-D-2 H and 6305/7-D-3 H in those three geological groups. The resultant ROP and the filtered ROP are then plotted against each other and presented in Figures 34 and 35.

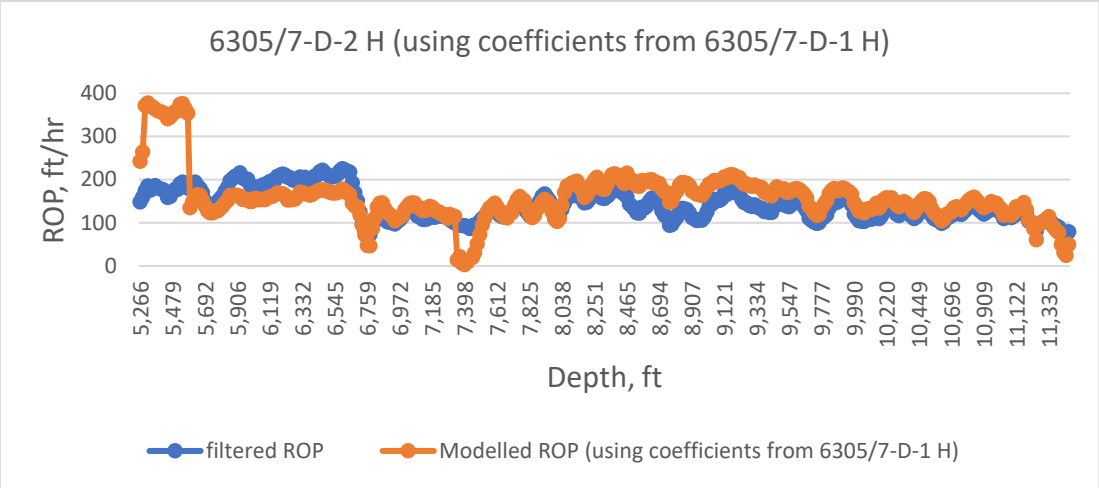

Figure 34. Multiple regression using geological group data from 6305/7-D-1 H on 6305/7-D-2 H.

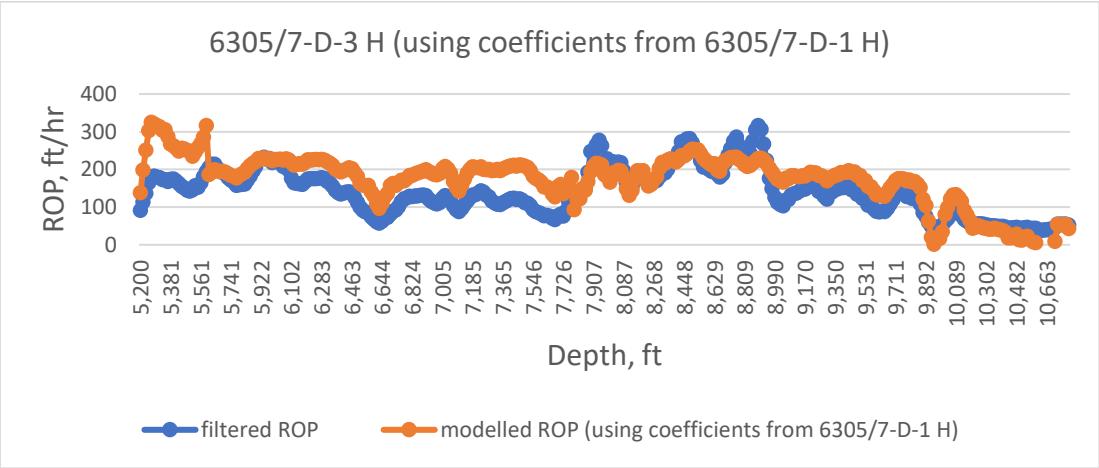

Figure 35. Multiple regression using geological group data from 6305/7-D-1 H on 6305/7-D-3 H.

Figures 34 and 35 of the modelled ROP, using the coefficients from 6305/7-D-1 H, vs. the filtered ROP gave good results, especially in well 6305/7-D-2 H, where the two graphs are correlated exceptionally well except for an overestimation of the ROP in the Nordland group. The modelled ROP In 6305/7-D-3 H showed an overestimation of the filtered ROP but with excellent correlation of the shape of the filtered ROP.

Testing the model with coefficients from 6305/7-D-2 H

Following the previous testing, the coefficients of well 6305/7-D-2 H from the different geological groups are implemented in the model and tested in wells 6305/7-D-1 H and

6305/7-D-3 H. The modelled ROP compared to the filtered ROP can be seen in Figures 36 and 37.

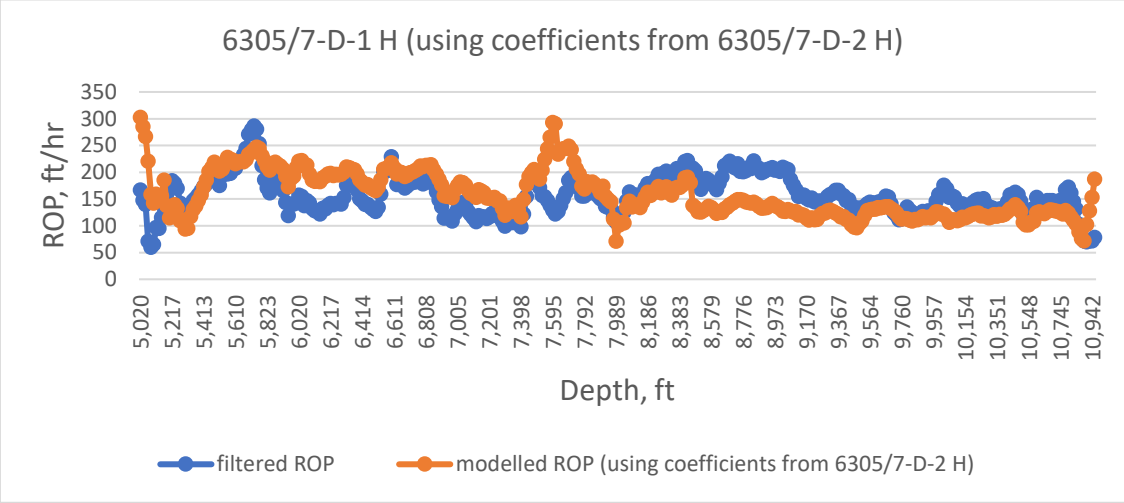

Figure 36. Multiple regression using geological group data from 6305/7-D-2 H on 6305/7-D-1 H.

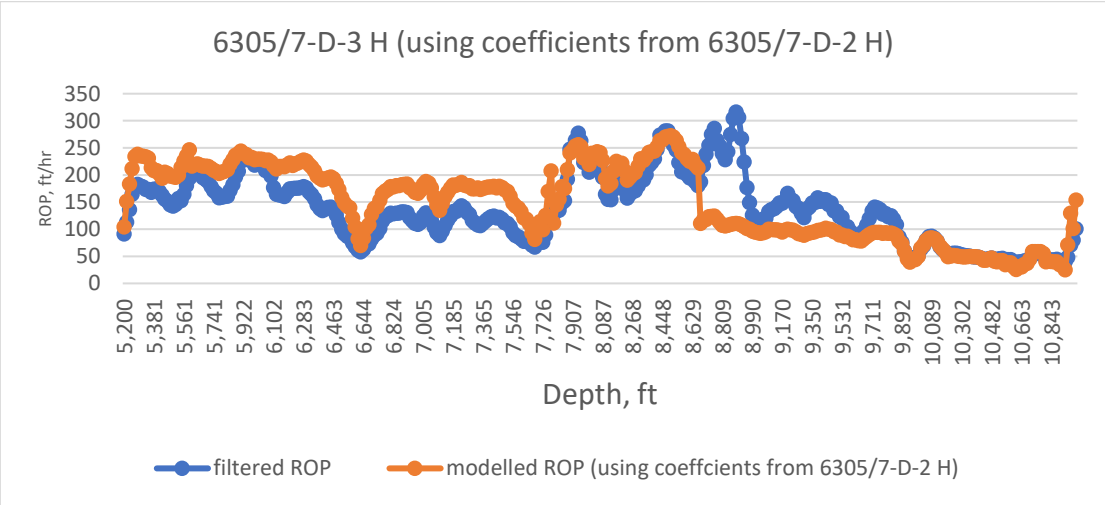

Figure 37. Multiple regression using geological group data from 6305/7-D-2 H on 6305/7-D-3 H.

The modelled ROP values for both wells using coefficients from 6305/7-D-2 H gave good result, which is seen when comparing Figures 27 and 36 and Figures 28 and 37. This indicates that the when modelling the whole well, the difference in the geology between the different wells resulted in an inconsistent ROP modelling. This inconsistency was

mostly eliminated as seen in Figures 36 and 37, where the modelled ROP and the filtered ROP values are near each other and follow the same pattern.

Testing the model with coefficients from 6305/7-D-3 H

The coefficients from well 6305/7-D-3 H presented in tables 14,15 and 16 are used to model the ROP of wells 6305/7-D-1 H and 6305/7-D-2 H. The resultant modelled ROP and the filtered ROP then are presented in Figures 38 and 39 respectively.

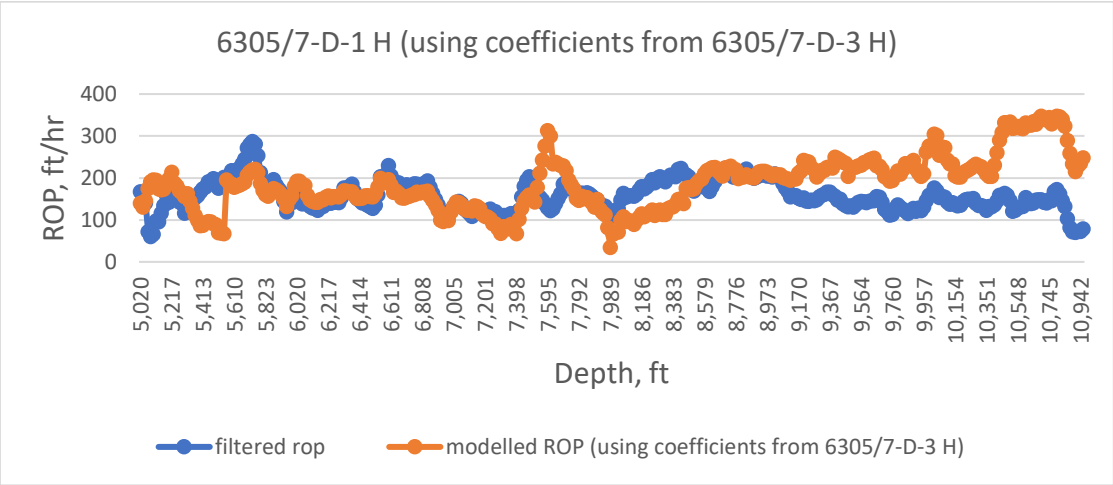

Figure 38. Multiple regression using geological group data from 6305/7-D-3 H on 6305/7-D-1 H.

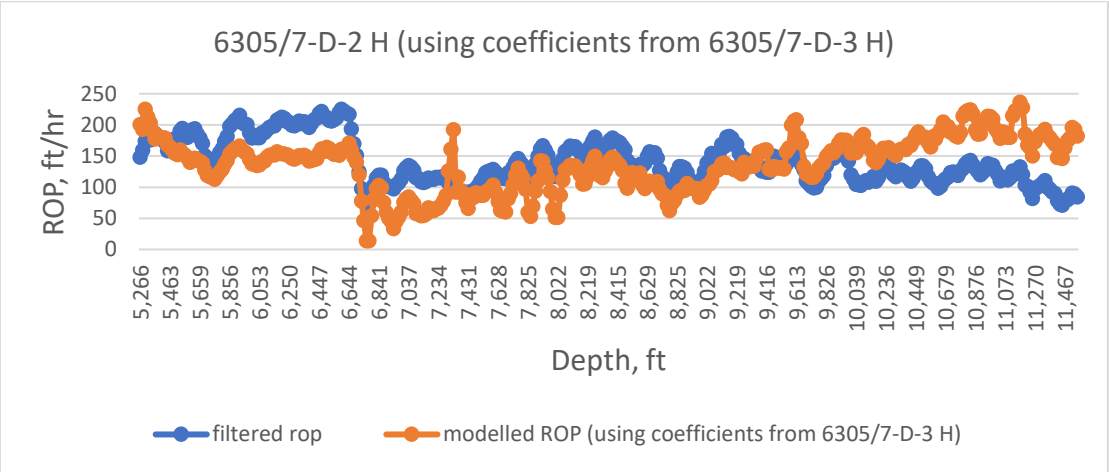

Figure 39. Multiple regression using geological group data from 6305/7-D-3 H on 6305/7-D-2 H.

The modelled ROP for wells 6305/7-D-1 H and 6305/7-D-2 H using the coefficients from 6305/7-D-3 H gave a good result, where the modelled ROP followed the pattern of the filtered ROP in both Figures. However, we can observe towards the end of the field after entering the Rogaland formation that the model deviates and overestimates the values of the ROP. This could be due to the difference of the inclination and total depth of the wells. The results show a better overall correlation opposed to modelling the whole well, as shown in Figures 29 and 30.

It is worth mentioning that modelling using the geological groups gave exceptionally good patterns for the modelled ROP that were almost identical to the filtered ROP for all cases, this indicates a good correlation between the modelling technique and the actual dataset.

5.2 MSE

The concept of MSE proposed by Teale in 1965 generates a physical model that describes the relationship between the energy to excavate one volume of formation rock, the drilling parameters such as the WOB, drill bit, the ROP, etc. Using this relationship to model the ROP, assumes that the MSE between different wells for the same depth is correlative or equal. This can create inaccuracies since the geology between wells and the formation strength can differ greatly, especially for wells that are far away. The model is adequate for wells that are nearby and will be tested in this thesis work using the workflow described in Figure 20.

This section presents the ROP modelling using MSE and the results.

MSE values for the three wells:

The MSE values for all three wells are calculated using Eq. 3.17. The resultant MSE values are presented in Figure 40 against the total depth of the three wells.

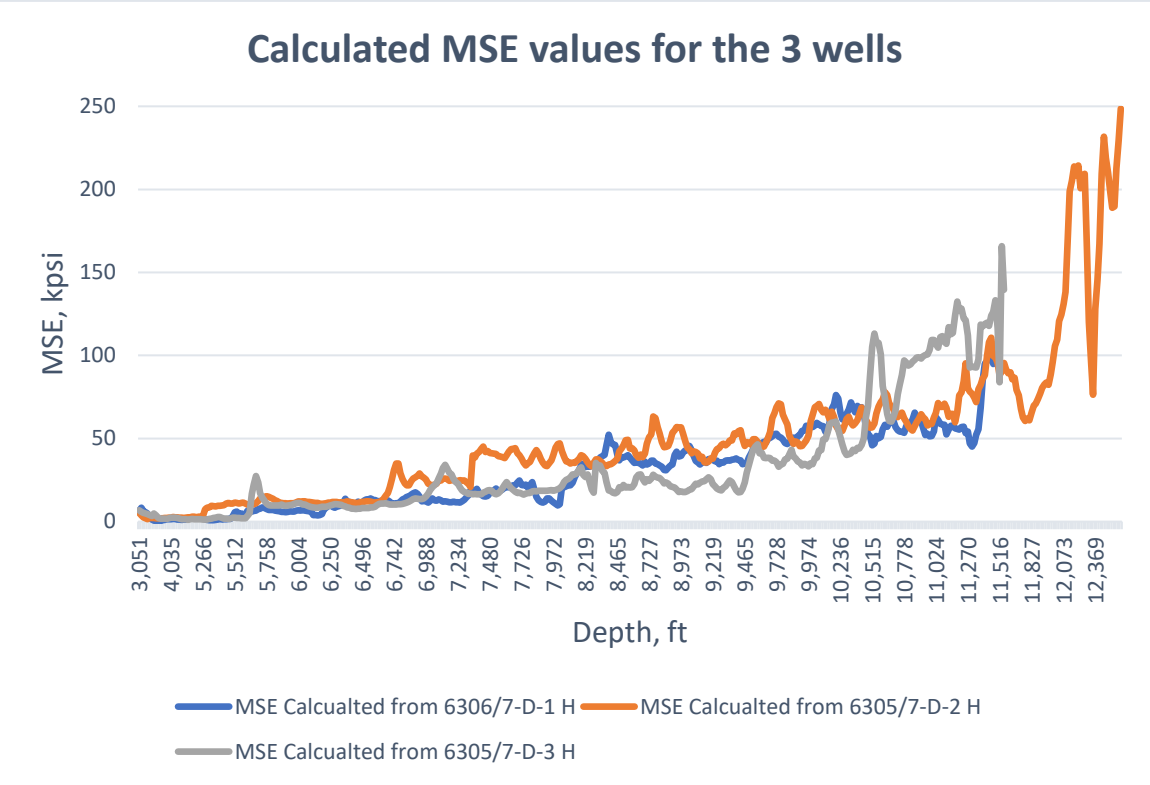

Figure 40. Calculated MSE for wells 6305/7-D-1 H, 6305/7-D-2 H and 6305/7-D-3 H vs. total depth.

The results show good correlation between the three wells when it comes to the MSE. This indicates that the formation strength and the formation pressure for the three wells are close to each other at the depths presented in the Figure. This is true until we reach a total depth of 10563 ft where the MSE of well 6305/7-D-3 H increases rapidly compared to the other two wells.

Testing the model using MSE values from 6305/7-D-1 H:

The MSE model is tested using the calculated MSE values from well 6305/7-D-1 H. The modelled ROP are presented in Figures 41 and 42.

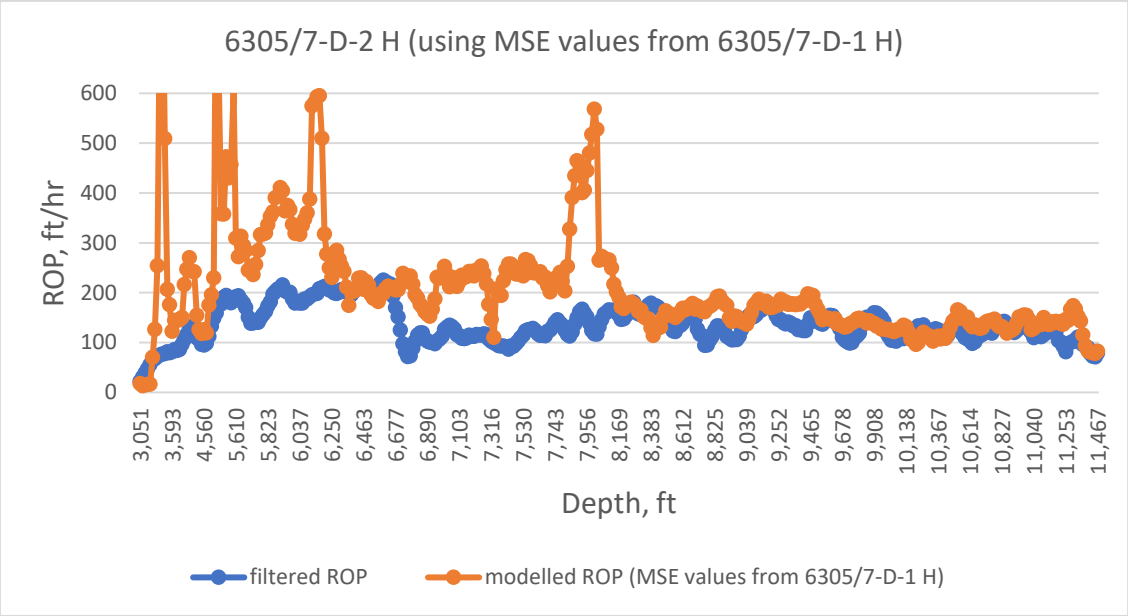

Figure 41. Modelled ROP (using MSE values from 6305/7-D-1 H).

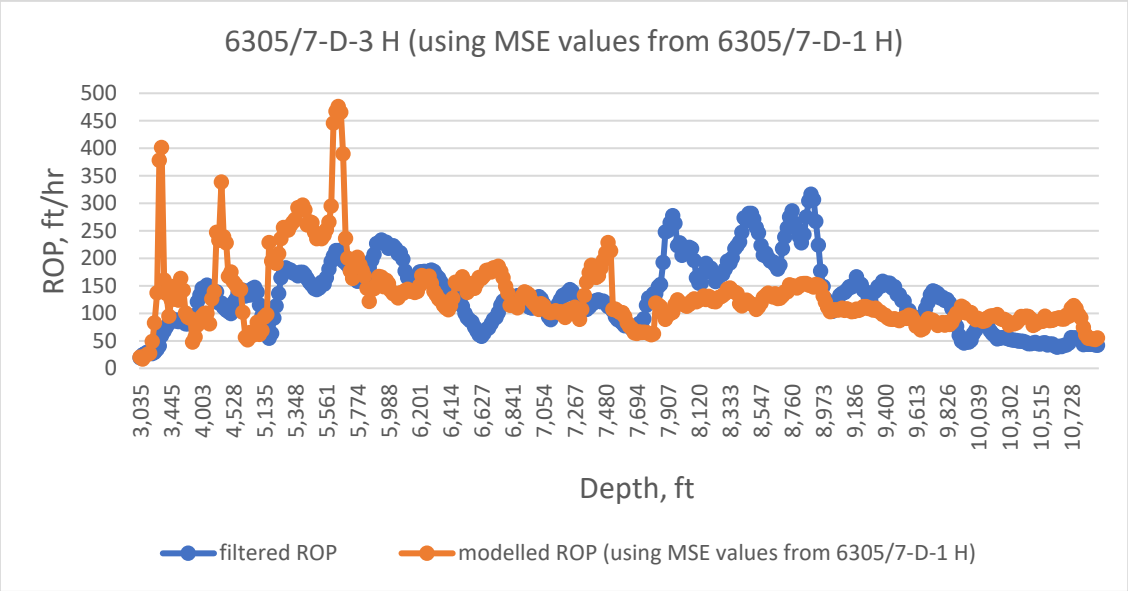

Figure 42. Modelled ROP (using MSE values from 6305/7-D-1 H).

The two Figures give decent results after a certain depth. This depth is 8219 ft for 6305/7-D-2 H and 5906 for 6305/7-D-3 H. It can be noticed that both modelled curves have the same pattern as the filtered ROP, but with different amplitudes for the ROP values. This is because of the difference in the MSE values between well 6307/5-D-1 H and the other two; where the MSE values of 6305/7-D-1 H were much lower and ROP increases with the decrease in MSE. Thus, the values of the ROP for 6305/7-D-2 H and 6305/7-D-3 H

where overestimated. This indicates that well 6305/7-D-1 H has lower formation strength at the top formations while drilling compared to the other two wells.

Testing the model using MSE values from 6305/7-D-2 H:

The MSE values extracted from 6305/7-D-2 H are used in the ROP model to calculate the ROP for the two other wells. The resultant ROP curves are shown in Figures 43 and 44.

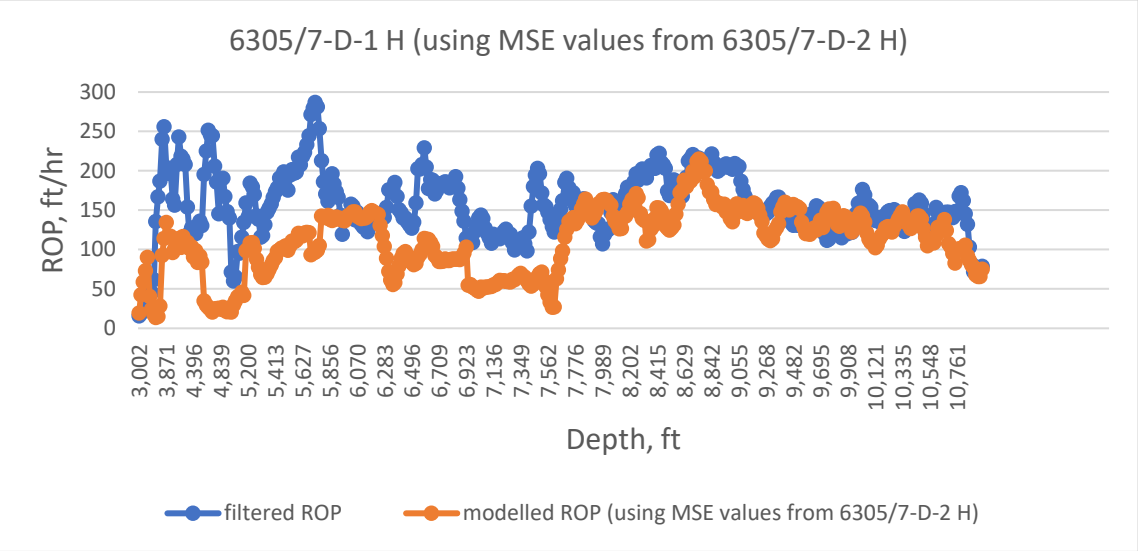

Figure 43. Modelled ROP (using MSE values from 6305/7-D-1 H).

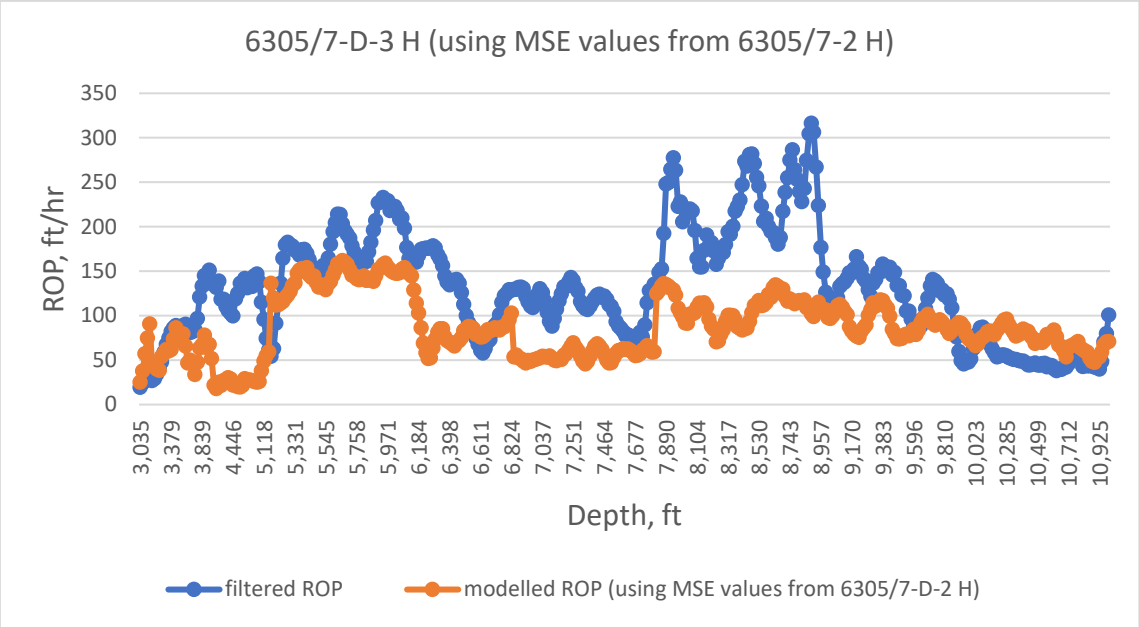

Figure 44. Modelled ROP (using MSE values from 6305/7-D-2 H).

The model shows correlation between the filtered ROP and the modelled ROP using data from 6305/7-D-2 H. However, as seen when we used the MSE values from 6305/7-D-1 H, the difference in the MSE values between the wells results in either an overestimation of the ROP in the cases where the MSE is lower, or an underestimation of the ROP when the MSE is higher. This behavior is observed again when we model the ROP for 6305/7-D-1 H and 6305/7-D-2 H using MSE values from 6305/7-D-3 H and can be seen in Figures 45 and 46.

The MSE changes between the wells for the same total depth are results of multiple differences between the wells for the same total depth. These could be the formation located at those depths, the deviation of the well at that depth, the hole size. These differences will affect the energy needed to drill a volume of formation rock.

Testing the model using MSE values from 6305/7-D-3 H:

The resultant ROP curves for wells 6305/7-D-1 H and 6305/7-D-2 H when using the MSE values from 6305/7-D-3 H are presented in Figures 45 and 46.

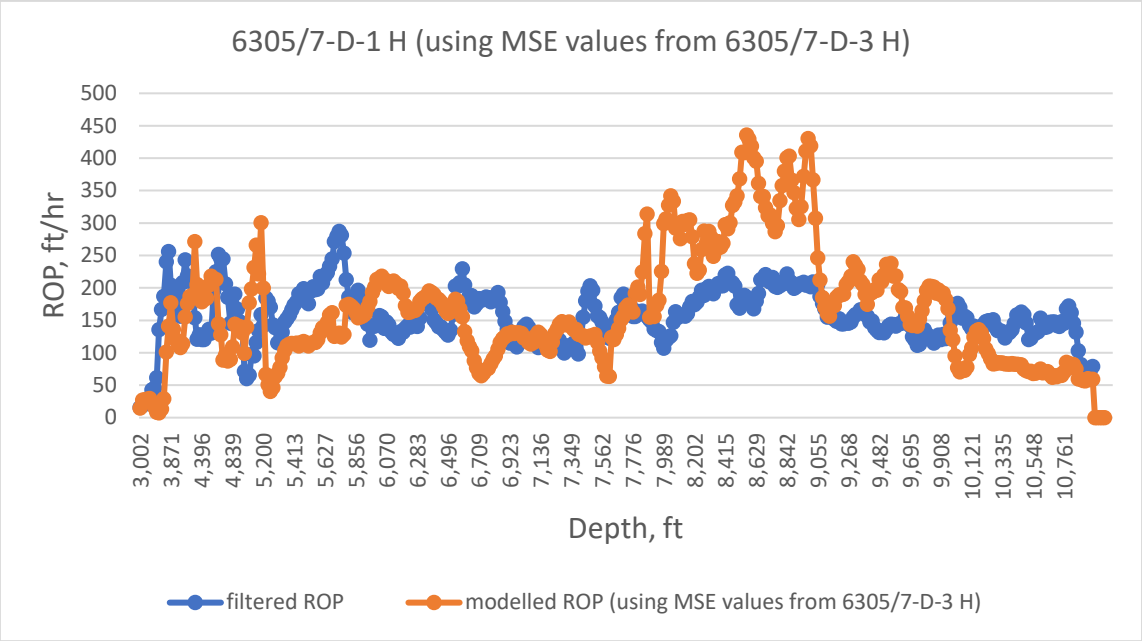

Figure 45. Modelled ROP (using MSE values from 6305/7-D-3 H).

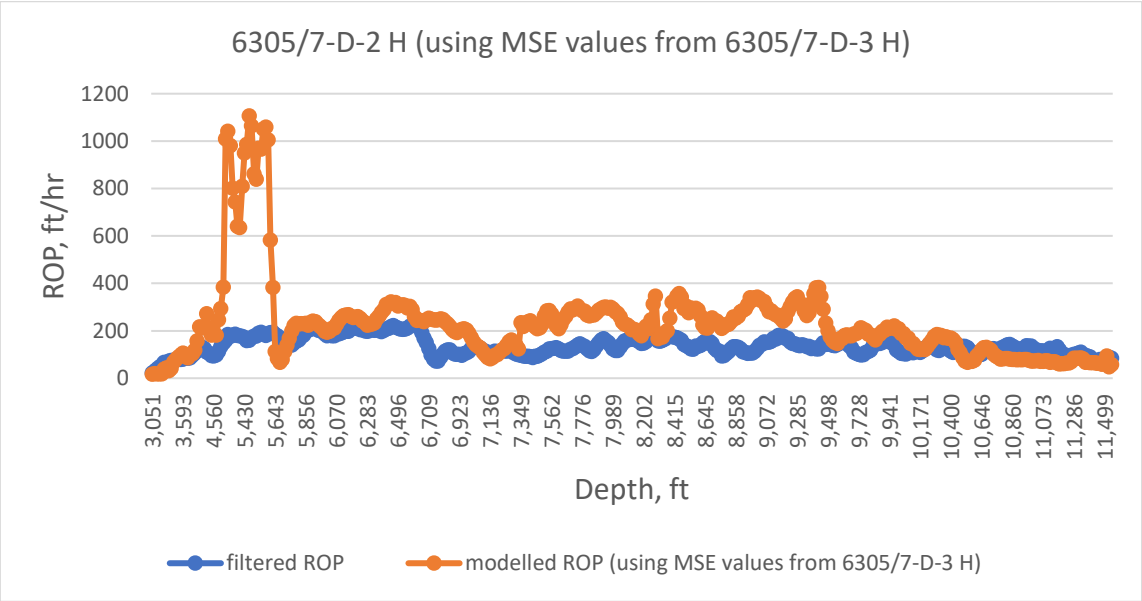

Figure 46. Modelled ROP (using MSE values from 6305/7-D-3 H).

5.3 D-exponent

The drilling exponent (d-exponent) is a drilling parameter that is derived while drilling and that describes the drill ability of a formation. This value indicates how easy or hard it is to penetrate a formation and is a function of multiple drilling parameters as well as

ROP. The d-exponent is proportional to the formation strength and increases linearly with depth for formations that are normally pressurized. ROP can be modelled as long as the d-exponent between wells is assumed to be correlative or equal for the same depths. This creates uncertainties in the modelled ROP where they drill ability of the formations for different depths are bound to be different due to geological differences between the different wells. The workflow presented in Figure 19 is used to model the ROP along with Eq. 4.6.

This chapter will present and discus the results of the D-exponent modelling

D-exponent values for the wells:

The calculated D-exponent from the 3 wells is presented in Figure 47. This was done using Eq. 3.24 and the drilling data along with the filtered ROP. It is observed that the calculated D-exponent for the same depths are very close between the wells, indicating a good correlation of the drill ability of the 3 wells.

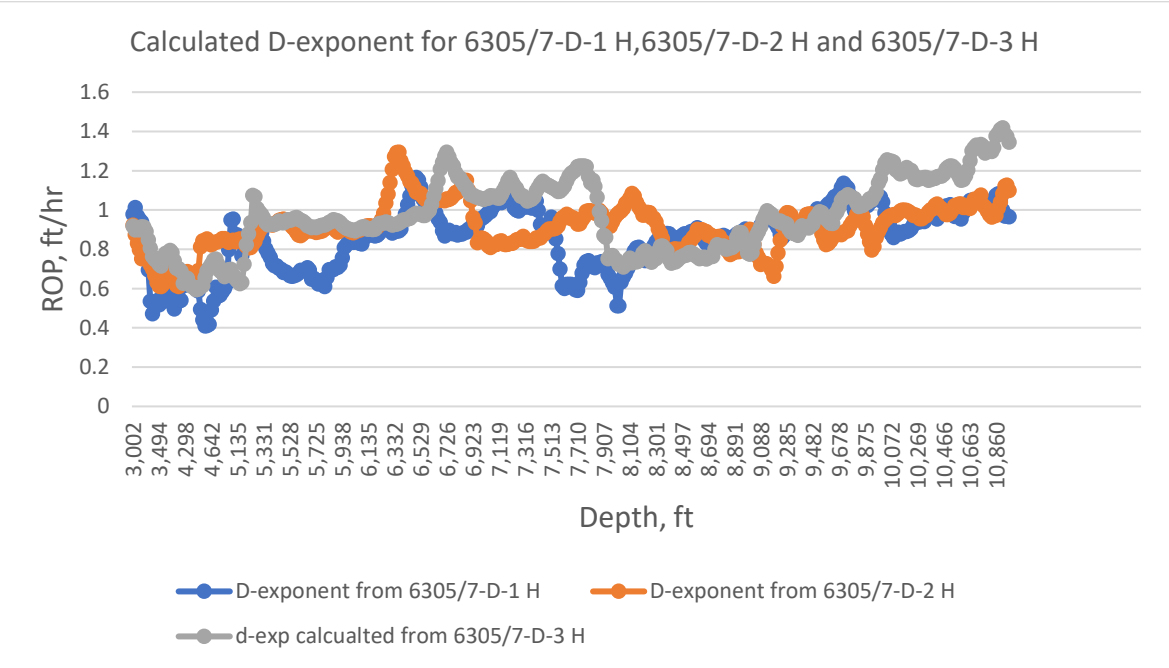

Figure 47. Calculated d-exponent for 6305/7-D-1 H, 6305/7-D-2 H and 6305/7-D-3 H.

Testing the model using d-exponent values from 6305/7-D-1 H:

The d-exponent values computed from the drilling data of well 6305/7-D-1 H are used in Eq. 4.6, along with the bit diameter, WOB and surface rotary speed, to predict the ROP for wells 6305/7-D-2 H and 6305/7-D-3 H. The results of this modelling are illustrated in Figures 48 and 49.

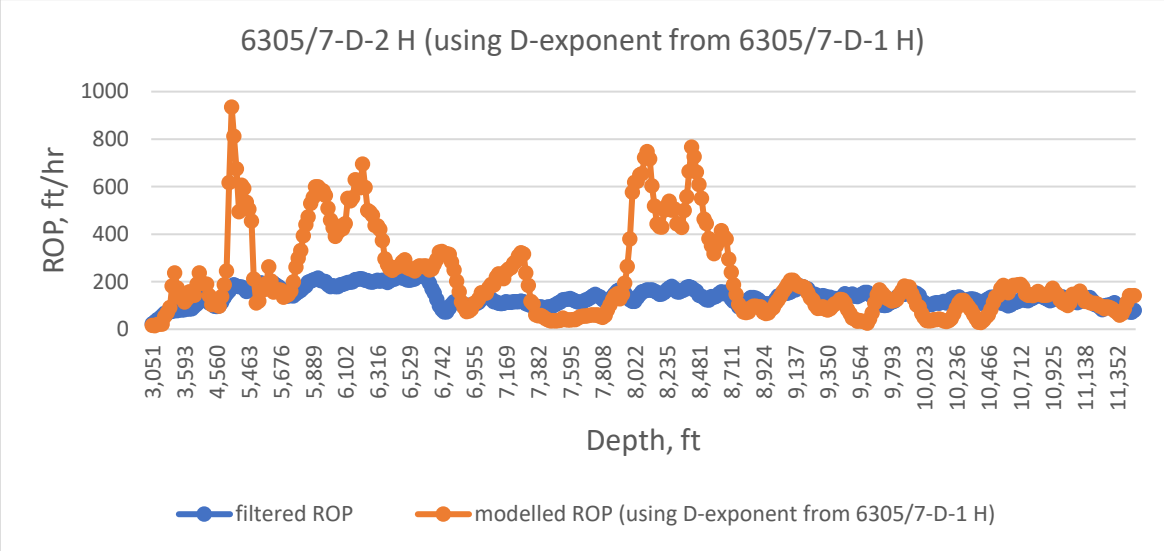

Figure 48. Modelled ROP (using d-exponent from 6305/7-D-1 H).

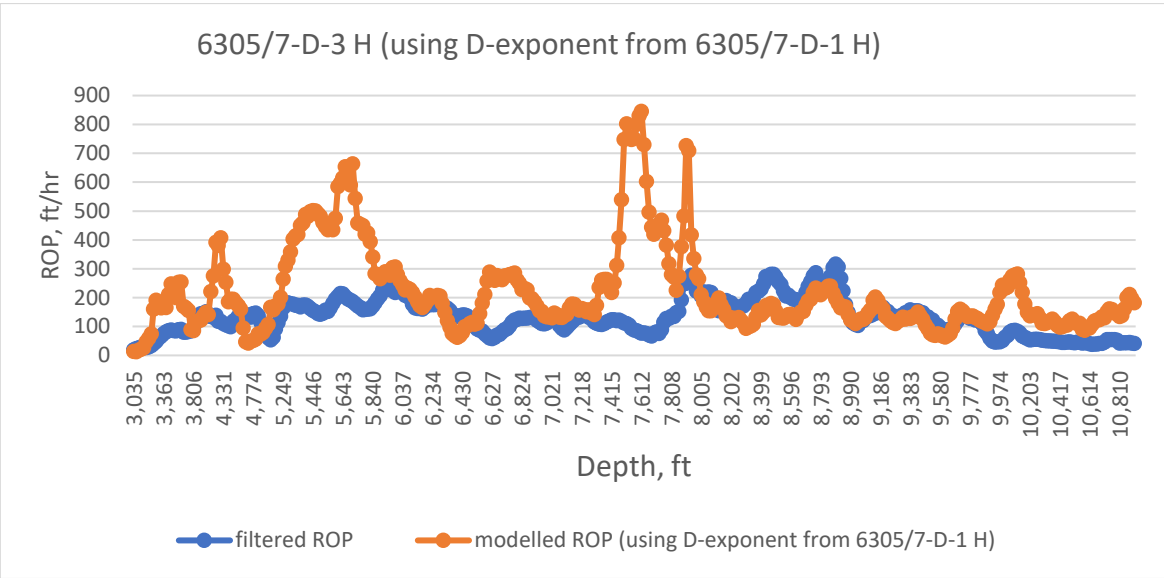

Figure 49. Modelled ROP (using d-exponent from 6305/7-D-1 H).

The results' pattern correlates well with the filtered ROP. However, some peaks in the data are noticeable. This is due to a difference in the D-exponent between the multiple wells for the same depth. ROP has an exponential relationship with the d-exponent and thus any small increase in the d-exponent will result in huge increases for the ROP. This is the reason for the huge peaks seen in the Figures.

Testing the model using d-exponent values from 6305/7-D-2 H:

The model is tested using d-exponent values from 6305/7-D 2 H and implemented to calculate the ROP for wells 6305/7-D-1 H and 6305/7-D-3 H. The resultant ROP values for the two wells are plotted and illustrated in figures 50 and 51.

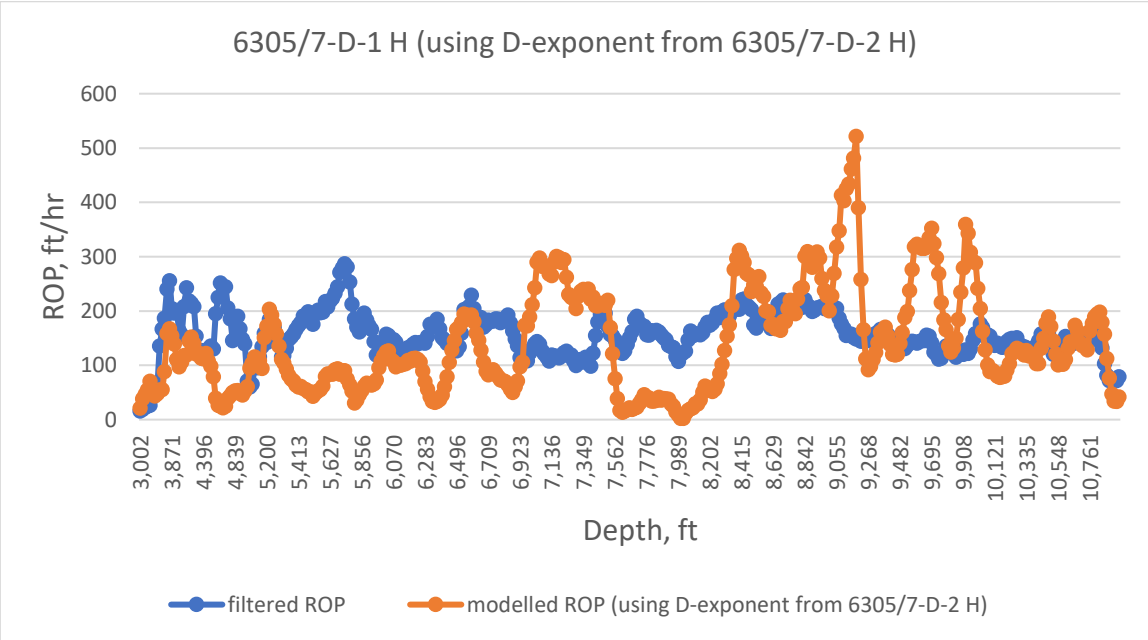

Figure 50. Modelled ROP (using d-exponent from 6305/7-D-2 H).

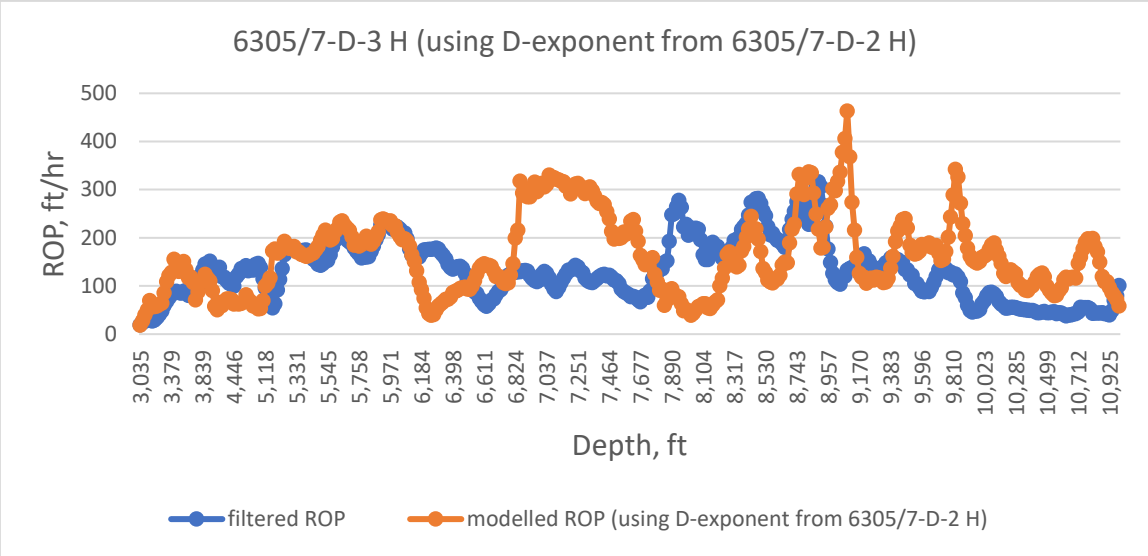

Figure 51. Modelled ROP (using d-exponent from 6305/7-D-2 H)

The results show good correlation but with the same peaks as we saw when using the d-exponent values from 6305/7-D-1 H. This is also seen when using the d-exponent values from 6305/7-D-3 H on wells 6305/7-D-2 H and 6305/7-D-3 H in Figures 52 and 53.

Testing the model using d-exponent values from 6305/7-D-3 H:

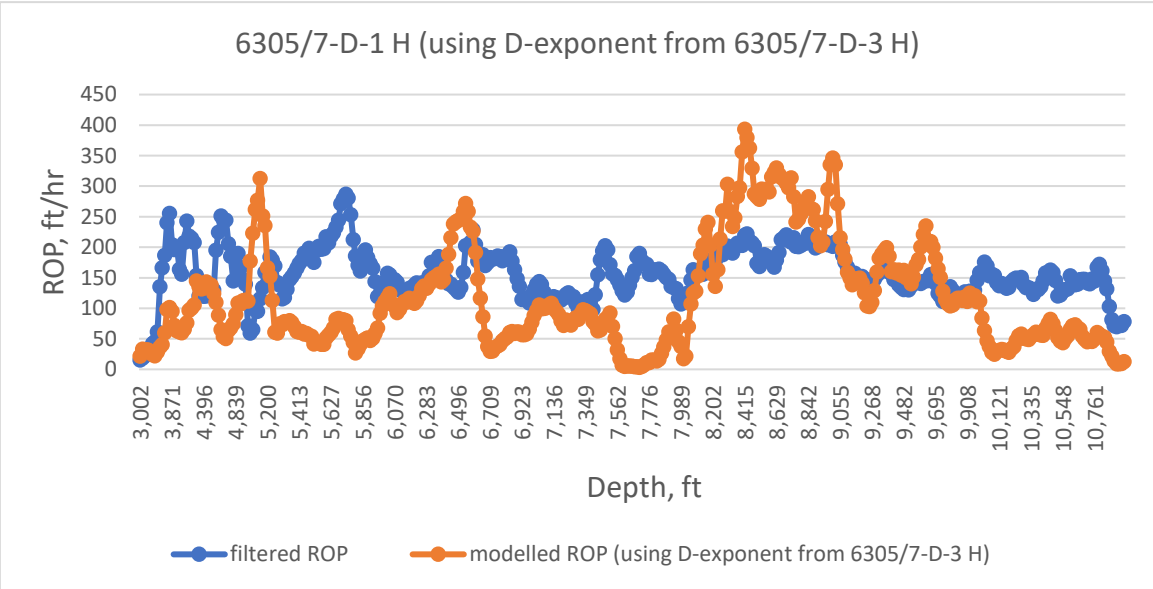

Figure 52. Modelled ROP (using d-exponent from 6305/7-D-3 H).

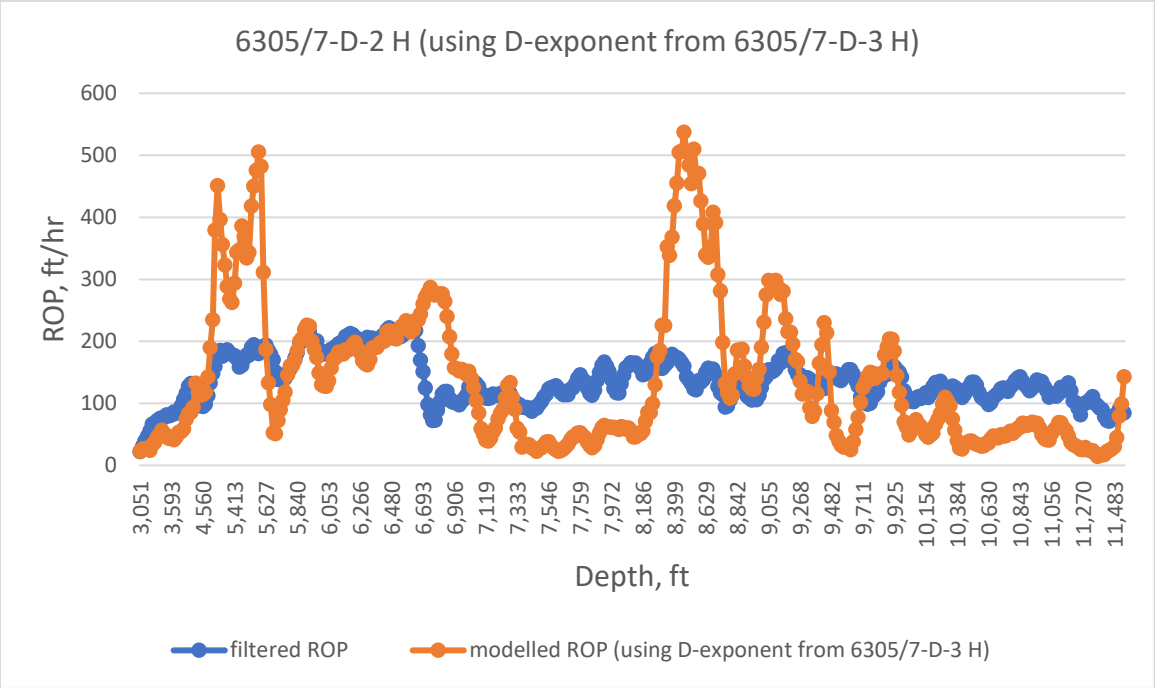

Figure 53. Modelled ROP (using d-exponent from 6305/7-D-3 H).

5.4 Warren Model

The Warren model estimates the ROP based on multiple drilling parameters. This model takes into account the cleaning of the hole and the flow of the fluids in the well. The model used in the thesis is the "imperfect-cleaning" model that assumes that the rate of cuttings generations does not equal the rate of cuttings removal. This model has three coefficients "a", "b" and "c" that are field specific and can be derived if all the data in the model is available. The workflow in this thesis is presented in Figure 21 and Eq. 4.8 is used to calculate the modelled ROP.

This thesis will attempt to model the ROP based on the Warren model using two methods:

- Modelling the whole well
- Modelling sections based on geological groups

The results of both these techniques are presented below.

5.4.1 Modelling with data from the whole well

For this part, the coefficients are derived from all of the well data and then used to model the ROP for a nearby well. The coefficients “a”, “b” and “c” are calculated for each well using Matlab. The calculated coefficients for each of the three wells are presented in tables 17, 18 and 19:

Table 17. Warren coefficients for 6305/7-D-1 H (using data from the whole well).

6305/7-D-1 H	Warren coefficients
a	2,1062E-08
b	4,62
c	6,8354E-08

Table 18. Warren coefficients for 6305/7-D-2 H (using data from the whole well).

6305/7-D-2 H	Warren coefficients
a	6,3431E-06
b	11,00
c	2,4683E-08

Table 19. Warren coefficients for 6305/7-D-3 H (using data from the whole well).

6305/7-D-3 H	Warren coefficients
a	6,9160E-05
b	8,67
c	5,1891E-09

Testing the Warren coefficients on the wells they were extracted from:

Using the Warren coefficients located in tables 17, 18 and 19, The modelled ROP for wells 6305/7-D-1 H, 6305/7-D-2 H and 6305/7-D-3 H, respectively. These modelled ROP values are then compared to the filtered ROP for the wells. This is seen in Figures 54, 55 and 56

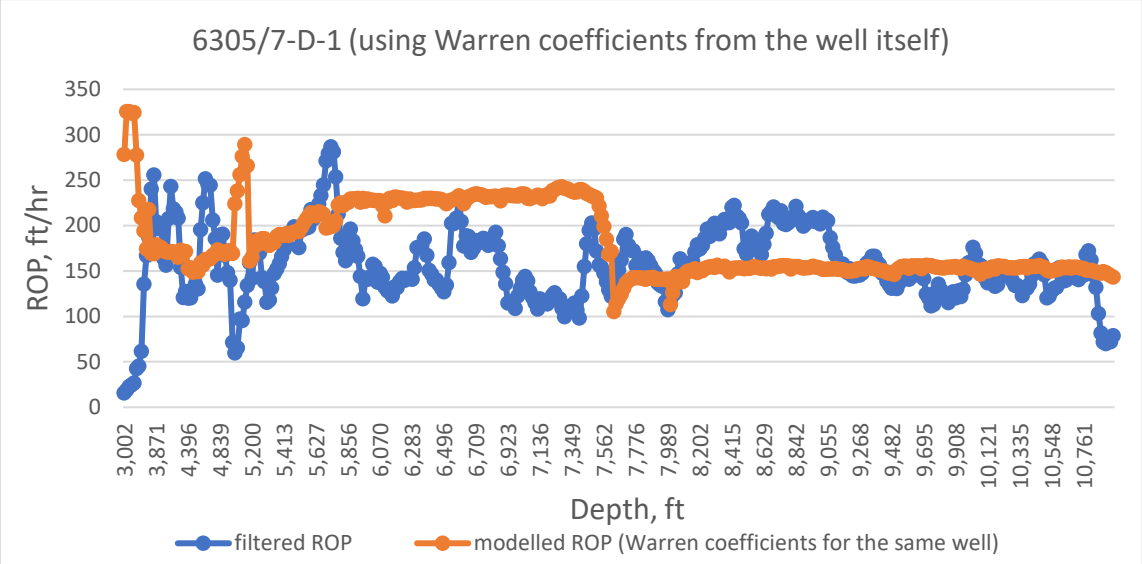

Figure 54. Warren ROP for 6305/7-D-1 H (using coefficients for the same well).

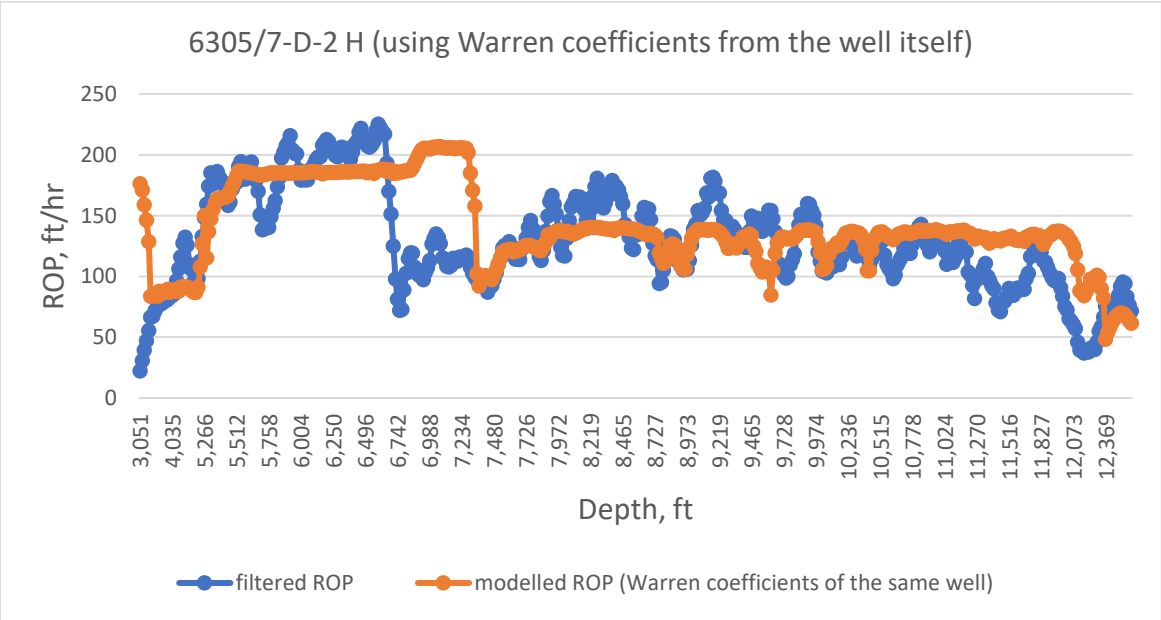

Figure 55. Warren ROP for 6305/7-D-2 H (using coefficients for the same well).

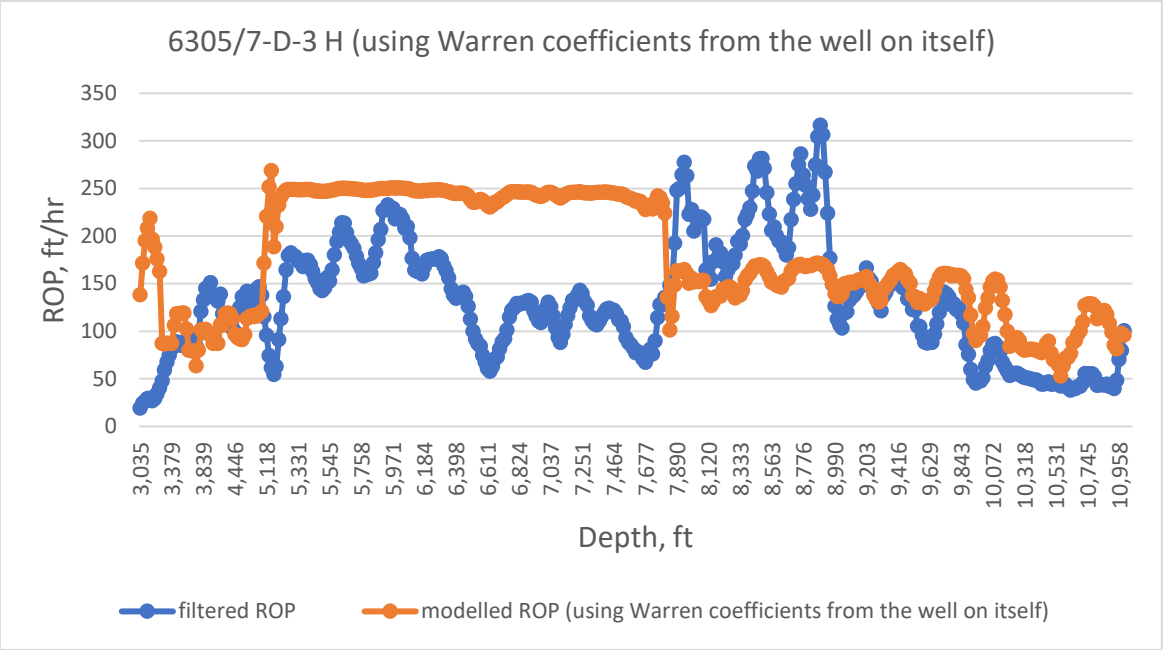

Figure 56. Warren ROP for 6305/7-D-3 H (using coefficients for the same well).

The model follows the filtered ROP, however most of the time it tries to average the ROP values to give a flat line instead of the jumps that the ROP experiences, that might be due to multiple factors such as bit bounces or different lithology in a formation.

Using Warren coefficients from 6305/7-D-1 H:

The Warren coefficients from well 6305/7-D-1 H located in table 17 are used to model the ROP for the other two wells. The modelled ROP is found in Figures 57, 58.

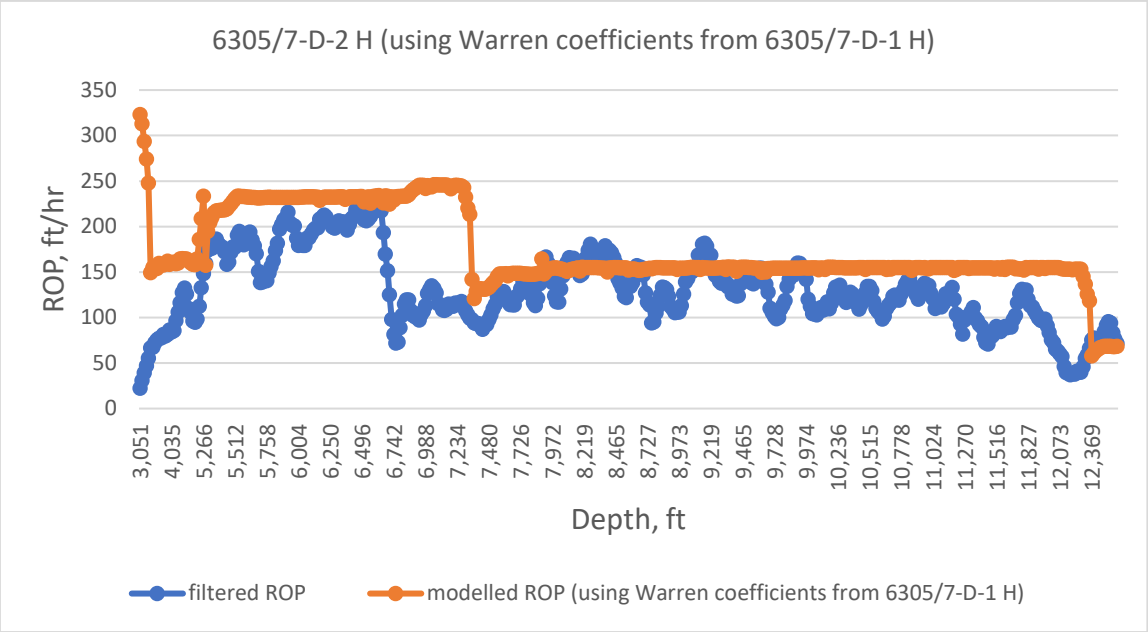

Figure 57. Warren ROP for 6305/7-D-2 H (using coefficients from 6305/7-D-1 H).

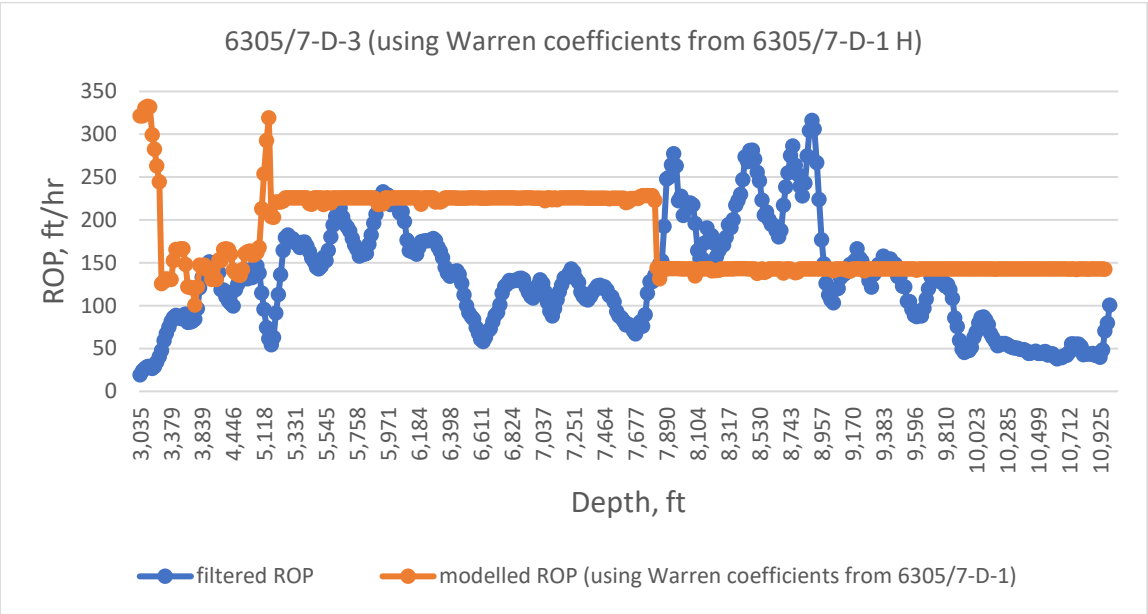

Figure 58. Warren ROP for 6305/7-D-3 H (using coefficients from 6305/7-D-1 H).

The resultant Warren ROP behave similarly as mentioned above where they give a flat line for the majority of the data. However, an overestimation and an underestimation of the ROP values can be seen in both cases which could be due geological differences between the wells as well as differences in the inclinations. The ROP for 6305/7-D-2 H gave a better fit overall than the graph of 6305/7-D-3 H.

Using Warren coefficients from 6305/7-D-2 H:

The calculated Warren coefficients from 6305/7-D-2 H are used to model the ROP for the wells 6305/7-D-1 H and 6305/7-D-3 H. The resultant Warren ROPs are presented in Figures 59 and 60.

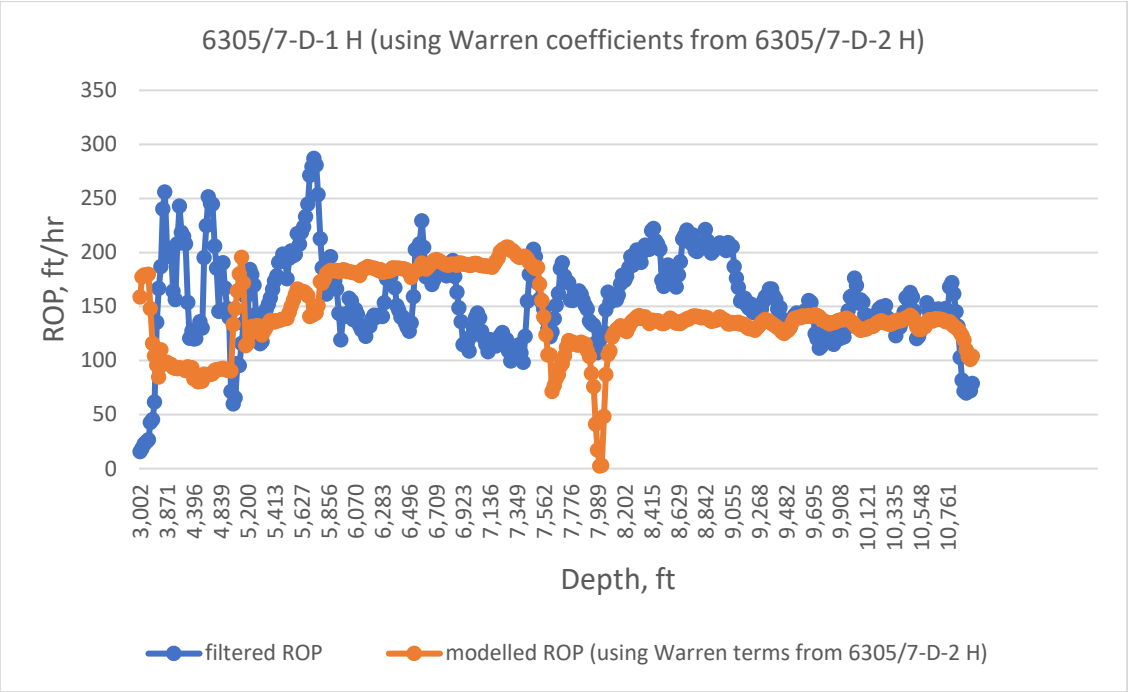

Figure 59. Warren ROP for 6305/7-D-1 H (using coefficients from 6305/7-D-2 H).

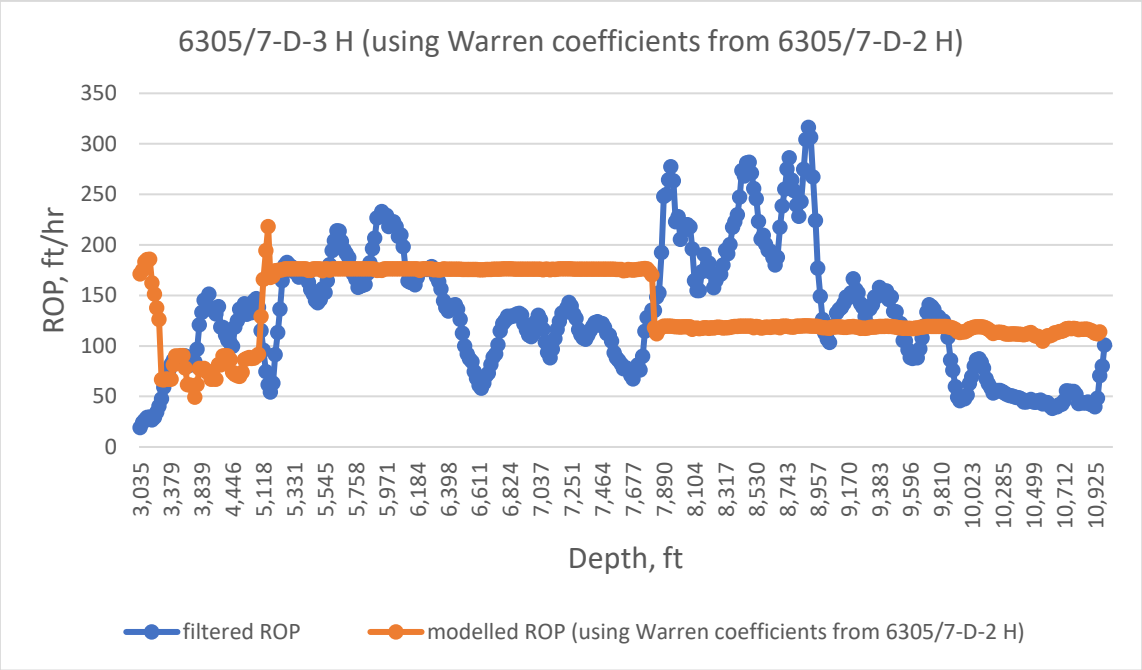

Figure 60. Warren ROP for 6305/7-D-3 H (using coefficients from 6305/7-D-2 H).

The modelled ROP for well 6305/7-D-1 H gave better fit than that of 6305/7-D-3 H. This observation and that of Figure 57, is an indication that the geological environment of these two wells is similar to some extent with 6305/7-D-3 H being the different one. The modelled ROP for 6305/7-D-3 H shows the flat lines with overestimations and underestimations of the filtered ROP.

Using Warren coefficients from 6305/7-D-3 H:

The Warren coefficients from well 6305/7-D-3 H are used to model the ROP of wells 6305/7-D-1 H and 6305/7-D-2 H. The modelled ROPs are illustrated in Figures 61 and 62 and compared to the filtered ROP for the wells.

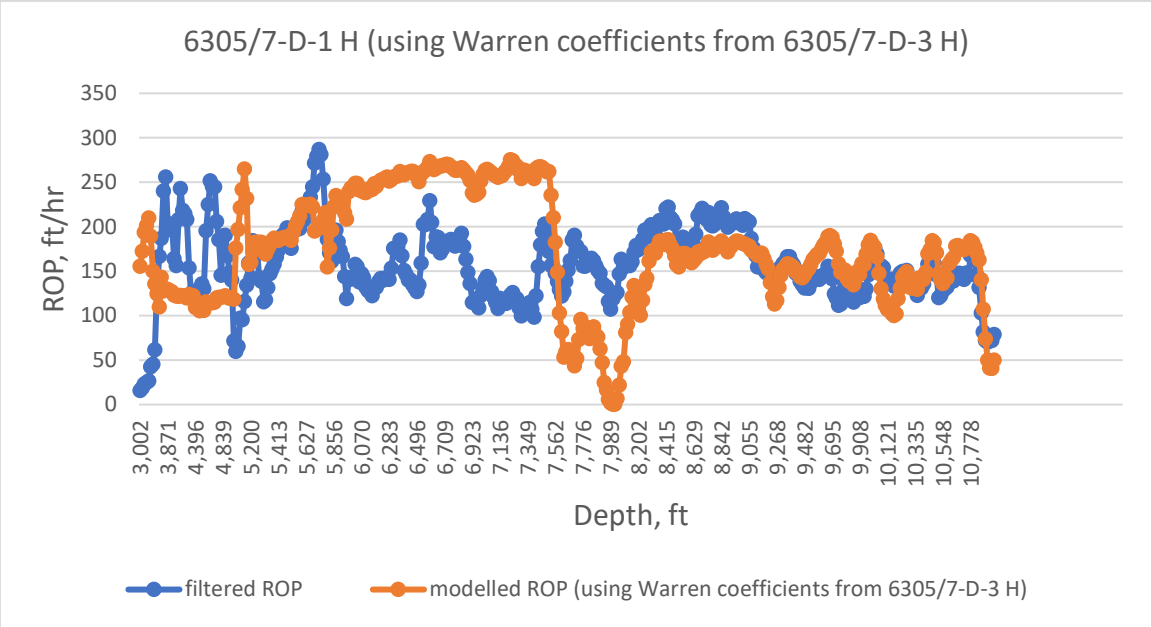

Figure 61. Warren ROP for 6305/7-D-1 H (using coefficients from 6305/7-D-3 H).

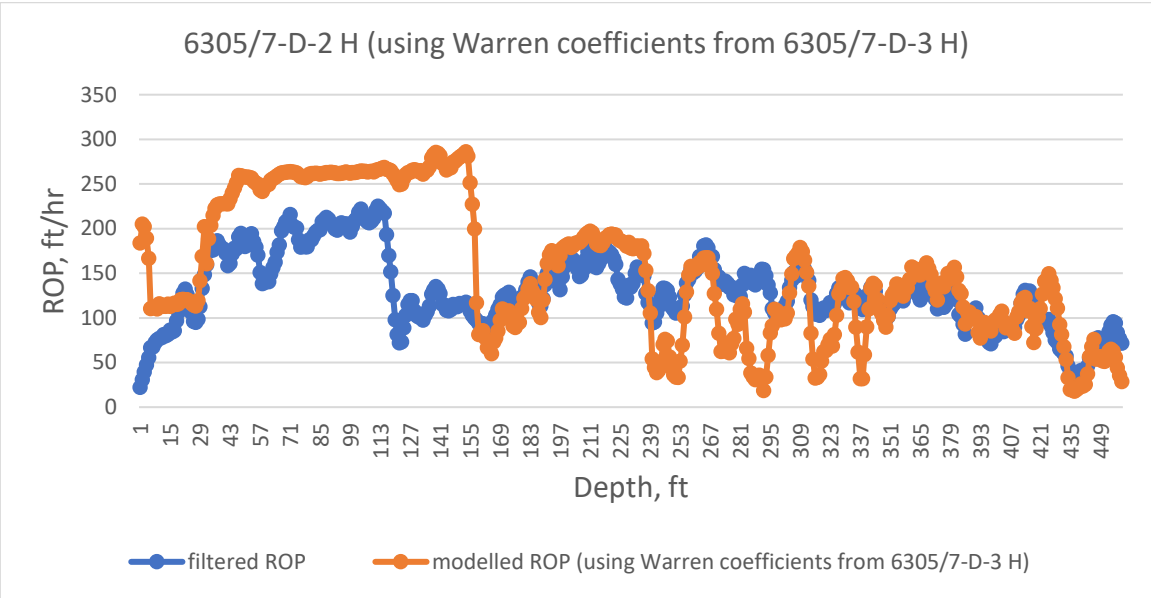

Figure 62. Warren ROP for 6305/7-D-3 H (using coefficients from 6305/7-D-2 H).

The modelled ROP in both curves follows the ROP and correlates fairly well with a bit of overestimation and underestimation. The model here seems to be very good and thus the coefficients from 6305/7-D-3 H seems best fit out of the three wells.

5.4.2 Modelling with data from geological groups

For this part, the well is dissected into three sections based on the geological groups of the wells. These groups are the Nordland group, the Hordaland group and the Rogaland group. Their depth for each well is presented in tables 5,6 and 7. Each one of these groups is then modelled to extract the Warren coefficients in Matlab and then implemented in the model to calculate the ROP for the other wells in the same sections. The derived coefficients for the sections for each well are located in tables 20→28.

Well 6305/7-D-1 H:

Table 20. Warren coefficients for 6305/7-D-1 H (Nordland group).

Nordland Warren coeffcients	
a	-1,368E-05
b	7,6630594
c	4,176E-08

Table 21. Warren coefficients for 6305/7-D-1 H (Hordaland group).

Hordaland Warren coeffcients	
a	1,98E-08
b	8,4217543
c	3,585E-08

Table 22. Warren coefficients for 6305/7-D-1 H (Rogaland group).

Rogaland Warren coeffcients	
a	3,79E-05
b	9,0099139
c	1,109E-08

Well 6305/7-D-2 H:

Table 23. Warren coefficients for 6305/7-D-2 H (Nordland group).

Nordland warren coeffcients	
a	0,00120932
b	13,70520782
c	-8,59327E-08

Table 24. Warren coefficients for 6305/7-D-2 H (Hordaland group).

Hordaland warren coeffcients	
a	1,41038E-05
b	16,46613309
c	-3,4005E-08

Table 25. Warren coefficients for 6305/7-D-2 H (Rogaland group).

Rogaland warren coeffcients	
a	5,17683E-06
b	19,57852892
c	-4,25508E-08

Well 6305/7-D-3:

Table 26. Warren coefficients for 6305/7-D-3 H (Nordland group).

Nordland warren coeffcients	
a	0,000807196
b	1,794284605
c	1,27182E-07

Table 27. Warren coefficients for 6305/7-D-3 H (Hordaland group).

Hordaland warren coeffcients	
a	0,000120838
b	62,3132419
c	-5,86563E-07

Table 28. Warren coefficients for 6305/7-D-3 H (Rogaland group).

Rogaland warren coeffcients	
a	0,000184203
b	42,29251281
c	-3,64301E-07

Testing the models on the fields they were derived from

The coefficients that where derived from the three wells are applied, using the model, on the wells they were extracted from to evaluate the model. The results of this is seen in Figures 63, 64 and 65.

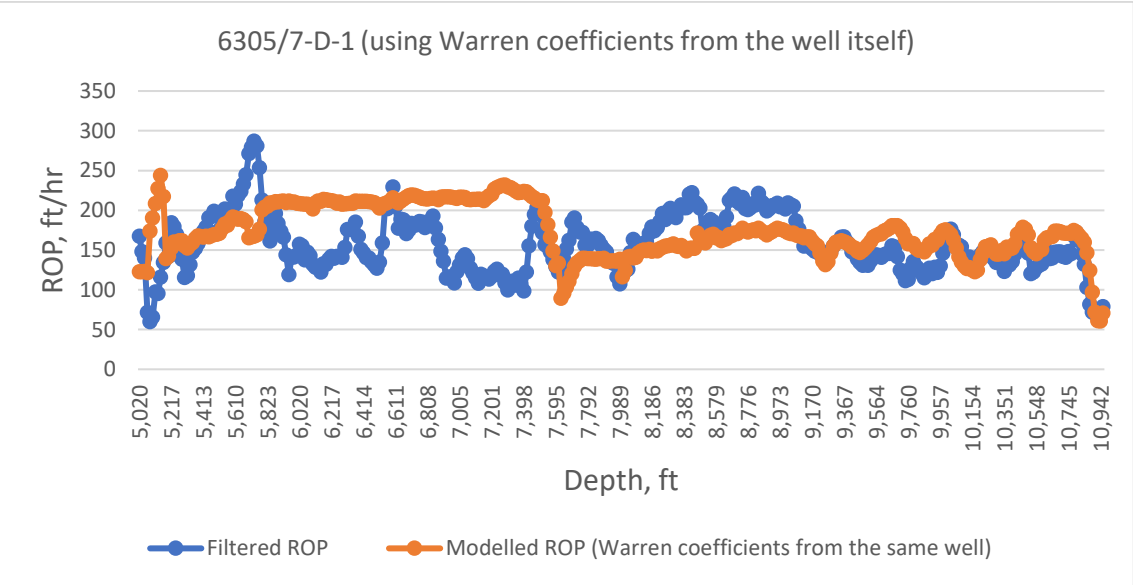

Figure 63. Warren ROP for 6305/7-D-1 H (using coefficients from the geological groups for the same well).

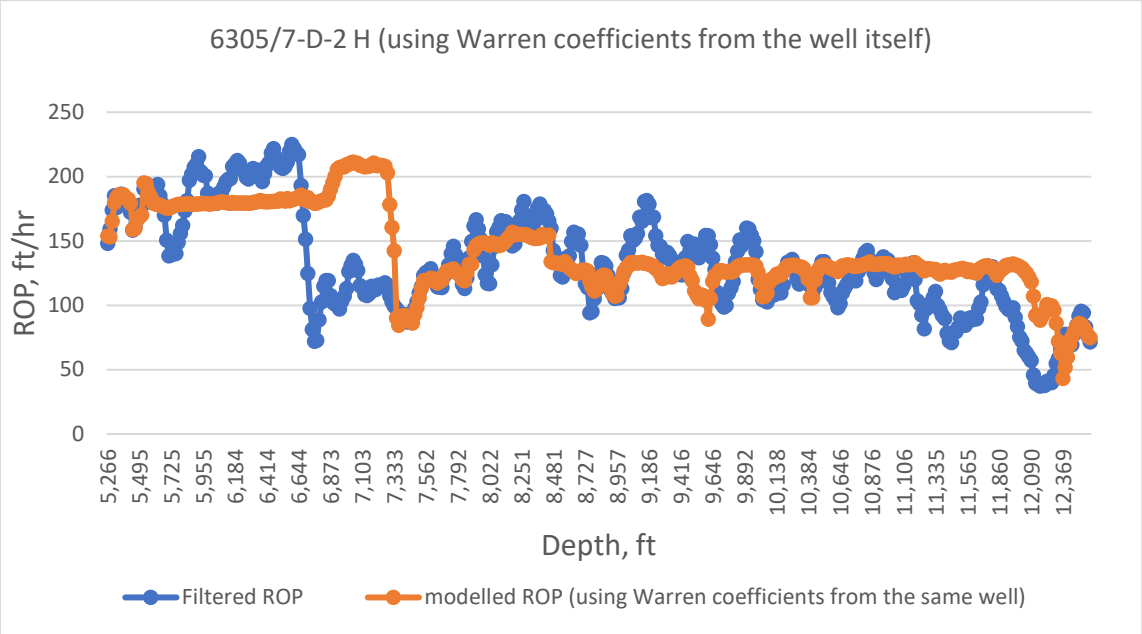

Figure 64. Warren ROP for 6305/7-D-2 H (using coefficients from the geological groups for the same well).

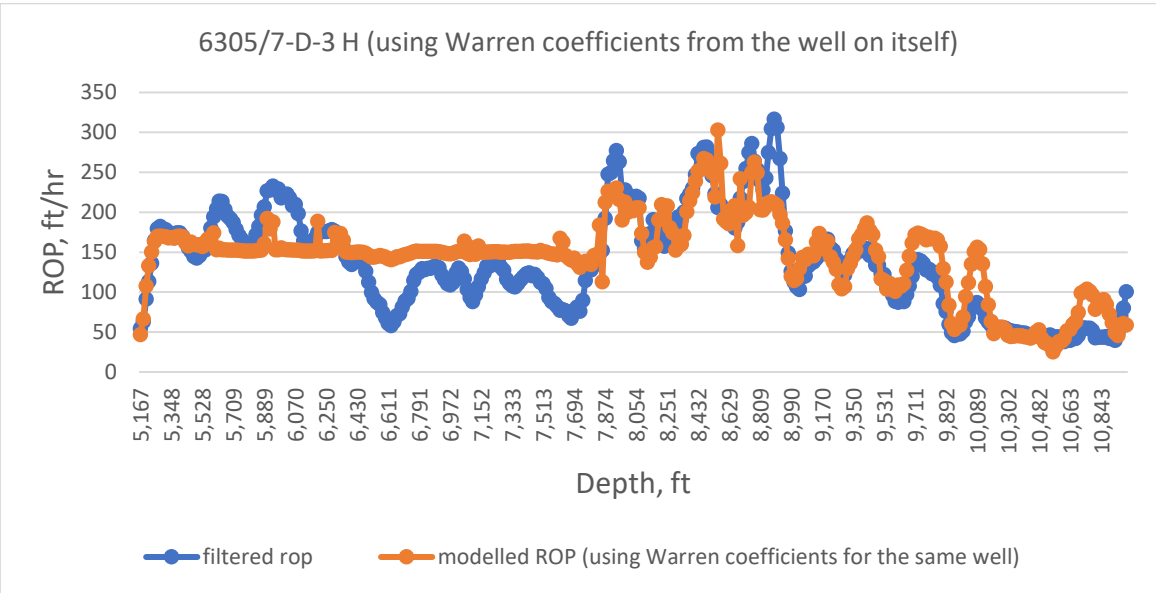

Figure 65. Warren ROP for 6305/7-D-3 H (using coefficients from the geological groups for the same well).

The resultant Warren ROP curves show good correlation with the filtered ROP and further validates the model, indicating that the model has a solid start. This can be seen when comparing Figures 63, 64 and 65 with Figures 54, 55 and 56, respectively.

Using coefficients from 6305/7-D-1 H:

The coefficients extracted from well 6305/7-D-1 H located in tables 20, 21 and 22 are used to model the Nordland, Hordaland and Rogaland groups in the respective geological groups. The results of this modeling are seen as graphs that compare the modelled Warren ROP and the filtered ROP in Figures 66 and 67.

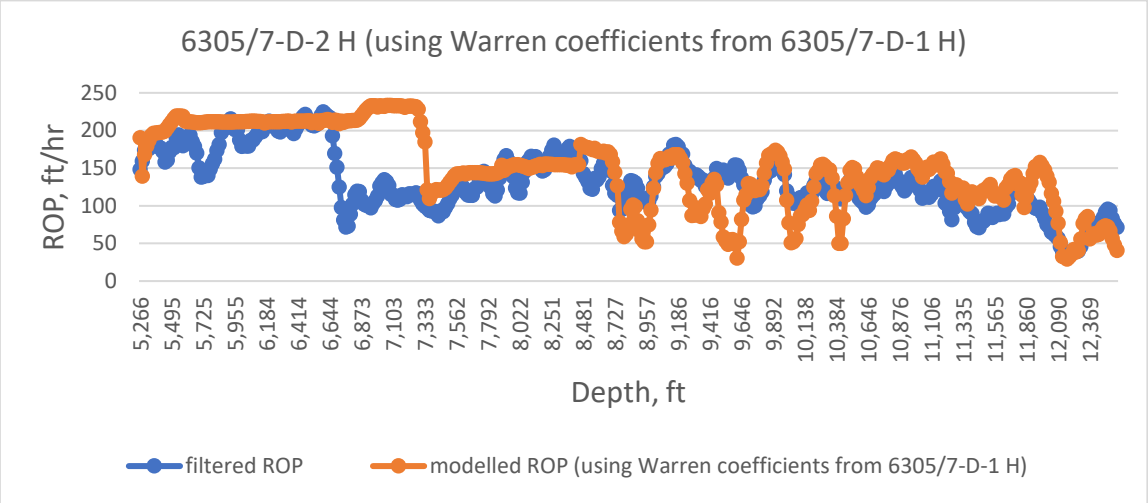

Figure 66. Warren ROP for 6305/7-D-2 H (using coefficients from the geological groups from 6305/7-D-1 H).

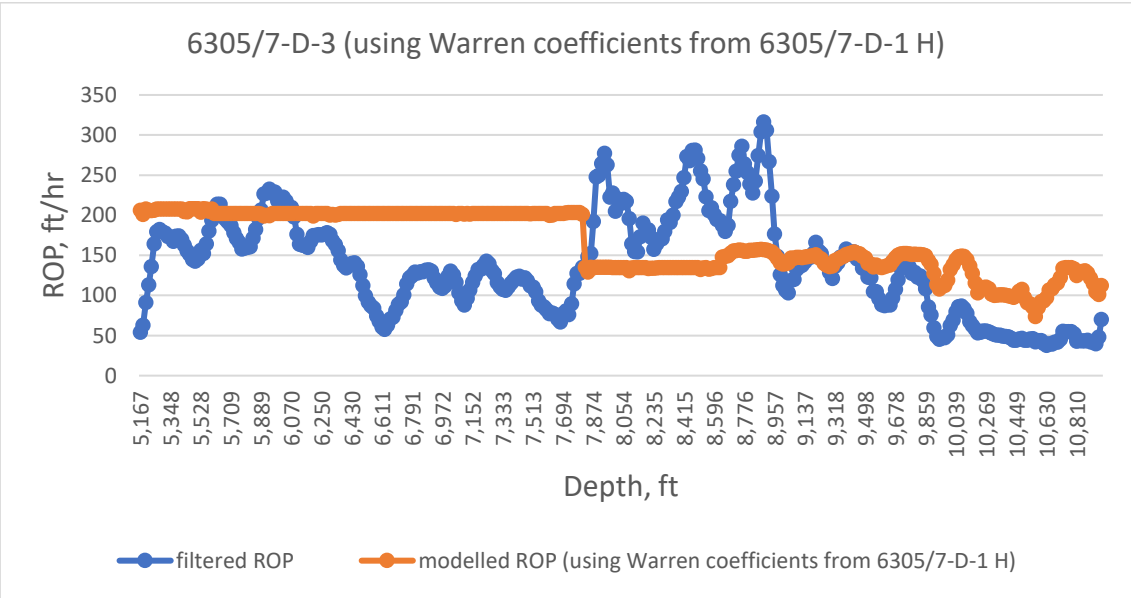

Figure 67. Warren ROP for 6305/7-D-3 H (using coefficients from the geological groups from 6305/7-D-1 H).

The results presented in Figures 66 and 67 show a smoother and better correlated modelled ROP than what was presented when the modelling was done for the whole well. This serves to prove that the geological group correlation improves the accuracy of ROP modelling and can serve to give more accurate values.

Using coefficients from 6305/7-D-2 H:

The coefficients extracted from well 6305/7-D-2 H found in tables 23, 24 and 25 are used to model the ROP for the three geological groups and then be compared to the filtered ROP of the wells 6305/7-D-1 H and 6305/7-D-2 H. The results of such modelling is illustrated in Figures 68 and 69

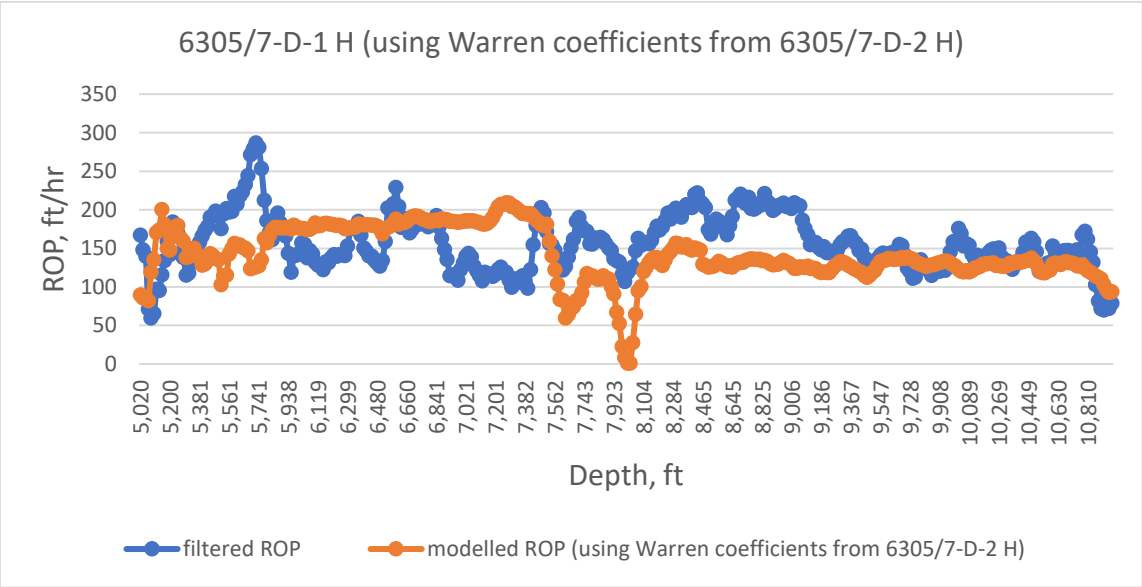

Figure 68. Warren ROP for 6305/7-D-1 H (using coefficients from the geological groups from 6305/7-D-2 H).

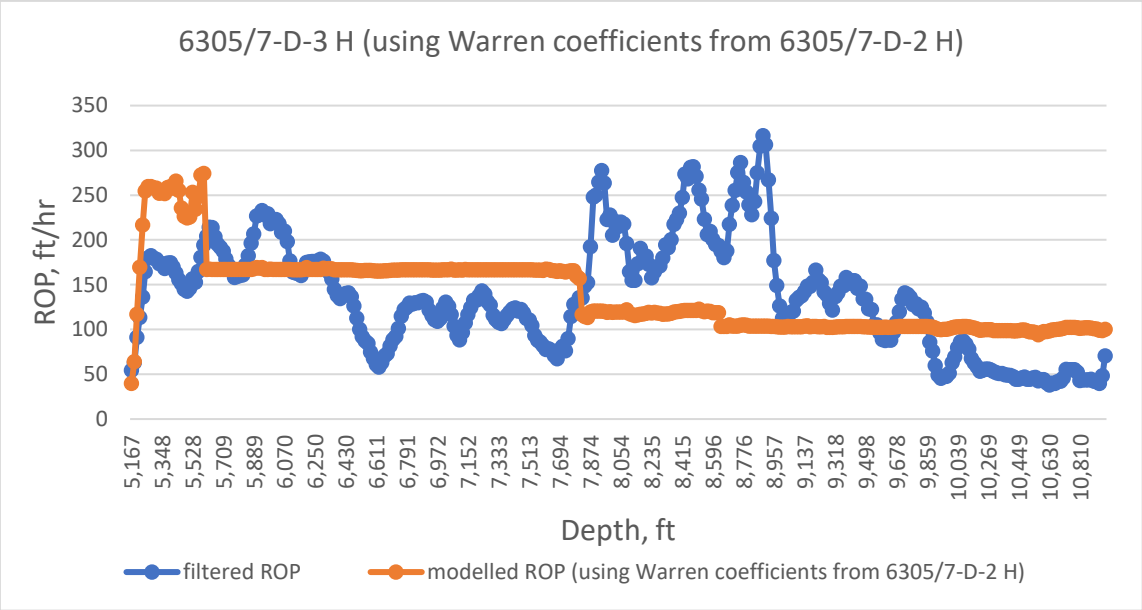

Figure 69. Warren ROP for 6305/7-D-3 H (using coefficients from the geological groups from 6305/7-D-2 H).

The results here again show smoother flow with the filtered ROP for both curves, where the modelled Warren ROP tries to match the filtered ROP even more than when we modelled the whole well. However, the results still show flat lines for well 6305/7-D-3 H and overestimation and underestimation in both cases above.

6 SUMMARY AND DISCUSSION

This chapter will analyze the results of the modelling presented in chapter 5 and review the rigidity of each modelling technique. This will be done through multiple methods to test how accurate the modelled ROP values are to the filtered ROP values. The methods used for the evaluation in the thesis work will be presented in this chapter.

6.1 Plot comparisons

As with all data-based modellings, achieving 100 % accuracy to the actual data is highly unlikely. However, to assess any model, a degree of accuracy needs to be made for the different data points. This is the goal of this subchapter and will done by testing if the modelled ROP values stay within a specific margin of the filtered ROP values. For this, two margins are used in this thesis and the multiple modelling techniques are tested.

The margins used in this thesis work are 5 % and 10 % deviations from the filtered ROP values. If the modelled ROP values stay within a margin of 5 %, then they share very strong correlation with the data and the difference can be considered insignificant statistically. The modelled ROP values that are within a -5 % to a +5 % deviation of the filtered ROP values will be included there.

The 10 % margin indicates a good correlation but not a perfect one, where the values might not be completely identical but are still close to the filtered ROP. The modelled ROP values that are within a -10 % to 10 % deviation of the filtered ROP will be included in this margin. Figure 70 gives an overview of how such deviations will look for a set of ROP values.

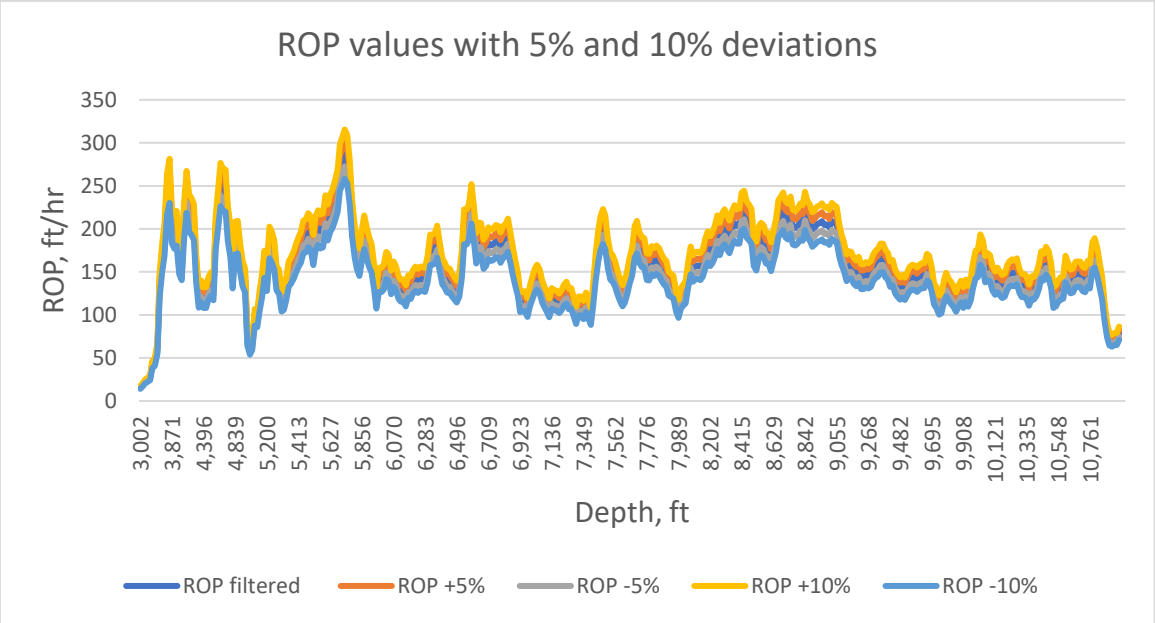

Figure 70. ROP deviations plot vs total depth.

In order to evaluate how much of the modelled values are inside the margins, the equation developed by Morten Husvæg [53], shown in Eq. 6.1, is used. This equation is applied for all the modelled ROP values using the multiple modelling methods. It returns "1" if the values are within the margins or "0" if they are not. The resultant "1" and "0" are then averaged and multiplied by 100 to give the percentage of modelled ROP values that are within the margins. Figures 71 and 72 give a demonstration of this model is used in Excel.

$$IF((ROP_{predicted}) = MEDIAN((ROP_{-X\%}):(ROP_{+X\%})); 1; 0 \quad (6.1)$$

SUM =IF(G2=MEDIAN(B2:D2);1;0)

	A	B	C	D	E	F	G	H
1	ROP filtered	-5 %	5 %	ROP geologically modelled	-10 %	10 %	ROP geologically modelled	if 5%
2	167,1456693	158,788386	175,502953	169,5616358	150,431102	183,860236	169,5616358	B2:D2);1;0)
3	148,0774278	140,673556	155,481299	129,4806709	133,269685	162,885171	129,4806709	0
4	139,8490814	132,856627	146,841535	116,3650084	125,864173	153,83399	116,3650084	0
5	71,46981627	67,8963255	75,0433071	96,36009649	64,3228346	78,6167979	96,36009649	0
6	59,79658793	56,8067585	62,7864173	67,29106092	53,8169291	65,7762467	67,29106092	0
7	65,40026247	62,1302493	68,6702756	75,48537956	58,8602362	71,9402887	75,48537956	0
8	97,17191601	92,3133202	102,030512	100,358585	87,4547244	106,889108	100,358585	1
9	95,22965879	90,4681759	99,9911417	95,75605625	85,7066929	104,752625	95,75605625	1
10	115,7217848	109,935696	121,507874	111,2789704	104,149606	127,293963	111,2789704	1

Figure 71. Application of the "IF" model.

SUM =100*AVERAGE(H2:H363)

	A	B	C	D	E	F	G	H	I
354	161,7716535	153,683071	169,860236	159,3053234	145,594488	177,948819	159,3053234	1	1
355	145,1574803	137,899606	152,415354	144,78719	130,641732	159,673228	144,78719	1	1
356	131,7650919	125,176837	138,353346	135,6534151	118,588583	144,941601	135,6534151	1	1
357	102,8674541	97,7240814	108,010827	102,4601531	92,5807087	113,154199	102,4601531	1	1
358	81,59448819	77,5147638	85,6742126	66,2546745	73,4350394	89,753937	66,2546745	0	0
359	71,74540682	68,1581365	75,3326772	46,2790335	64,5708661	78,9199475	46,2790335	0	0
360	69,92125984	66,4251969	73,4173228	57,34965034	62,9291339	76,9133858	57,34965034	0	0
361	71,9816273	68,3825459	75,5807087	62,54312096	64,7834646	79,17979	62,54312096	0	0
362	72,02755906	68,4261811	75,628937	66,2489077	64,8248031	79,230315	66,2489077	0	1
363	78,66141732	74,7283465	82,5944882	88,94256459	70,7952756	86,5275591	88,94256459	0	0
364								H2:H363)	73,2044199

Figure 72. Calculation of the percentage deviation of the modelled ROP.

The model demonstrated in the Figures is applied for all the modelling techniques and the resultant percentage deviations are presented in tables 29 and 30.

Table 29. percentage of data that are within a 5 % margin using all the modelling methods.

5 % margin	**Well**		
Modelling method applied	**6305/7-D-1 H**	**6305/7-D-2 H**	**6305/7-D-3 H**
multiple regressions (whole well) using coefficients from the well	31,26 %	21,04 %	11,27 %
multiple regressions (whole well) using coefficients from 6305/7-D-1 H		8,5 %	7,37 %

multiple regressions (whole well) using coefficients from 6305/7-D-2 H	6,63 %		10,57 %
multiple regressions (whole well) using coefficients from 6305/7-D-3 H	13,26 %	4,70 %	
multiple regressions (geo groups) using coefficients from the well	53,04 %	41,53 %	29,18 %
multiple regressions (geo groups) using coefficients from 6305/7-D-1 H		12,66 %	9,73 %
multiple regressions (geo groups) using coefficients from 6305/7-D-2 H	12,16 %		12,54 %
multiple regressions (geo groups) using coefficients from 6305/7-D-3 H	19,60 %	10,56 %	
MSE (coefficients from 6305/7-D-1 H)		9,97 %	5,72 %
MSE (coefficients from 6305/7-D-2 H)	10,17 %		4,66 %
MSE (coefficients from 6305/7-D-3 H)	5,96 %	3,93 %	
D-exponent (coefficients from 6305/7-D-1 H)		6,78 %	5,71 %
D-exponent (coefficients from 6305/7-D-2 H)	7,44 %		7,11 %
D-exponent (coefficients from 6305/7-D-3 H)	5,71 %	7,11 %	
Warren model (whole well) using coefficients from the well	15,14 %	21,81 %	4,93 %
Warren model (whole well) using coefficients from 6305/7-D-1 H		8,64 %	6,90 %
Warren model (whole well) using coefficients from 6305/7-D-2 H	11,60 %		9,36 %

Warren model (whole well) using coefficients from 6305/7-D-3 H	10,70 %	8,93 %	
Warren model (geo groups) using coefficients from the well	12,15 %	28,18 %	14,25 %
Warren model (geo groups) using coefficients from 6305/7-D-1 H		14,09 %	13,56 %
Warren model (geo groups) using coefficients from 6305/7-D-2 H	13,40 %		12,75 %

Table 30. percentage of data that are within a 10 % margin using all the modelling methods.

10 % margin	**Well**		
Modelling method applied	**6305/7-D-1 H**	**6305/7-D-2 H**	**6305/7-D-3 H**
multiple regressions (whole well) using coefficients from the well	54,59 %	38,61 %	23,53 %
multiple regressions (whole well) using coefficients from 6305/7-D-1 H		22,75 %	18,67 %
multiple regressions (whole well) using coefficients from 6305/7-D-2 H	19,06 %		19,90 %
multiple regressions (whole well) using coefficients from 6305/7-D-3 H	24,59 %	10,44 %	
multiple regressions (geo groups) using coefficients from the well	73,20 %	69,84 %	55,81 %
multiple regressions (geo groups) using coefficients from 6305/7-D-1 H		31,27 %	18,29 %
multiple regressions (geo groups) using coefficients from 6305/7-D-2 H	28,54 %		24,50 %
multiple regressions (geo groups) using coefficients from 6305/7-D-3 H	36,48 %	19,90 %	

MSE (coefficients from 6305/7-D-1 H)		19,18 %	10,70 %
MSE (coefficients from 6305/7-D-2 H)	19,35 %		9,07 %
MSE (coefficients from 6305/7-D-3 H)	11,41 %	7,86 %	
D-exponent (coefficients from 6305/7-D-1 H)		13,07 %	11,66 %
D-exponent (coefficients from 6305/7-D-2 H)	13,65 %		14,22 %
D-exponent (coefficients from 6305/7-D-3 H)	11,17 %	14,22 %	
Warren model (whole well) using coefficients from the well	27,30 %	40,60 %	8,62 %
Warren model (whole well) using coefficients from 6305/7-D-1 H		18,79 %	13,79 %
Warren model (whole well) using coefficients from 6305/7-D-2 H	23,76 %		15,02 %
Warren model (whole well) using coefficients from 6305/7-D-3 H	20,65 %	22,66 %	
Warren model (geo groups) using coefficients from the well	27,07 %	46,42 %	33,05 %
Warren model (geo groups) using coefficients from 6305/7-D-1 H		28,87 %	12,54 %
Warren model (geo groups) using coefficients from 6305/7-D-2 H	24,81 %		9,97 %

The results of this analysis show an improvement in the accuracy of the models when geologically-grouped well data. This is observed when we compare the percentages of the ROP models that are within the 5 % and 10 % margins for the modelled ROP values

using the geological groups and for the ones using the whole well. This pattern is again observed when using the Warren model.

The multiple regression method using the geological groups and the model described in 4.3.1 gave good results, followed by the Warren's model using the geological groups as well. These where followed by the same models, however using the whole well data to model the ROP.

The d-exponent and MSE both came worst and close to each other when it comes to the number of ROP values that are within the 5 % and 10 % margins. This is mostly because they both assume identical geological correlation for the same depths between the multiple wells. This inaccurate assumption is most likely the reason for the errors in the modelled ROP values.

6.2 Mean absolute percentage error (MAPE)

The mean absolute percentage error (MAPE) is a method used to compute the accuracy of a forecast based on a model. This gives a percentage value that shows the average deviation the modelled dataset has from the actual dataset. The lower the MAPE value, the more accurate the forecast is to the actual dataset and a MAPE value of 0 indicates no deviation at all. This statistical technique is used in this thesis work to analyze the modelled ROP values for each modelling technique and observe how much the average modelled ROP value deviates from the filtered one. The technique is applied using Eq. 6.2 for all the modelled ROP values and is illustrated in Figures 73 and 74.

$$MAPE = \frac{100\ \%}{n} \sum_{i=1}^{n} \left| \frac{(ROP_{mod})_i - ROP_i}{ROP_i} \right| \tag{6.2}$$

Where "n" is the number of datapoints, ROP_{mod} is the modelled ROP and ROP is the filtered ROP.

SUM =ABS((A2-G2)/A2)

	A	B	C	D	E	F	G	H	I	J	K
1	ROP [ft/hr]	-5 %	5 %	ROP whole well	-10 %	10 %	ROP whole well	if 5%	if 10%	MAPE	
2	19,2191601	18,2582021	20,1801181	72,16201079	17,2972441	21,1410761	72,16201079	0	0	G2)/A2)	
3	24,1338583	22,9271654	25,3405512	77,35520087	21,7204724	26,5472441	77,35520087	0	0	2,20525628	
4	26,6272966	25,2959318	27,9586614	81,74576963	23,9645669	29,2900262	81,74576963	0	0	2,06999884	
5	29,1666667	27,7083333	30,625	83,23036356	26,25	32,0833333	83,23036356	0	0	1,85361246	
6	29,4619423	27,9888451	30,9350394	84,85640882	26,515748	32,4081365	84,85640882	0	0	1,88020417	
7	26,8307087	25,4891732	28,1722441	93,11237424	24,1476378	29,5137795	93,11237424	0	0	2,47036582	

Figure 73. calculating the MAPE for each datapoint

SUM =(100/408)*SUM(J2:J409)

	A	B	C	D	E	F	G	H	I	J	K	L	M
1	ROP [ft/hr]	-5 %	5 %	ROP whole well	-10 %	10 %	ROP whole well	if 5%	if 10%	MAPE			MAPE error
2	19,2191601	18,2582021	20,1801181	72,16201079	17,2972441	21,1410761	72,16201079	0	0	2,75469117			J409)
3	24,1338583	22,9271654	25,3405512	77,35520087	21,7204724	26,5472441	77,35520087	0	0	2,20525628			
4	26,6272966	25,2959318	27,9586614	81,74576963	23,9645669	29,2900262	81,74576963	0	0	2,06999884			
5	29,1666667	27,7083333	30,625	83,23036356	26,25	32,0833333	83,23036356	0	0	1,85361246			
6	29,4619423	27,9888451	30,9350394	84,85640882	26,515748	32,4081365	84,85640882	0	0	1,88020417			
7	26,8307087	25,4891732	28,1722441	93,11237424	24,1476378	29,5137795	93,11237424	0	0	2,47036582			
8	29,1535433	27,6958661	30,6112205	98,70506177	26,238189	32,0688976	98,70506177	0	0	2,38569692			
9	34,2454068	32,5331365	35,9576772	94,57076854	30,8208661	37,6699475	94,57076854	0	0	1,76156067			
10	40,3937008	38,3740157	42,4133858	97,62866767	36,3543307	44,4330709	97,62866767	0	0	1,41692803			

Figure 74. Calculating the MAPE for the modelling technique

The resultant MAPE values are presented in table 31.

Table 31. MAPE values for the multiple modelling methods.

MAPE values	**Well**		
Modelling method applied	**6305/7-D-1 H**	**6305/7-D-2 H**	**6305/7-D-3 H**
multiple regressions (whole well) using coefficients from the well	20,25 %	15,82 %	29,77 %
multiple regressions (whole well) using coefficients from 6305/7-D-1 H		23,98 %	61,70 %
multiple regressions (whole well) using coefficients from 6305/7-D-2 H	23,85 %		37,33 %
multiple regressions (whole well) using coefficients from 6305/7-D-3 H	42,20 %	33,53 %	
multiple regressions (geo groups) using coefficients from the well	7,944 %	8,75 %	13,76 %

multiple regressions (geo groups) using coefficients from 6305/7-D-1 H		17,84 %	40,77 %
multiple regressions (geo groups) using coefficients from 6305/7-D-2 H	27,19 %		27,05 %
multiple regressions (geo groups) using coefficients from 6305/7-D-3 H	24,29 %	37,33 %	
MSE (coefficients from 6305/7-D-1 H)		62,63 %	49,41 %
MSE (coefficients from 6305/7-D-2 H)	32,80 %		40,86 %
MSE (coefficients from 6305/7-D-3 H)	42,53 %	78,26 %	
D-exponent (coefficients from 6305/7-D-1 H)		103,38 %	111,73 %
D-exponent (coefficients from 6305/7-D-2 H)	52,87 %		76,76 %
D-exponent (coefficients from 6305/7-D-3 H)	48,06 %	57,60 %	
Warren model (whole well) using coefficients from the well	4,17 %	27,54 %	76,23 %
Warren model (whole well) using coefficients from 6305/7-D-1 H		52,18 %	97,99 %
Warren model (whole well) using coefficients from 6305/7-D-2 H	27,03 %		63,01 %
Warren model (whole well) using coefficients from 6305/7-D-3 H	49,69 %	41,09 %	
Warren model (geo groups) using coefficients from the well	26,96 %	22,94 %	25,74 %
Warren model (geo groups) using coefficients from 6305/7-D-1 H		28,45 %	61,72 %

Warren model (geo groups) using coefficients from 6305/7-D-2 H	37,37 %		50,81 %

The MAPE analysis gave results that further confirm the finding in the plot comparisons in the subchapter above. The multiple regression modelling, using the geological groups, gave the least MAPE values, indicating that it had the least deviation from the filtered ROP. This was then followed by using the Warren model, using the geological groups, which gave some deviation.

The multiple regression model using data from the whole well and the MSE model both gave decent MAPE values, this indicates a somewhat good correlation between the modelled values and the filtered ROP values.

The Warren model, using well data from the whole well, and the d-exponent modelling gave the worst results with the average modelled ROP values being furthest away from the average filtered ROP value.

6.3 Time analysis

Time analysis is applied on the resultant ROP values from the different models to evaluate results of real-life application of the models and how late or soon the drilling will be completed for the wells if the model was used to predict the ROP. This analysis procedure allows models that had fluctuation in their data to still predict a good drilling time for the whole well. Eq. 6.3 represents the method to calculate the drilling time for each well, assuming no nonproductive time and the whole well is drilled in one go.

$$t_d = \frac{depth_{drilled}}{ROP} \tag{6.3}$$

Where t_d is the drilling time, $depth_{drilled}$ is the drilling depth and ROP is the average rate of penetration for the depth drilled.

Considering that we have all the depth intervals for the wells and the start and finish ROP for these intervals, calculating the drilling time for each interval is possible. Thus, the well is dissected into multiple depth intervals and the time to drill each section is calculated. This is then summed up to calculate the drilling time for the whole well. This is presented in Eq. 6.4 and Figure 75.

$$t_d = \sum_{i=1}^{n} \frac{2((depth_{drilled})_{i+1} - (depth_{drilled})_i)}{ROP_{i+1} + ROP_i} \tag{6.4}$$

SUM =2*(K3-K2)/(A3+A2)

	A	B	C	D	E	F	G	H	I	J	K	L
1	ROP filtered	-5 %	5 %	ROP geologically modelled	-10 %	10 %	ROP geologically modelled	if 5%	if 10%	MAPE	Tot Depth [ft	drilling time
2	167,1456693	158,788386	175,502953	169,5616358	150,431102	183,860236	169,5616358	1	1	0,01445426	3001,9685	A3+A2)
3	148,0774278	140,673556	155,481299	129,4806709	133,269685	162,885171	129,4806709	0	0	0,12558806	3018,3727	

Figure 75. calculating drilling time for interval.

The calculated drilling time of the modelled ROP from the multiple techniques is then compared to the drilling time of filtered ROP. Thus, the time deviation from using the modelling techniques can be calculated. The lower the time deviation percentage, the more accurate the model. This is presented in table 31.

Table 32. Drilling time deviation for the different models.

Time deviation (%)	**Well**		
Modelling method applied	**6305/7-D-1 H**	**6305/7-D-2 H**	**6305/7-D-3 H**
multiple regressions (whole well) using coefficients from the well	-0,25 %	-0,28 %	+3,45E-13 %
multiple regressions (whole well) using coefficients from 6305/7-D-1 H		+10,91 %	+22,07 %
multiple regressions (whole well) using coefficients from 6305/7-D-2 H	-13,16 %		-9,48 %

multiple regressions (whole well) using coefficients from 6305/7-D-3 H	+18,71 %	-1,89 %	
multiple regressions (geo groups) using coefficients from the well	+7,41E-13 %	-0,13 %	+9,48E-12 %
multiple regressions (geo groups) using coefficients from 6305/7-D-1 H		+0,82 %	-2,71 %
multiple regressions (geo groups) using coefficients from 6305/7-D-2 H	+0,46 %		+7,30 %
multiple regressions (geo groups) using coefficients from 6305/7-D-3 H	-3,33 %	-9,48 %	
MSE (coefficients from 6305/7-D-1 H)		+54,23 %	-0,85 %
MSE (coefficients from 6305/7-D-2 H)	-29,48 %		-34,15 %
MSE (coefficients from 6305/7-D-3 H)	+7,33 %	+69,93 %	
D-exponent (coefficients from 6305/7-D-1 H)		+59,47 %	+65,54 %
D-exponent (coefficients from 6305/7-D-2 H)	-9,24 %		+23,53 %
D-exponent (coefficients from 6305/7-D-3 H)	-24,90 %	+2,18 %	
Warren model (whole well) using coefficients from the well	+15,87 %	+8,05 %	+34,18 %
Warren model (whole well) using coefficients from 6305/7-D-1 H		+34,03 %	+36,61 %
Warren model (whole well) using coefficients from 6305/7-D-2 H	-9,31 %		+4,37 %

Warren model (whole well) using coefficients from 6305/7-D-3 H	+10,94 %	+17,55 %	
Warren model (geo groups) using coefficients from the well	+10,26 %	+6,58 %	+5,88 %
Warren model (geo groups) using coefficients from 6305/7-D-1 H		+13,22 %	+20,11 %
Warren model (geo groups) using coefficients from 6305/7-D-2 H	-9,49 %		+0,67 %

The results in the time deviation give the models a better usability in operations, where the deviations that where seen for the modelled ROP values gets minimized in this analysis and the models give more accurate prediction of the drilling time.

The best fit model at predicting the drilling time is the multiple linear regressions, using the geological model. This model gave extremely good results that might be considered within margins of error. This reinforces the observations that this model has been, consistently, the best model at predicting the ROP.

The Warren model by geological groups and the regression model, using whole well data, follow at predicting the drilling time, where both show small deviation from the calculated drilling time. This is then followed by the Warren model, using the whole well data and trailing just behind. The MSE and d-exponent modelling both gave similar deviations from the drilling time and where worst at predicting the drilling time.

6.4 Parametric sensitivity study

The aim of a parametric sensitivity study is to analyze which of the operational parameters are the ones that affect the ROP the most. By doing so, these parameters can be optimized and changed to control the ROP and achieve the ROP values desired. This gives the operators a better understanding for when they plan to drill a well nearby to an already drilled one.

In order to do the sensitivity study, the operational parameters used in the modelling process are increased and decreased by 10% and then the new ROP is modelled and compared to the old one. When doing so for each parameter independently, we can see which one is the most dominant in the model and what combination of increases or decreases will promote the highest ROP. The operational parameters that will be tested in this thesis are the WOB, Torque, RPM and the flow rate.

After the parametric study is done and the parameters are deduced. The drilling time using the new ROP will be calculated and compared with the old ROP values to observe how much time and money could be saved by such an analysis.

The parametric analysis will be applied on well 6305/7-D-1 H using the geological model that was applied in chapter 5 for the well on itself. The results will be presented in Figures 76 to 79.

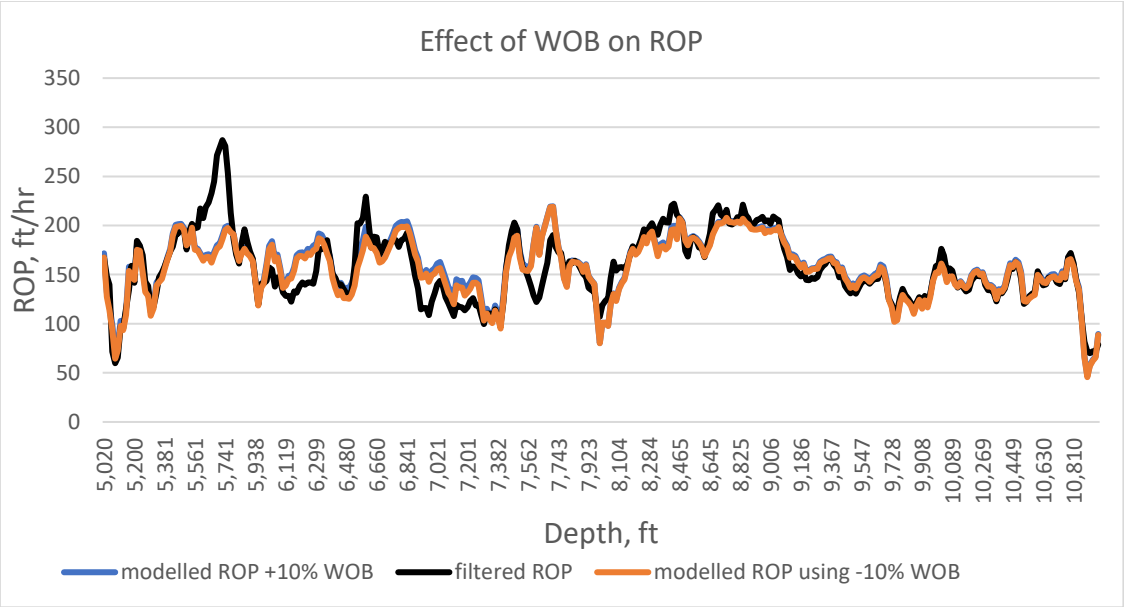

Figure 76. The effect of increasing or decreasing WOB by 10% on the modelled ROP.

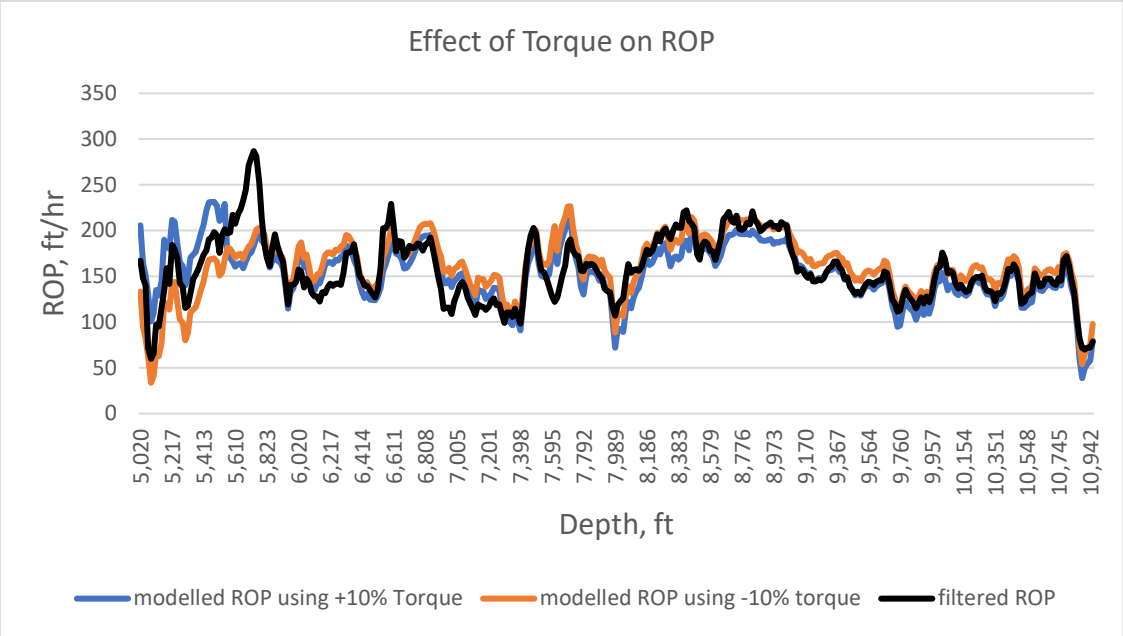

Figure 77. The effect of increasing or decreasing torque by 10% on the modelled ROP.

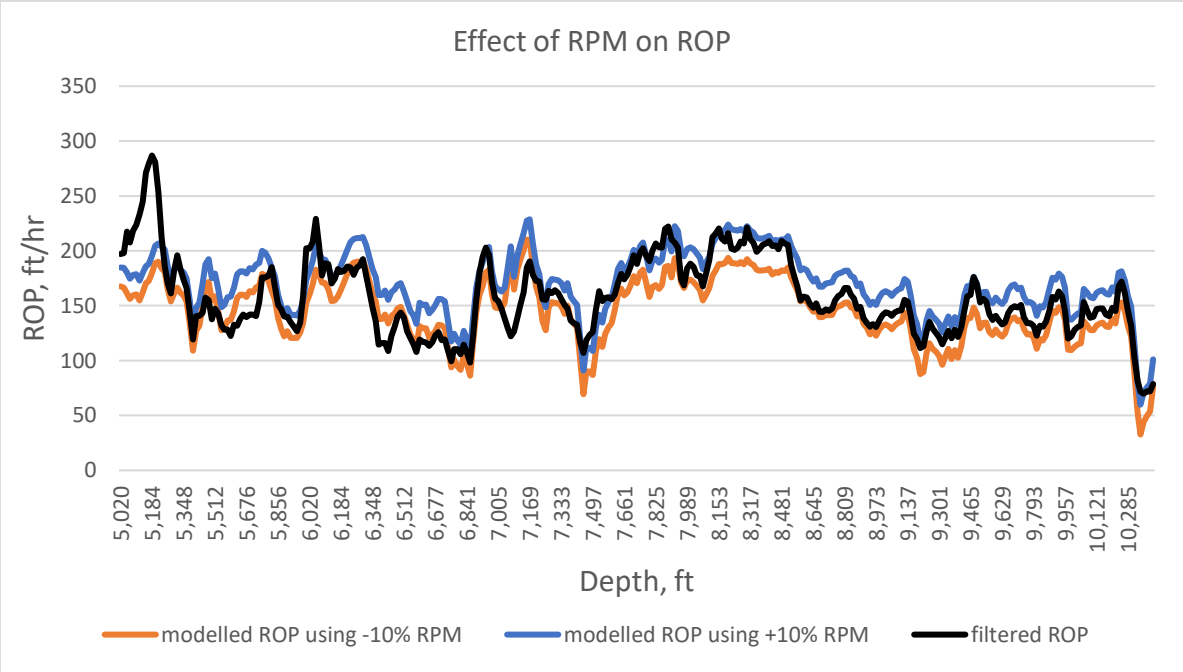

Figure 78. The effect of increasing or decreasing RPM by 10% on the modelled ROP.

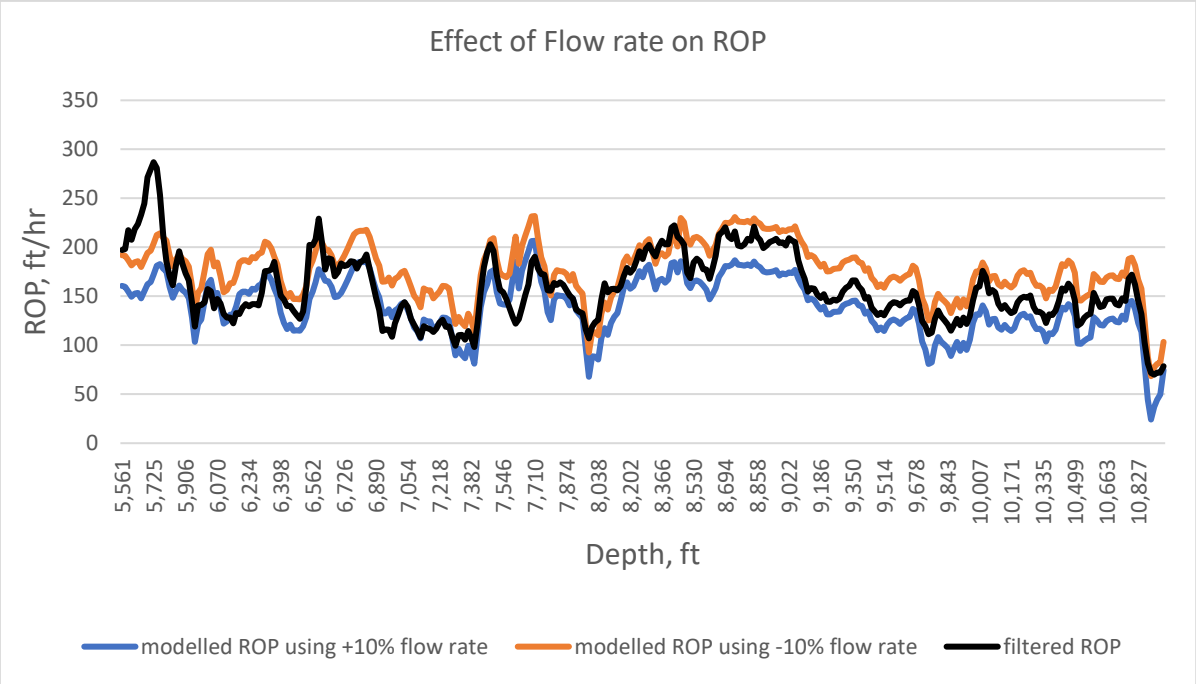

Figure 79. The effect of increasing or decreasing flow rate by 10% on the modelled ROP.

Figure 80 illustrates the impact that each operational parameter has on the modelled ROP. It compares the average modelled ROP values after a 10 % increase or decrease to each parameter. The most dominant parameters that can be seen in both the Figures and the table are both the RPM and the Torque, where an increase in RPM and a decrease in torque will be the factors that mostly affect the ROP. This is due to the coefficients from the model we extracted for this well, where the higher the coefficient, the more emphasis it has on the modelled ROP.

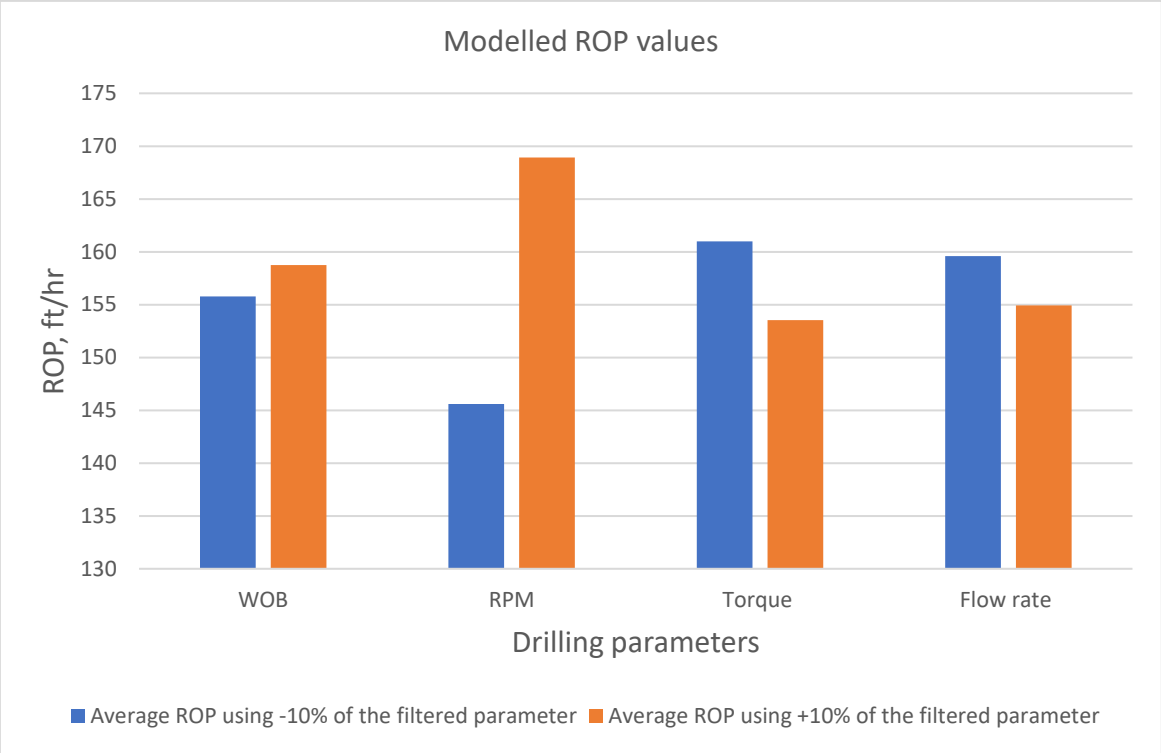

Figure 80. Average of the modelled ROP (using 10% deviations from the filtered operational parameters).

These two parameters are combined to optimize the drilling of a new well using this model. This is demonstrated by increasing the RPM by 10 % and decreasing the torque by 10 % for wells 6305/7-D-2 H and 6305/7-D-3 H as shown in Figures 81 and 82. Doing so will yield the highest modelled ROP for the wells.

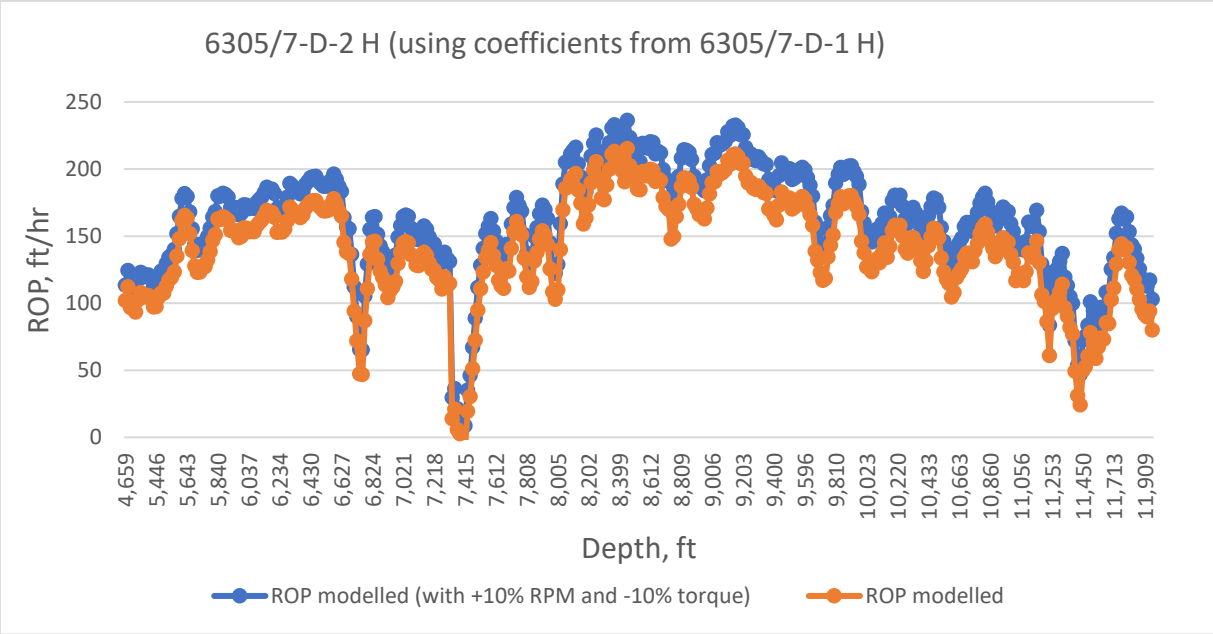

Figure 81. Sensitivity analysis – modelled ROP for 305/7-D-2 H after increasing RPM by 10 % and decreasing torque by 10 % vs. modelled ROP (using coefficients from 6305/7-D-1 H).

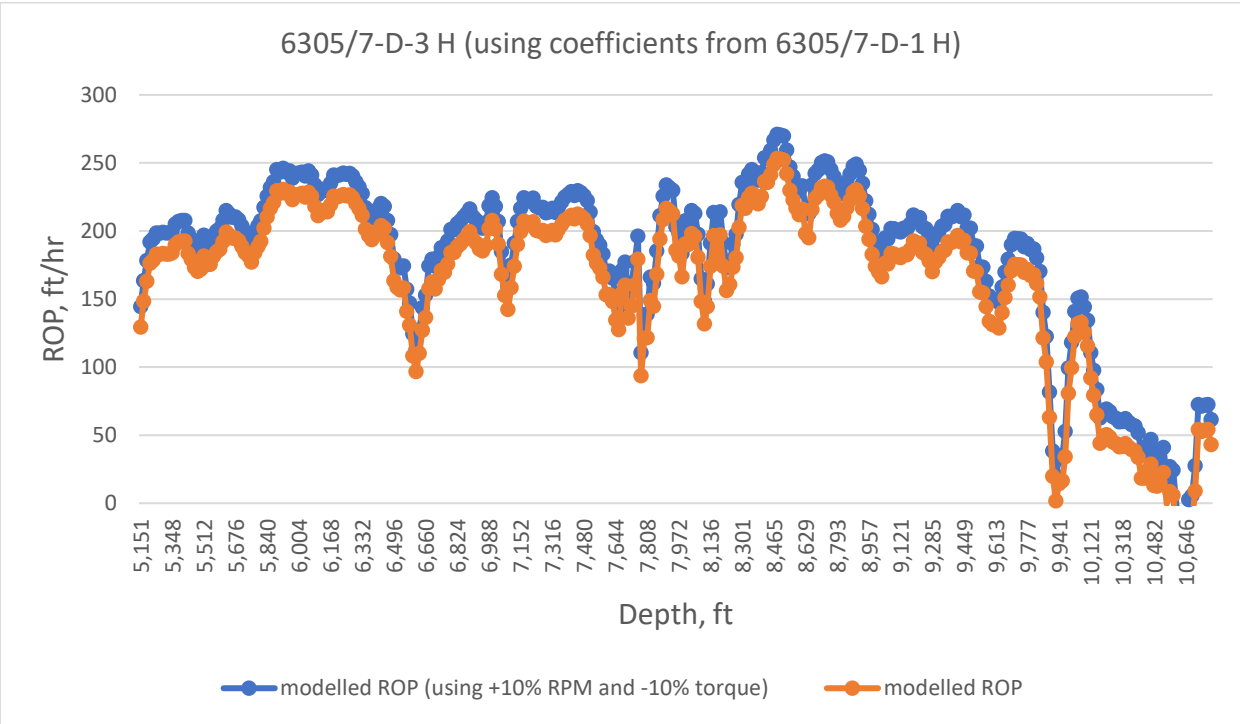

Figure 82. Sensitivity analysis – modelled ROP for 305/7-D-3 H after increasing RPM by 10 % and decreasing torque by 10 % vs. modelled ROP (using coefficients from 6305/7-D-1 H).

Both wells saw an increase in the modelled ROP, this increase in ROP will lead to a decrease in drilling time and the drilling expenses. The new drilling time is calculated in the same manner as in the time analysis and compared to the drilling time for the well without any changes in the parameters. This is shown in Figure 83 below, where both wells 6305/7-D-2 H and 6305/7-D-3 H had a reduction between 10.49 % and 12.49 % in their drilling time and since the drilling time is proportional to the drilling cost, this will lower the drilling cost by the same percentages.

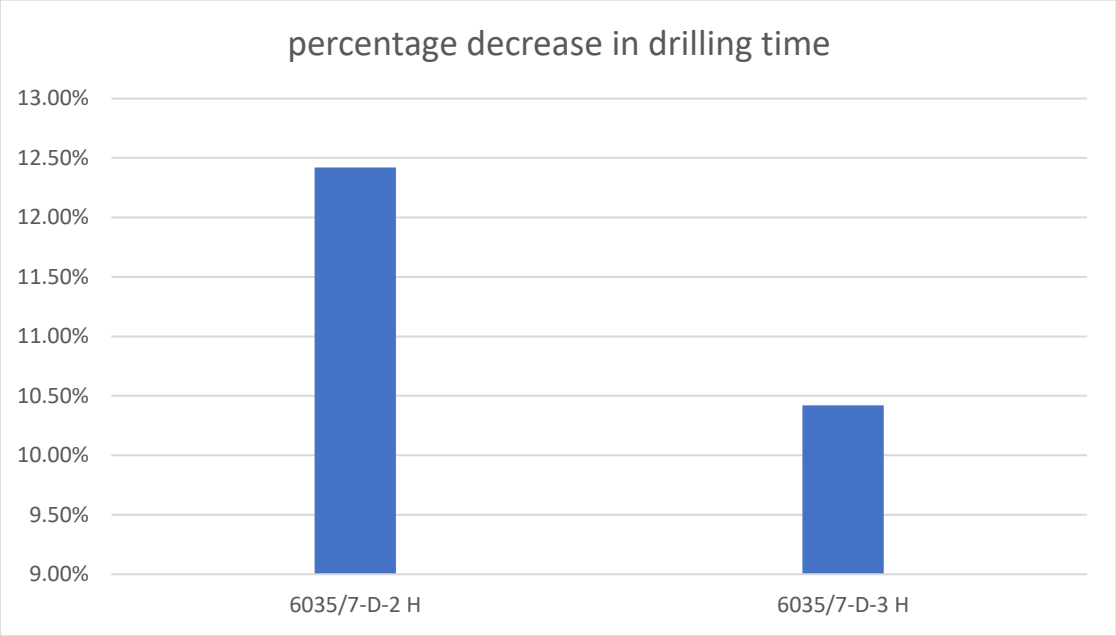

Figure 83. percentage decrease in drilling time for wells 6305/7-D-2 H and 6305/7-D-3 H when using +10% RPM and -10% torque.

6.5 Analysis summary

In order to achieve good modelling of the ROP, multiple modelling techniques need to be evaluated in order to decide which of the methods results in the best fit model for the datasets. This subchapter will evaluate the results of the analysis performed on the multiple modelling techniques in chapter 6 and discuss the feasibility of the modelling techniques used in this thesis.

As observed in the works of Malik and Morten, the modelling techniques used in this thesis give good correlation with the well data when the coefficients are used from one

well to another. The aim was to improve on the modelling techniques for the regression method. The analysis results can be expressed in Table 33.

Table 33. Analysis of the modelling techniques.

Method	Analysis of modelling techniques		
	Plot comparison	MAPE	Time analysis
Linear regression (whole well)	Good correlation with the filtered ROP values with some deviation	Low deviation of the average ROP value from the average filtered ROP value	Good prediction of the drilling time with little deviation from the actual one
Linear regression (geological groups)	Excellent correlation with the filtered ROP values	Deviations are small enough to be considered statistically insignificant	The expected drilling time using this modelling is almost identical
MSE	Bad correlation with the ROP values when compared to the other models	Higher deviations of the average modelled ROP compared to the other models	Worse drilling time prediction when compared to the other modelling techniques
d-exponent	Bad correlation with the ROP values when compared to the other models	Higher deviations of the average modelled ROP compared to the other models	Worse drilling time prediction when compared to the other modelling techniques
Warren model (whole well)	Good correlation with the filtered ROP values with some deviation	Low deviation of the average ROP value from the average filtered ROP value	Good prediction of the drilling time with little deviation from the actual one
Warren model (geological groups)	Excellent correlation with the filtered ROP values	Deviations are small enough to be considered statistically insignificant	Good prediction of the drilling time with little deviation from the actual one

6.6 Optimization methods for the field application

ROP optimization has been the focus of this thesis, and the method devised that resulted in the highest prediction of ROP for a nearby well are:

1. **Step 1** For the application of the modelling, the best approach is first to identify the stratigraphic section of the old drilled well and the well to be drilled at nearby.

2. **Step 2** The data from the old well is filtered to remove any data outliers using a moving average filter.

3. **Step 3** The Linear regression coefficients and Warren coefficients for each stratigraphic section are derived (depending on the section that is to be drilled and the geology in it)

4. **Step 4** Model can be tested on pre-drilled wells to be verified.

5. **Step 5** The modelled ROP values from the pre-drilled wells are checked against the filtered ones using plot comparisons, MAPE and time analysis.

6. **Step 6** Based on the correlation coefficient, do a parameter sensitivity analysis with a certain +/- increment, to calculate the ROP and the time to drill out the section. The operational parameters with the highest impact on the ROP to not be changed during application for the nearby well.

7. **Step 7** Time analysis is applied on the resultant ROP values from the different models to evaluate results of real-life application of the models and how late or soon the drilling will be completed for the wells if the model was used to predict the ROP.

8. **Step 8** The sensitivity study can be redone as many times as needed until the best realistic combination of the parameters that give the lowest drilling time is decided.

7 CONCLUSIONS

Drilling operations are still at the age of optimizing their operations, with a lot of headroom ahead and more to improve upon. One such thing for drilling operations is the rate of penetration, where more research is still needed to devise a physical model that describes it. The primary goal of this thesis is to improve the drilling ROP modelling and increase its efficiency.

Based on previous work on the subject, the modelling was applied to nearby wells and the focus was improving the ROP models used. This was done by dissecting the well into stratigraphic or geological sections and modelling each of the sections to extract coefficients for them. The extracted coefficients were used to model the other wells and the resultant ROP values were then compared to the filtered ROP values. This was done for the Ormen Lange field using wells 6305/7-D-1 H, 6305/7-D-2 H and 6305/7-D-3 H.

The results of applying the different models show that that the regression based on geological groups gave the best fit values for the filtered ROP values. The approach of dissecting the well into geological sections before modelling also improved the accuracy of well-established models such as the Warren model. This was validated by the analysis done in chapter 6. This analysis was applied to all the modelling techniques to evaluate their efficiency and accuracy in predicting the ROP. This validates the power of modelling as a method of estimating the ROP when drilling a nearby well.

The model devised in this thesis does not consider the deviation of the wells. This is a factor that affects the ROP that was not considered and could be one of the factors that caused some deviation and mispredictions of the ROP values.

The modelled ROP for a well can be then optimized as shown in chapter 6.6 by the usage of a parametric sensitivity analysis. This is done to observe what operational parameters matter most and which changes will increase the ROP most to decrease both drilling time and drilling cost.

8 REFERENCES

1. Hareland, G., et al., *Increased Drilling Efficiency of Gas Storage Wells Proven Using Drilling Simulator*, in *CIPC/SPE Gas Technology Symposium 2008 Joint Conference*. 2008, Society of Petroleum Engineers: Calgary, Alberta, Canada. p. 7.
2. Berre, T., L.W. Tunbridge, and K. Hoeg, *The measurement of small strains and Ko-values in triaxial tests on clay-shales*. Vol. 197. 1996. 194-X.
3. Zausa, F., et al., *Real-Time Wellbore Stability Analysis at the Rig-Site*, in *SPE/IADC Drilling Conference*. 1997, Society of Petroleum Engineers: Amsterdam, Netherlands. p. 10.
4. Tokle, K., P. Horsrud, and R.K. Bratli, *Predicting Uniaxial Compressive Strength From Log Parameters*, in *SPE Annual Technical Conference and Exhibition*. 1986, Society of Petroleum Engineers: New Orleans, Louisiana. p. 8.
5. Rampersad, P.R., G. Hareland, and P. Boonyapaluk, *Drilling Optimization Using Drilling Data and Available Technology*, in *SPE Latin America/Caribbean Petroleum Engineering Conference*. 1994, Society of Petroleum Engineers: Buenos Aires, Argentina. p. 9.
6. Hareland, G., et al., *Cutting Efficiency of a Single PDC Cutter on Hard Rock.* Journal of Canadian Petroleum Technology, 2009. **48**(06): p. 60-65.
7. Hareland, G., et al., *Drilling Simulation Improves Field Communication and Reduces Drilling Cost in Western Canada*, in *Canadian International Petroleum Conference*. 2007, Petroleum Society of Canada: Calgary, Alberta. p. 7.
8. Rastegar, M., et al., *Optimization of Multiple Bit Runs Based on ROP Models and Cost Equation: A New Methodology Applied for One of the Persian Gulf Carbonate Fields*, in *IADC/SPE Asia Pacific Drilling Technology Conference and Exhibition*. 2008, Society of Petroleum Engineers: Jakarta, Indonesia. p. 7.
9. Gjelstad, G., et al., *The Method of Reducing Drilling Costs More Than 50 Percent*, in *SPE/ISRM Rock Mechanics in Petroleum Engineering*. 1998, Society of Petroleum Engineers: Trondheim, Norway. p. 7.
10. Teale, R., *The concept of specific energy in rock drilling.* International Journal of Rock Mechanics and Mining Sciences & Geomechanics Abstracts, 1965. **2**(1): p. 57-73.
11. (U.S.), S.o.P.E. *Rotary drilling mechanism*. 29 August 2012 [cited 2019 17.04]; Available from: https://petrowiki.org/File:Devol2_1102final_Page_223_Image_0002.png.
12. Mitchell, R.F. and E. Society of Petroleum, *Petroleum engineering handbook. Vol. II Vol. II*. Vol. II. 2006, Richardson, Tex: SPE.
13. Varhaug, M. *Bits* The defining 2016; Available from: https://www.slb.com/-/media/Files/resources/oilfield_review/defining_series/Defining-Bits.pdf?la=en&hash=7AFD27FEAA283A428BEE202D460E458A604D0688.
14. (U.S.), s.o.P.E. *PDC drill bits* 8 August 2018 [cited 2019 20.04]; Available from: https://petrowiki.org/PDC_drill_bits?rel=2#Important_factors_to_consider_before_the_use_and_design_of_PDC_bits.

15. bits, S. *PDC and its components* 2012 29.08.2012 [cited 2019 27.04.2019]; Available from: https://petrowiki.org/File:Devol2_1102final_Page_242_Image_0001.png.
16. bits, S. *PDC cutter components* 2012 29.08.2012 [cited 2019 27.04.2019]; Available from: https://petrowiki.org/File:Devol2_1102final_Page_243_Image_0001.png.
17. Hughes, B. *Hughes Christensen Kymera hybrid drill bit* [cited 2019; an example of a hybrid bit]. Available from: https://no.pinterest.com/pin/476677941780303526/.
18. Ismail, A., et al., *Hybrid Drill Bit Combining Fixed-Cutter and Roller-Cone Elements Improves Drilling Performance in Challenging Application in the Western Desert*, in *SPE Middle East Oil and Gas Show and Conference*. 2013, Society of Petroleum Engineers: Manama, Bahrain. p. 9.
19. Onyia, E.C., *Relationships Between Formation Strength, Drilling Strength, and Electric Log Properties*, in *SPE Annual Technical Conference and Exhibition*. 1988, Society of Petroleum Engineers: Houston, Texas. p. 14.
20. Minaeian, B. and K. Ahangari, *Estimation of uniaxial compressive strength based on P-wave and Schmidt hammer rebound using statistical method*. Vol. 6. 2013. 1925-1931.
21. Bieniawski, Z.T. and M.J. Bernede, *Suggested methods for determining the uniaxial compressive strength and deformability of rock materials: Part 1. Suggested method for determining deformability of rock materials in uniaxial compression.* International Journal of Rock Mechanics and Mining Sciences & Geomechanics Abstracts, 1979. **16**(2): p. 138-140.
22. Anupoju, S. *Laboratory tests for determining strength of Rocks*. Available from: https://theconstructor.org/building/laboratory-tests-determine-strength-rocks/11665/.
23. William Calhoun, C.R.E., ChevronTexaco *New Confined Compressive Strength Calculation Improves Bit Selection*
and Bit Performance American association of drilling engineers 2005.
24. Mirzaei-Paiaman, A., et al., *Effect of Drilling Fluid Properties on Rate of Penetration*. Vol. 60. 2009.
25. Akpabio, J.U., 2Inyang, P. N., Iheaka, C. I. , *The Effect of Drilling Mud Density on Penetration Rate.* International Research Journal of Engineering and Technology (IRJET), 2015. **02**(09).
26. Cheatham, C.A. and J.J. Nahm, *Effects of Selected Mud Properties on Rate of Penetration in Full-Scale Shale Drilling Simulations*, in *SPE/IADC Drilling Conference*. 1985, Society of Petroleum Engineers: New Orleans, Louisiana. p. 9.
27. Mitchell Robert, F., et al., *Fundamentals of drilling engineering*. SPE textbook series. xiv, 696 pages.
28. Irawan, S., et al., *Optimization of Weight on Bit During Drilling Operation Based on Rate of Penetration Model*. Vol. 4. 2012.

29. Erdogan, Y., M. Yıldız, and O. Kök, *Correlating Rate of Penetration with the Weigth on Bit, Rotation per Minute, Flow Rate and Mud Weight of Rotary Drilling*. Vol. 3. 2018. 378-385.
30. Bourgoyne, A.T., *Applied drilling engineering*. SPE textbook series. 502 pages.
31. Morton, E.K. and W.R. Clements, *The Role of Bit Type and Drilling Fluid Type in Drilling Performance*, in *International Meeting on Petroleum Engineering*. 1986, Society of Petroleum Engineers: Beijing, China. p. 7.
32. Warren, T.M. and W.K. Armagost, *Laboratory Drilling Performance of PDC Bits.* SPE Drilling Engineering, 1988. **3**(02): p. 125-135.
33. Bahari, M., et al., *Drilling Rate Prediction Using Bourgoyne and Young Model Associated with Genetic Algorithm*. 2009.
34. Warren, T.M., *Drilling Model for Soft-Formation Bits.* Journal of Petroleum Technology, 1981. **33**(06): p. 963-970.
35. Warren, T.M., *Penetration Rate Performance of Roller Cone Bits.* SPE Drilling Engineering, 1987. **2**(01): p. 9-18.
36. Hareland, G. and L.L. Hoberock, *Use of Drilling Parameters To Predict In-Situ Stress Bounds*, in *SPE/IADC Drilling Conference*. 1993, Society of Petroleum Engineers: Amsterdam, Netherlands. p. 15.
37. Teale, R., *The concept of specific energy in rock drilling*. Vol. 2. 1965. 57-73.
38. Dupriest, F.E. and W.L. Koederitz, *Maximizing Drill Rates with Real-Time Surveillance of Mechanical Specific Energy*, in *SPE/IADC Drilling Conference*. 2005, Society of Petroleum Engineers: Amsterdam, Netherlands. p. 10.
39. Pessier, R.C. and M.J. Fear, *Quantifying Common Drilling Problems With Mechanical Specific Energy and a Bit-Specific Coefficient of Sliding Friction*, in *SPE Annual Technical Conference and Exhibition*. 1992, Society of Petroleum Engineers: Washington, D.C. p. 16.
40. Jorden, J.R. and O.J. Shirley, *Application of Drilling Performance Data to Overpressure Detection.* Journal of Petroleum Technology, 1966. **18**(11): p. 1387-1394.
41. Guo, B., G. Liu, and Knovel (Firm), *Applied drilling circulation systems : hydraulics, calculations, and models*. 1 online resource.
42. Bingham, M.G., *A new approach to interpreting-- rock drillability*. 1965, [Place of publication not identified]: Petroleum Pub. Co.
43. Rehm, B. and R. McClendon, *Measurement of Formation Pressure from Drilling Data*, in *Fall Meeting of the Society of Petroleum Engineers of AIME*. 1971, Society of Petroleum Engineers: New Orleans, Louisiana. p. 11.
44. Hareland, G. and P.R. Rampersad, *Drag - Bit Model Including Wear*, in *SPE Latin America/Caribbean Petroleum Engineering Conference*. 1994, Society of Petroleum Engineers: Buenos Aires, Argentina. p. 11.
45. C. Maurer, W., *The "Perfect - Cleaning" Theory of Rotary Drilling*. Vol. 14. 1962. 1270-1274.
46. Elahifar, B., et al., *ROP Modeling using NeuralNetwork and Drill String Vibration Data*, in *SPE Kuwait International Petroleum Conference and Exhibition*. 2012, Society of Petroleum Engineers: Kuwait City, Kuwait. p. 13.

47. Directorate, N.P. *Ormen Lange* 02.06.2019 02.06]; Available from: https://www.norskpetroleum.no/en/facts/field/ormen-lange/.
48. NPD. *Factmaps* [cited 2019 15. May]; NCS Factmaps]. Available from: http://gis.npd.no/factmaps/html_21/.
49. Mathuranathan. *Moving Average Filter (MA filter)*. 2010; Available from: https://www.gaussianwaves.com/2010/11/moving-average-filter-ma-filter-2/.
50. Smith, S.W., *The scientist and engineer's guide to digital signal processing*. 1997: California Technical Publishing. 625.
51. Deviant, S., *The Practically Cheating Statistics Handbook, the Sequel! (2nd Edition)*. 2010: CreateSpace Independent Publishing Platform.
52. Montgomery, D.C., *Introduction to Linear Regression Analysis*. 5th ed. ed. Wiley Series in Probability and Statistics, ed. E.A. Peck and G.G. Vining. 2013, Hoboken: Wiley.
53. Husvæg, M.A., *ROP modelling and analysis*. 2015, University of Stavanger, Norway.

APPENDIX I: More Reviewed ROP Models

Bourgoyne and Young model

As mentioned in chapter 3.1, the model devised by Bourgoyne and Young aims at defining the ROP as a function of 8 different parameters under drilling operations. The parameters are assumed to be the ones that mostly affect the ROP and are as follows: formation drill ability, formation strength and bit type, compaction on drilling penetration, overbalance on drilling rate, undercompaction found in abnormally pressured formations, weight on bit, rotary speed, tooth wear and the bit hydraulics. The model that they devised can be written as follows [33]:

$$ROP = f_1 x f_2 x f_3 x f_4 x f_5 x f_6 x f_7 x f_8 \quad \text{(A.1)}$$

Where functions 1 to 8 represent the parameters mentioned above and have coefficients (a_1 to a_8) are model constants that are determined experimentally and are specific for the well being drilled.

Term f_1 represents the formation strength the formation drill ability and can be expressed as follows [27]:

$$f_1 = e^{2.303a_1} \quad \text{(A.2)}$$

The term f_2 represents the effect of the compaction on the ROP and can be expressed as:

$$f_2 = e^{2.303a_2(10{,}000-D)} \quad \text{(A.3)}$$

Where D is the depth in feet. The term f_3 models the undercompaction that is found in abnormally pressured formations and is expressed as:

$$f_3 = e^{2.303a_3 D^{0.69}(g_p-9.0)} \quad \text{(A.4)}$$

Where $g_p$is the pore pressure gradient in pounds per gallon equivalent. The fourth term f_4 represents the effect of the overpressure on the ROP and is represented by the following model:

$$f_4 = e^{2.303 a_4 D(g_p - \rho_c)} \tag{A.5}$$

Where ρ_c is the mud weight in pound per gallon. The fifth term describes the effect of the weight on bit on the ROP. This can be described as:

$$f_5 = \left[\frac{\left(\frac{WOB}{d_b}\right) - \left(\frac{WOB}{d_b}\right)_t}{4.0 - \left(\frac{WOB}{d_b}\right)_t}\right]^{a_5} \tag{A.6}$$

Where $\left(\frac{WOB}{d_b}\right)_t$ represents the threshold weight on bit and can usually be neglected since its value is low. It can be estimated from drillof tests done at very low weight on bit. The sixth term represents the effect of rotary speed (N) on the ROP. This can be represented as:

$$f_6 = \left(\frac{N}{60}\right)^{a_6} \tag{A.7}$$

The term f_7 expresses the effect of bit wear on the ROP. This model can be expressed as:

$$f_7 = e^{-a_7 h} \tag{A.8}$$

Where h represents the fractional height of the worn away tooth and is expressed as following:

$$h = \frac{Dg}{8} * \frac{Depth_{current} - Depth_{initial}}{Depth_{cout} - Depth_{initial}} \tag{A.9}$$

Where Dg is the dull bit grade (IADC) for the bit when it is pulled out of the whole. The last term describes the effect of bit hydraulics on the ROP. This can be modelled as follows:

$$f_8 = \left(\frac{F_j}{1000}\right)^{a_8} \tag{A.10}$$

Where F_j represents the hydraulic jet impact force that the bit applies on the formation.

Drag Bit Model

The Drag bit model developed by Hareland and Rampersad assumes perfect wellbore cleaning under drilling operations using drag bits. The model devised by them can be described as [44]:

$$ROP = W_f\left(\frac{G * RPM^{\gamma} * WOB^{\alpha}}{d_b * UCS}\right) \tag{A.11}$$

Where γ is the RPM exponent and α is the WOB exponent. W_f represents the wear function and G is the ROP model constant that is dependent on the bit geometry.

Maurer Model

The Maurer model was developed with the assumption that the cleaning of the whole under drilling is perfect and that all cutting produced by the teeth are removed before the bit makes contact with the formation again. The model developed by Maurer can be expressed as following:

$$ROP = \frac{K}{S^2}\left[\frac{WOB}{d_b} - \left(\frac{WOB}{d_b}\right)_t\right]^2 N \tag{A.12}$$

Where K is constant of proportionality and $\left(\frac{WOB}{d_b}\right)_t$ is the threshold WOB.

Bingham Model

The Bingham model discussed in chapter 3.7 is a simplified version of the Maurer model that is only applicable for low values of WOB and rotary speed. This model assumes that the threshold WOB in the Maurer model is negligible and thus removed. The model is expressed as:

$$ROP = K\left(\frac{WOB}{d_b}\right)^{a_5} N \tag{A.13}$$

Where K is the constant of proportionality and a_5 is the WOB exponent and can be determined experimentally.

APPENDIX II: Modelling Application

Moving Average

The data used for the modelling in this thesis is filtered before application in order to remove any outliers in the dataset. Filtering data before applying multiple linear regression, increases the accuracy and reliability of a model. This is done in Excel using the Data Analysis package and the procedure can be seen in Figures 84 and 85.

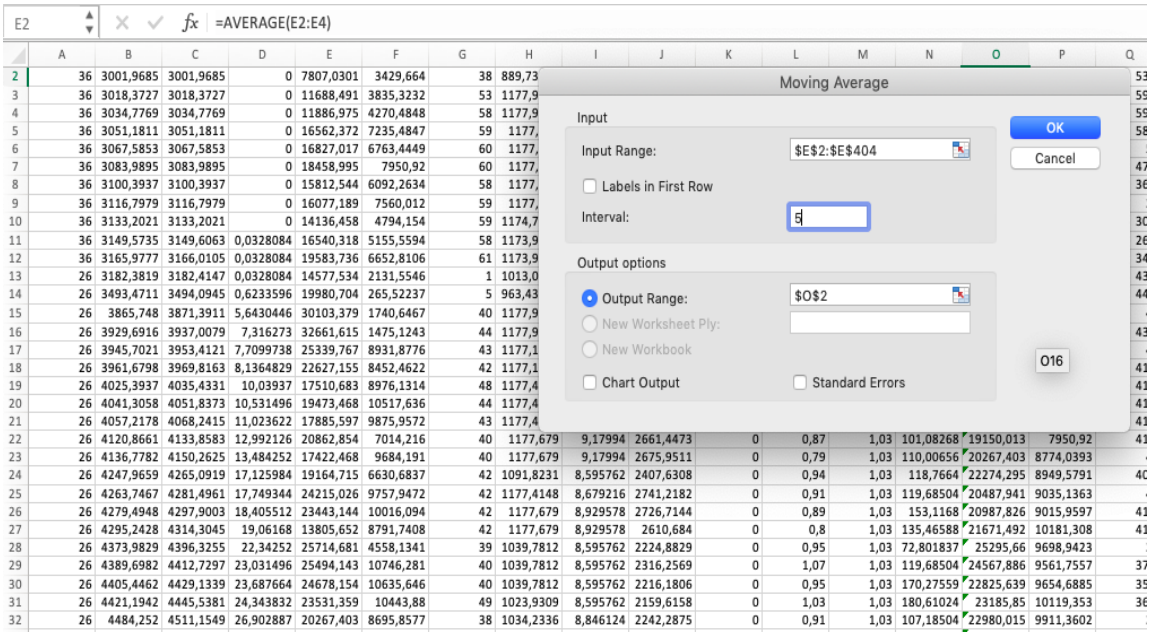

Figure 84. Moving Average filter using the data analysis package

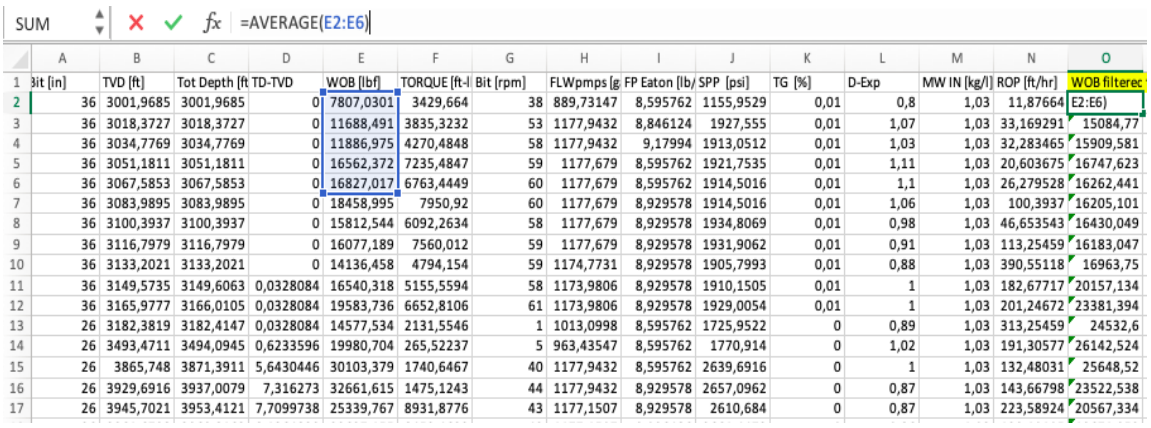

	A	B	C	D	E	F	G	H	I	J	K	L	M	N	O
1	Bit [in]	TVD [ft]	Tot Depth [ft	TD-TVD	WOB [lbf]	TORQUE [ft-l	Bit [rpm]	FLWpmps [g	FP Eaton [lb/	SPP [psi]	TG [%]	D-Exp	MW IN [kg/l]	ROP [ft/hr]	WOB filterec
2	36	3001,9685	3001,9685	0	7807,0301	3429,664	38	889,73147	8,595762	1155,9529	0,01	0,8	1,03	11,87664	E2:E6)
3	36	3018,3727	3018,3727	0	11688,491	3835,3232	53	1177,9432	8,846124	1927,555	0,01	1,07	1,03	33,169291	15084,77
4	36	3034,7769	3034,7769	0	11886,975	4270,4848	58	1177,9432	9,17994	1913,0512	0,01	1,03	1,03	32,283465	15909,581
5	36	3051,1811	3051,1811	0	16562,372	7235,4847	59	1177,679	8,595762	1921,7535	0,01	1,11	1,03	20,603675	16747,623
6	36	3067,5853	3067,5853	0	16827,017	6763,4449	60	1177,679	8,595762	1914,5016	0,01	1,1	1,03	26,279528	16262,441
7	36	3083,9895	3083,9895	0	18458,995	7950,92	60	1177,679	8,929578	1914,5016	0,01	1,06	1,03	100,3937	16205,101
8	36	3100,3937	3100,3937	0	15812,544	6092,2634	58	1177,679	8,929578	1934,8069	0,01	0,98	1,03	46,653543	16430,049
9	36	3116,7979	3116,7979	0	16077,189	7560,012	59	1177,679	8,929578	1931,9062	0,01	0,91	1,03	113,25459	16183,047
10	36	3133,2021	3133,2021	0	14136,458	4794,154	59	1174,7731	8,929578	1905,7993	0,01	0,88	1,03	390,55118	16963,75
11	36	3149,5735	3149,6063	0,0328084	16540,318	5155,5594	58	1173,9806	8,929578	1910,1505	0,01	1	1,03	182,67717	20157,134
12	36	3165,9777	3166,0105	0,0328084	19583,736	6652,8106	61	1173,9806	8,929578	1929,0054	0,01	1	1,03	201,24672	23381,394
13	26	3182,3819	3182,4147	0,0328084	14577,534	2131,5546	1	1013,0998	8,595762	1725,9522	0	0,89	1,03	313,25459	24532,6
14	26	3493,4711	3494,0945	0,6233596	19980,704	265,52237	5	963,43547	8,595762	1770,914	0	1,02	1,03	191,30577	26142,524
15	26	3865,748	3871,3911	5,6430446	30103,379	1740,6467	40	1177,9432	8,595762	2639,6916	0	1	1,03	132,48031	25648,52
16	26	3929,6916	3937,0079	7,316273	32661,615	1475,1243	44	1177,9432	8,929578	2657,0962	0	0,87	1,03	143,66798	23522,538
17	26	3945,7021	3953,4121	7,7099738	25339,767	8931,8776	43	1177,1507	8,929578	2610,684	0	0,87	1,03	223,58924	20567,334

Figure 85. Moving average equation applied in Excel by the package

Multiple Linear Regression

Regressions is applied using the data analysis tool in Excel. The coefficients extracted (β_{0-7}) are extracted with β_0 being the intercept for the model and β_{1-7} being the regression coefficients that are multiplied to the used regressors in the model. These are represented in Excel in cells Z17 to Z24 and are donated by a $ sign to keep them constant while the model is applied for all the dataset. For the modelling technique applied in this thesis, the regressors are the filtered values of the WOB, torque, RPM, flow rate, flow rate, mud weight and the UCS. These are represented in columns O to U respectively.

This is represented in Figure 86 and the model in Excel can be represented as:

$$Modelled\ ROP = \$Z\$17 + \$Z\$18 * O2 + \$Z\$19 * P2 + \$Z\$20 * Q2 + \$Z\$21 * R2 + \$Z\$22 * S2 + \$Z\$23 * T2 + \$Z\$24 * U2 \quad (A.14)$$

SUM =$Z$17+$Z$18*O2+$Z$19*P2+$Z$20*Q2+$Z$21*R2+$Z$22*S2+$Z$23*T2+$Z$24*U2

	M	N	O	P	Q	R	S	T	U	V	W	X	Y	Z
1	MW IN [kg/l	ROP [ft/hr]	WOB filterec	torque filtere	RPM average	flow rate filtered	FP filtered	mw filtered	MSE Calcualt	ROP filtered	ROP modelled	ROP modelled for the geological groups	SUMMARY OUTPUT	
2	1,03	11,8766404	12954,377	5106,88033	53,6	1120,195169	8,76267	1,03	6,50179416	15,6	96 $Z$24*U2			
3	1,03	33,1692913	16747,6233	7120,425	59,2	1177,679008	8,7960516	1,03	8,35901284	18,7139108	129,786801		*Regression Statistics*	
4	1,03	32,2834646	16262,4406	6632,15885	59,2	1177,097829	8,8628148	1,03	6,38603504	22,828084	129,9986983		Multiple R	0,658707
5	1,03	20,6036745	16205,1009	6310,58176	58,8	1176,358148	8,929578	1,03	5,60855072	24,5734908	129,2366535		R Square	0,433895
6	1,03	26,2795276	16430,0492	6050,95988	59	1175,618466	8,929578	1,03	4,97700833	26,6535433	126,8712627		Adjusted R Sq	0,423913
7	1,03	100,393701	16183,0471	5258,81813	47,6	1142,702628	8,8628148	1,03	2,19497947	42,5459318	120,5614139		Standard Erro	32,03192
8	1,03	46,6535433	16963,7501	3799,9202	36,8	1099,853921	8,7960516	1,03	1,16141207	45,2427822	98,80812605		Observations	405
9	1,03	113,254593	20157,1342	3189,21874	33	1100,487934	8,7292884	1,03	0,6542634	61,4370079	87,59498337			
10	1,03	390,551181	23381,3935	2453,13171	30,2	1101,28045	8,7292884	1,03	0,22558053	135,426509	75,94069004		ANOVA	
11	1,03	182,677165	24532,5996	2908,94512	26,6	1101,914463	8,7292884	1,03	0,19601213	166,706037	81,87333875			*df*
12	1,03	201,246719	26142,5239	4173,12664	34,8	1134,724632	8,8294332	1,03	0,31350411	186,87664	101,1648192		Regression	7
13	1,03	313,254593	25648,5198	5915,24844	43,4	1177,520505	8,8294332	1,03	0,80721818	240,19685	126,5636968		Residual	397
14	1,03	191,305774	23522,5376	7670,64636	44,2	1177,414836	8,9629596	1,03	0,9854054	255,807087	155,479008		Total	404
15	1,03	132,480315	20567,3341	9350,81294	44	1177,309167	8,929578	1,03	1,46946257	204,192913	179,4693424			
16	1,03	143,667979	19671,9515	8967,28062	43,4	1177,414836	8,9796504	1,03	1,44414649	196,391076	176,602514			*Coefficients*
17	1,03	223,589239	18631,0142	9213,62638	43	1177,520505	8,9963412	1,03	1,43564916	200,85958	181,5648078		Intercept	-256,095
18	1,03	129,10105	18961,8205	8744,53685	41,8	1160,402156	8,9963412	1,03	1,61800898	164,028871	172,9996733		X Variable 1	-0,00102
19	1,03	152,198163	19910,1321	8592,59905	41,4	1160,402156	8,8795056	1,03	1,65453013	156,207349	167,0024571		X Variable 2	0,013662
20	1,03	390,813648	21021,6415	8620,62641	41,2	1160,45499	8,9128872	1,03	1,2527884	207,874016	168,1096142		X Variable 3	-0,20776
21	1,03	318,930446	19610,201	8976,13137	41,6	1160,45499	8,8628148	1,03	1,1283814	242,926509	173,359147		X Variable 4	0,095136
22	1,03	101,082677	21268,6436	7950,91998	41,4	1132,875428	8,7459792	1,03	1,11012273	218,425197	152,1736709		X Variable 5	25,2423
23	1,03	110,006562	22534,5292	8774,03934	41	1122,467049	8,7459792	1,03	1,23268622	214,606299	160,925261		X Variable 6	3,951088
24	1,03	118,766404	22627,155	8949,57913	40,6	1094,940321	8,7292884	1,03	1,28349016	207,919948	160,1495032		X Variable 7	-2,41145
25	1.03	119.685039	22644.798	9035.13634	42	1064.190694	8.6625252	1.03	1.79580899	153.694226	155.1634415			

Figure 86. Multiple rinear regression application

Warren Model

The Warren model presented in 4.3.4 describes ROP as a function of three terms $\left(\frac{S^2 d_b^3 ROP}{NWOB^2}\right)$, $\left(\frac{ROP}{N d_b}\right)$ and $\left(\frac{d_b \gamma_f \mu ROP}{F_{jm}}\right)$. These terms are calculated in Excel for each well using the already filtered datasets. The rock strength used for the calculations is derived from the calculated MSE for each datapoint in the well. The calculation of these terms can be seen in Figures 87, 88 and 89.

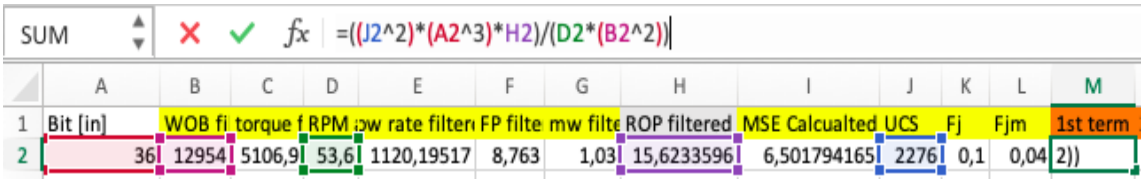

Figure 87. Calculating the first Warren Term in Excel

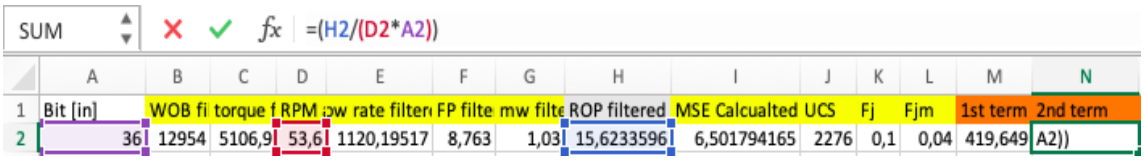

Figure 88. Calculating the second Warren Term in Excel

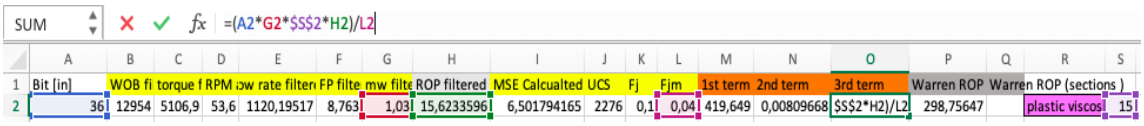

Figure 89. Calculating the third Warren Term in Excel

This is then followed by extracting the Warren coefficients “a”,” b” and “c” using MATLAB software. Application of this can be seen in Figure 90

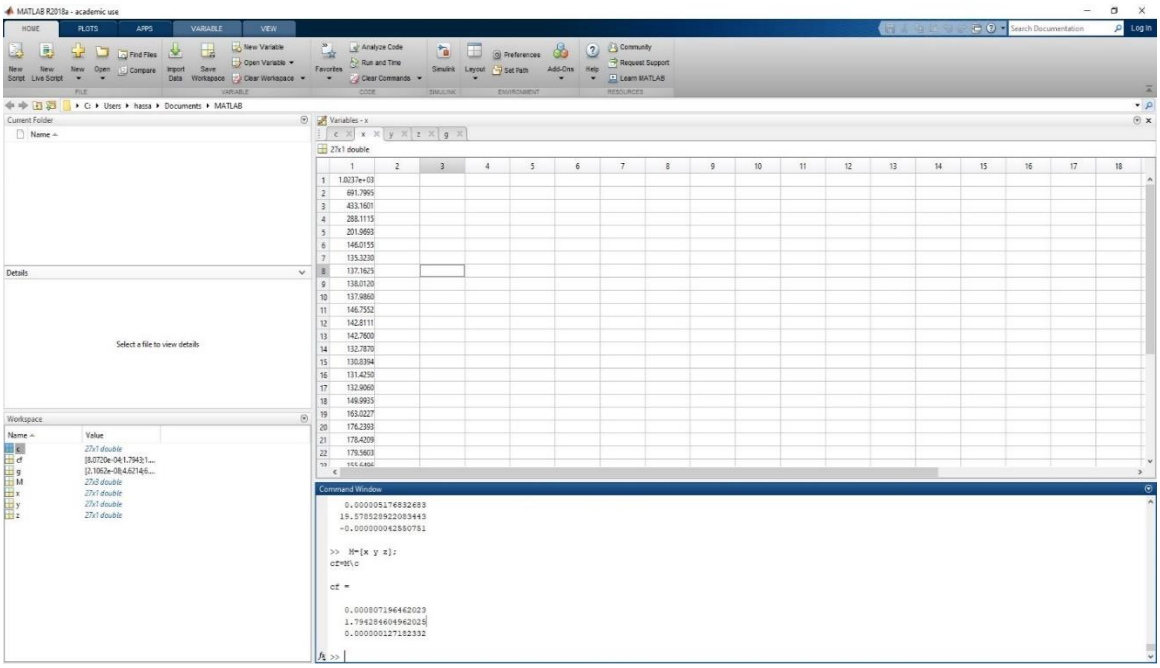

Figure 90. Calculation of Warren coefficients in Matlab

Once the coefficients have been extracted, the Warren ROP can be calculated using Eq. 3.6 as shown in Figure 91.

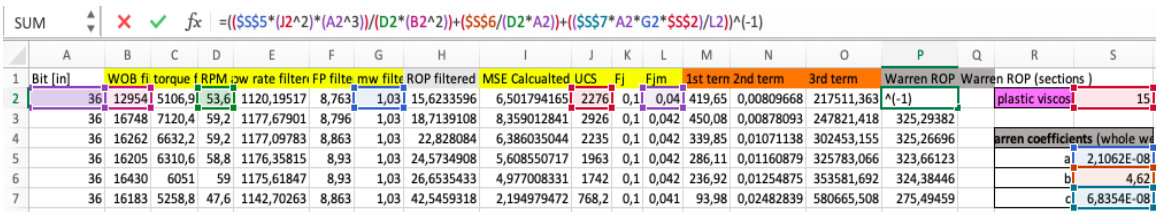

SUM =(($$5*(J2^2)*(A2^3))/(D2*(B2^2))+($$6/(D2*A2))+(($$7*A2*G2*$$2)/L2))^(-1)

	A	B	C	D	E	F	G	H	I	J	K	L	M	N	O	P	Q	R	S
1	Bit [in]	WOB fi	torque f	RPM	ow rate filter	FP filte	mw filte	ROP filtered	MSE Calcualted	UCS	Fj	Fjm	1st term	2nd term	3rd term	Warren ROP	Warren ROP (sections)		
2	36	12954	5106,9	53,6	1120,19517	8,763	1,03	15,6233596	6,501794165	2276	0,1	0,04	419,65	0,00809668	217511,363	^(-1)		plastic viscos	15
3	36	16748	7120,4	59,2	1177,67901	8,796	1,03	18,7139108	8,359012841	2926	0,1	0,042	450,08	0,00878093	247821,418	325,29382			
4	36	16262	6632,2	59,2	1177,09783	8,863	1,03	22,828084	6,386035044	2235	0,1	0,042	339,85	0,01071138	302453,155	325,26696		arren coefficients (whole w	
5	36	16205	6310,6	58,8	1176,35815	8,93	1,03	24,5734908	5,608550717	1963	0,1	0,042	286,11	0,01160879	325783,066	323,66123		a	2,1062E-08
6	36	16430	6051	59	1175,61847	8,93	1,03	26,6535433	4,977008331	1742	0,1	0,042	236,92	0,01254875	353581,692	324,38446		b	4,62
7	36	16183	5258,8	47,6	1142,70263	8,863	1,03	42,5459318	2,194979472	768,2	0,1	0,041	93,98	0,02482839	580665,508	275,49459		c	6,8354E-08

Figure 91. Warren ROP calculating in Excel